Regulation of *L. monocytogenes* PrfA regulon by environmental stimuli in gastrointestinal tract

A thesis submitted to The University of Manchester for the degree of Doctor of Philosophy in the Faculty of Biology, Medicine and Health

2023

Lamis A Alnakhli

School of Biological Sciences

Division of Immunology, Immunity to Infection and Respiratory Medicine

Table of content

Final words count: 29,271

Index of Figures

Index of Tables

Abbreviations

5-HT	Serotonin
actA/ActA	actin assembly inducing gene/protein
ADI	arginine deiminase
AMPs	antimicrobial peptides
Arp2/3	actin-related protein 2/3
ATR	acid tolerance response
BCFAs	branched chain fatty acids
BKD	branched chain alpha-keto acid dehydrogenase
Bp	base pair
ºC	degree Celsius
CDC	Cholesterol-Dependent Cytolysin
Cm	chloramphenicol
CNS	central nervous system
CT	cycle threshold
DNA	deoxyribonucleic acid
E-cadherin	epithelial-cadherin
EC	enterochromaffin cells
EDTA	ethylenediaminetetraacetic acid
EIIA/B	Enzyme IIA/B
Erm	erythromycin

EVH1	Ena/VASP homology domain 1
GABA	glutamate-γ-aminobutyrate antiporter
GAD	glutamate decarboxylase
gDNA	genomic deoxyribonucleic acid
Gfp	green fluorescent protein
GTP	guanosine triphosphate
GW	dipeptide Gly-Trp
H	hours
HDAC	Histone deacetylases
HEPES	hydroxyethyl piperazineethanesulfonic acid
Hpt	hexose phosphate transporter
IL-12	interleukin 12
IL-23	interleukin 23
InlA/B/C/J/I/L/D	Internalin A/B/C/J/I/L/D
Kb	kilo base
LAMP-1	lysosome-associated membrane protein-1
LB	lysogeny broth
LIPI-1	*Listeria* pathogenicity island 1
LLO	listeriolysin O
LLS	listeriolysin S
LPXTG	leucine-proline-X-threonine-glycine

LRR	leucine rich repeat
MAPK	mitogen-activated protein kinases
mEC1	murine E-cadherin
min	minutes
MOI	multiplicity of infection
mRNA	messenger ribonucleic acid
MucBP	mucin binding protein domains
NF-kB	nuclear factor kappa B
O/N	overnight
OD	optical density
PBS	phosphate buffered saline
PC	phosphatidylcholine
PC-PLC	broad-range phospholipases C
PCR	polymerase chain reaction
PE	phosphatidylethanolamine
PEST	proline, glutamic acid, serine and threonine-rich motif
PI3K	phosphatidylinositol 3-kinase
PlcA/B	phospholipase A/B
PrfA	positive regulatory factor A
PS	phosphatidylserine
PTS	phosphoenolpyruvate-sugar phosphotransferase system

qRTPCR	quantitative real time polymerase chain reaction
RFU	relative florescent unit
RNA	ribonucleic acid
rpm	revolutions per minute
SCFA	short chain fatty acid
SD	Shine-Dalgarno
SDS	sodium dodecyl sulphate
Sec	second
SERT	serotonin re-uptake transporter
SigB	alternative sigma factor B
SM	sphingomyelin
TSB	tryptone soya broth
UPR	unfolded protein response
VASP	Vasodilator-stimulated phosphoprotein
VCA	verprolin homology, cofilin homology and acidic
WASP	Wiskott-Aldrich syndrome protein
WAVE	WASP-family verprolin-homologous protein
ml	microliter
µM	micromolar

Abstract

Listeria monocytogenes, a Gram-positive bacterium*,* is a food-borne pathogen which causes listeriosis. It is an intracellular pathogen invading the epithelial cells where it escapes from the vacuole into the host cytoplasm to replicate, using actin-based motility to move within and between cells. The intracellular life cycle is well documented whereas the time spent in the lumen of the intestine is poorly understood. The aim of this study was to investigate the mechanism by which *L. monocytogenes* adapts to the environment of the small intestine prior to invasion. Specifically, to determine if the PrfA regulon, that encodes the virulence factors of *L. monocytogenes,* is switched on by signals within the intestinal lumen. Initially three signals were examined, butyrate, a short chain fatty acid molecule synthesised by bacteria within the gut microbiota, microaerobic conditions (5.5 %v/v oxygen) and serotonin (5-HT), a key neurotransmitter that modulates brain behaviour. 5-HT is secreted by enterochromaffin cells (EC) into the intestinal lumen where it acts to control gut motility, secretion and vasodilation. *L. monocytogenes* strains with either chromosomal *phly*::*gfp* or *pactA*::*gfp* transcriptional fusions were grown in MD10 medium with two different source of carbon either aerobically or microaerobically with and without 5 mM butyrate or 100 µM 5-HT and Gfp expression monitored. There was significant induction of the *pactA* and *phly* expression in microaerobic versus aerobic conditions. The addition of 5-HT had no effect while butyrate significantly lowered both *phly* and *pactA* activity. A *prfA* mutation abolished detectable transcription from *phly* and *pactA* while a *sigB* mutation led to increased expression from *phly* regardless of the oxygen concentration or carbon source used in the experiment. In contrast, the transcription from *pactA* showed a trend of increased activity in a *sigB* mutation but this increase was only significant in mid-log phase during aerobic growth. Western blot analysis demonstrated that under microaerobic conditions there was increased production of PrfA, LLO and ActA proteins. The RNA-seq analysis showed 27 annotated genes were specifically regulated by microaerobic conditions either up or down including the PrfA regulon virulence factors. Overall, these data indicated that *L. monocytogenes* PrfA regulon is highly responsive to signals likely to be encountered in the small intestine.

Declaration

No portion of the work referred to in the thesis has been submitted in support of an application for another degree or qualification of this or any other university or other institute of learning.

Copyright statement

Acknowledgements

It has been an honour to be a student of Professor Ian Roberts over the last four years, and I am grateful to you for your outstanding mentorship. I have gained invaluable insight and advice from you as I have grown as an individual and as a scientist. You have been the best supervisor that I could have ever asked for.

Many thanks to Marie Goldrick and Elizabeth Lord for their technical assistance and always being available to lend a helping hand with love and generosity. My thanks also extend to everyone in lab C.1202 for making it such an enjoyable work environment. Special thanks to Esraa Aldawood for her support in qRTPCR experiment even after she graduated.

I also thank Leo Zeef and Andy Hayes of the Bioinformatics and Genomic Technologies Core Facilities at the University of Manchester for providing support with regard to RNA-seq

I owe a big thank you to my friends Fatima Alhashim and Maryam Munawis. They were like sisters to me in exile and the only outlet I always turned to whenever I needed a breather from the stresses of my study.

My mother's love and prayers for me are the foundations of my life, and I am deeply grateful to her for that. My deepest gratitude reaches out to all of my siblings who held out hope in me that I would one day be able to achieve this goal. Especially for my sister Rawan Alnakhli, who was a constant source of laughter and joy in my life throughout the difficult days.

It would not be possible for me to survive without my dearest husband and best friend, Ali. There are no words that can properly describe my gratitude for you because you believed in me and encouraged me to pursue this degree. I appreciate your patience, love, support and for listening to me so well. I am deeply grateful to my children Alhussain and Hanan for making me stronger, better, and more fulfilled than I could ever imagine. It was you who shined the brightest during the darkest hours of this rough journey for me, you were my true stars.

Chapter 1 Introduction

1.1. Taxonomy

Listeria is a genus of Gram-positive bacteria of low G+C, currently it consists of twenty species of which *Listeria. monocytogenes* and *Listeria ivanovii*, are considered pathogenic to humans and animals (Korsak *et al*., 2012; Borcan *et al*., 2014; Townsend *et al.,* 2021; Nwaiwu, 2020). *Listeria species* are non-spore forming, rod shaped and facultatively anaerobic bacteria (Müller-Herbst *et al*., 2014). They produce small milky white colonies, are motile, positive for catalase, aesulin hydrolysis and Voges-Proskauer and negative in oxidase, indole and urea hydrolysis (Low and Donachie, 1997). *L. ivanovii* and *L. monocytogenes* are pathogenic species, with *L. ivanovii* considered to be a pathogen for animals, in particular ungulates like cattle and sheep, whereas *L. monocytogenes* is more prevalent in human infections but it can also infect animals (Wang, 2012).

1.2. Characteristics of *Listeria monocytogenes*

L. monocytogenes are able to grow at a range of te

mperatures from 1.7 °C to over 42 °C, as well as being able to survive and grow in a broad pH range and with a high salt concentration and long periods of freezing and drying (Junttila *et al*., 1988; Müller-Herbst *et al*., 2014). It can be readily isolated from soil, water, plant, forage and the natural environment (Korsak *et al.,* 2012). Therefore, it can contaminate foods consumed by humans such as meat, milk, seafood, dairy products, fresh vegetables and processed food products (Yan *et al*., 2010).

L. monocytogenes has four lineages (I, II, III, IV) and 13 serotypes (Ward *et al*., 2004; Zang *et al*., 2007). The serotypes 1/2b, 4b and 1/2a that are associated with human disease belong to lineages I and II respectively (Obaidat *et al*, 2015). Isolates belonging to serogroups 1/2b and 4b are frequently associated with bacteriemia and neurologic infections while serogroup 1/2a were associated with embryonic infections (Steckler *et al.,* 2018).

1.3. Diseases caused by *L. monocytogenes*

1.3.1 Listeriosis in animals:

A host of animal species, notably ruminants, are affected by listeria (Wesley *et al*., 2003; Dhama *et al*., 2015). *L. monocytogenes* is common globally and is implicated as the cause of significant disease in different animals (Low and Donachie, 1997). In contrast, the incidence of *L. ivanovii* in animal listeriosis is less common compared to *L. monocytogenes* (Gouin *et al*., 1994). *L. monocytogenes* is responsible for miscarriage and circling disease (encephalitis), and the spread of listeriosis has been observed in cattle and sheep herds (Schuchat *et al.,* 1991). The pathogen is ubiquitous, especially prevalent in regions with moderate temperatures and is prominent in niches such as soil, faeces, sewage, and can also be found on farm structures and surfaces (Dhama *et al*., 2015). A lack of nutritious food and bad weather are some of the factors that predispose animals to listeriosis (Wesley *et al*., 2003). Silage can contain approximately 10^6 *L. monocytogenes* per gram, thus animals fed with it are more likely to be affected (Wesley *et al*., 2003). Other factors include genetic makeup, abrupt alteration in feed content, mixing of animals from different farms, ill-health and weather (Wesley *et al*., 2003). An insult to the oral cavity and the wall lining the digestive tract increases the chance of *L. monocytogenes* colonisation (Wesley *et al*., 2003). In Canada, cattle are the most affected by listeriosis, accounting for 82 % of cases, compared to 17 % in the case of sheep and fewer still in pig (Wesley *et al*., 2003). Conversely, in Great Britain, sheep are mostly affected, 63 %, followed by cattle 32 % (Wesley *et al*., 2003). The disease can be treated using antibiotics, typically penicillin, but cephalosporins and chloramphenicol are not used due to high levels of resistance and therefore high clinical failure rates (Crum, 2002).

1.3.2 Listeriosis in humans:

L. monocytogenes causes listeriosis the symptoms which in most healthy adults are febrile gastroenteritis that is not life threatening (Lomonaco *et al*., 2015). However, in people with

reduced immunity such as the old, young, pregnant women or people whose immunity has been compromised by infection or medical treatment, then *L. monocytogenes* infection can have more serious consequences including septicaemia, meningitis and intrauterine infection of the unborn child (Lomonaco *et al*., 2015). Compared to other food borne bacterial infections, listeriosis has the highest morality rate of 30% in spite of early antibiotic treatment (Lecuit, 2007). Unpasteurized dairy products together with raw salad and vegetables, fruit, cold meat and smoked fish have all been implicated in out breaks of listeriosis (Wang, 2012).

1.3.2.1 Foetomaternal and neonatal listeriosis

L. monocytogenes has been implicated in neonatal meningitis in the western parts of the world (Lecuit, 2007). A pregnant woman infected by *L. monocytogenes* may be asymptomatic but commonly have flu-like or pyelonephritis symptoms before the early onset of labour. If the mother becomes symptomatic, it is usually in the third trimester. Symptoms include fever, myalgia, arthralgia, abortion, stillbirth and preterm labour (Vázquez-Boland *et al.*, 2001).

There are two types of neonatal listeriosis: early onset and late onset. Early stage of listeriosis manifests during the first seven days after delivery with a resulting illness observed in mothers. Clinical signs in the neonate include inflammation in the lungs and difficulty in breathing (Chen *et al*., 2007). Despite rapid intervention and treatment, remarkably high death rates occur from early form of the disease and it is common for infants to die intrauterine in the womb prior to birth. Perinatal listeriosis mainly occurs when the fetus is invaded through the placenta leading to inflammation of the amnion and chorion (Vázquez-Boland *et al.*, 2001).

On the other hand, late stage of listeriosis occurs during delivery and is transmitted via the vagina. Symptoms are observed 1 to 2 weeks after delivery and include swelling on the top part of the head, fever, and meningismus (Kessler and Dajani, 1990).

1.3.2.2 Listeriosis in adults

After ingestion of contaminated food, *L. monocytogenes* is able to cross the intestinal barrier and spread from there to mesenteric lymph nodes and move to the spleen and the liver (see section 4). If *L. monocytogenes* is not controlled by the immune system in the liver and spleen a systemic bacteraemia may occur leading to infection of brain (Lecuit, 2007).

In adults who are not pregnant, 55-70 % of listerial cases affect the central nervous system with bacteraemia present in 15-50 % while uncommon clinical manifestations such as myocarditis and colecystitis are seen in 5-10 % of cases (Vázquez-Boland *et al.*, 2001).

The most common infection of the CNS caused by *L. monocytogenes* is meningitis. Bacterial meningitis presents symptoms which include fever, headache, and stiff neck (Skogberg *et al.*, 1992). Another form of CNS listeriosis in adults is rhombencephalitis which affects the brainstem (Armstrong and Fung, 1993; Doganay, 2003). It is characterised at initial stage by fever, headache, and malaise. At later stages of the disease, the nerves coming out of the brain become inflamed causing a lack of voluntary coordination (Doganay, 2003).

Bacteraemia where the CNS is unaffected, accounts for about 33% of cases that affect adults. Patients that have underlying medical conditions such as diabetes, liver cirrhosis, and blood disorders are more vulnerable to listeria sepsis (Doganay, 2003). The presentation is unspecific and is similar to other types of bacteria sepsis with an infected individual typically having a fever, night sweats and general body weakness (Doganay, 2003; Yildiz *et al.,* 2007). There are other clinical syndromes in adults such as hepatitis, gastroenteritis, pleuritis, endocarditis, pneumonia, arthritis, conjunctivitis and peritonitis localised abscesses but such infections are uncommon (Vázquez-Boland *et al.*, 2001).

1.4. Infection route of *L. monocytogenes* in humans

The stomach of humans is naturally acidic therefore *L. monocytogenes* must be able to navigate and survive this hostile environment before it can proceed to the intestine. There has

been evidence that antacids and H2-blocking agents (types of medicines that neutralise the stomach's acid) can increase the risk for listeriosis, especially in experimental animals treated with cimetidine which an agent used to reduce acid in the stomach, (Vázquez-Boland *et al.*, 2001). This means that Listeria organisms swallowed with contaminated food are likely destroyed by gastric acidity.

Despite the sterilising action in the stomach, an estimated 0.9 % of listeria will successfully survive and invade the epithelium of the intestine (Melton-Witt *et al.*, 2012). Beginning from the intestine invasion, the *L. monocytogenes* (Figure 1.1) spreads through the portal vein until it reaches the liver. The basement membrane under the intestinal epithelium prevents extension of *L. monocytogenes* into the lamina propria. It is shed back from the tips of intestinal villi into the lumen inside extruded enterocytes. Then by re-infecting Peyer's patches and lamina propria macrophages, *L. monocytogenes* could disseminate in infected leukocytes via the portal vein directly to the liver and along afferent lymphatic vessels to the mesenteric lymph nodes. The bacteria disseminate further via the systemic circulation to liver and spleen (Figure 1.2) (Melton-Witt *et al.*, 2012).

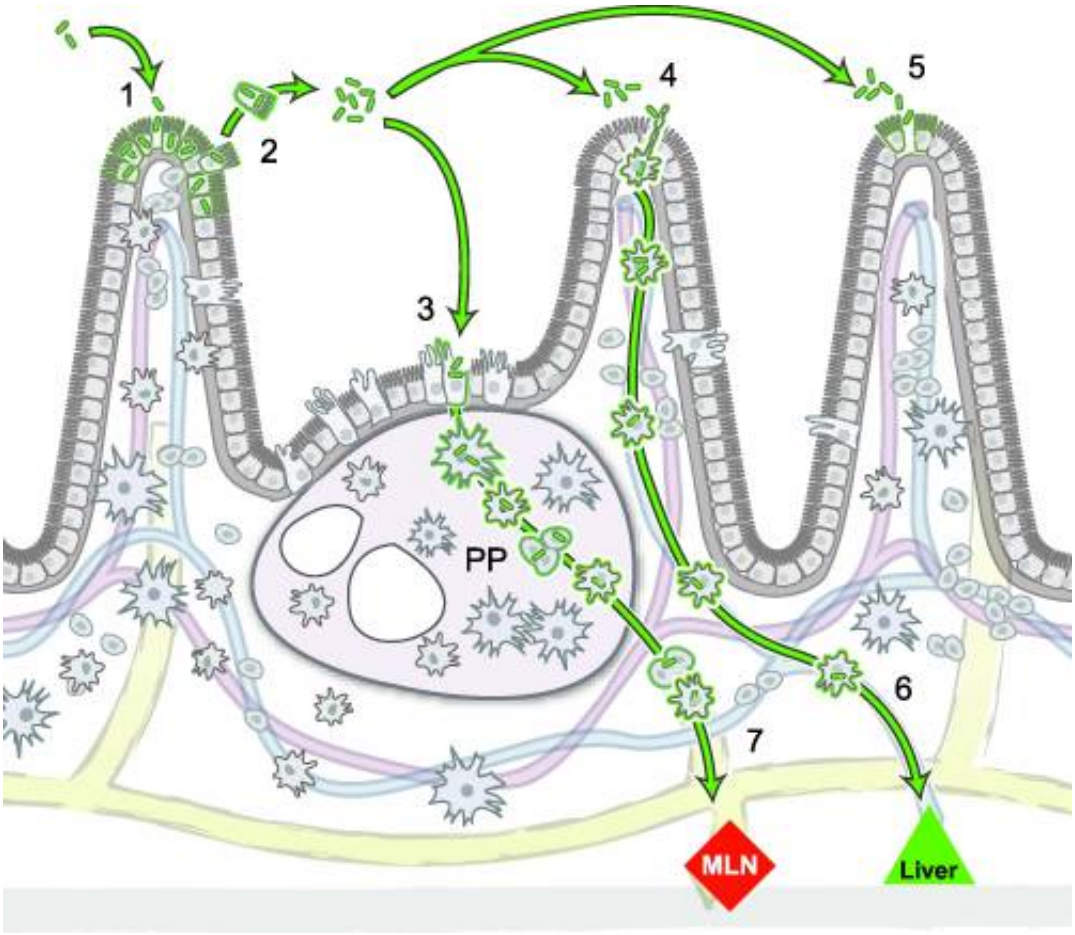

Figure 1.1 Model of bacterial dissemination from intestinal villi to liver and mesenteric lymph nodes. (arrow 1) Ingestion of *L. monocytogenes* leads to enterocyte invasion at the tip of intestinal villi. Once internalized, *L. monocytogenes* replicates and spreads to neighboring enterocytes via cell-to-cell spread. (arrow 2) The basement membrane under the intestinal epithelium prevents bacterial extension into the lamina propria. Bacteria are shed back from the tips of intestinal villi into the lumen inside extruded enterocytes. Subsequently, bacteria reinfect Peyer's patches (PP) (arrow 3), lamina propria macrophages (arrow 4), and other enterocytes (arrow 5). *L. monocytogenes* could disseminate in infected leukocytes (dendritic cells and/or macrophages) via the portal vein directly to the liver (arrow 6) and along afferent lymphatic vessels to the mesenteric lymph nodes (MLN) (arrow 7). The bacteria disseminate further via the systemic circulation to liver and spleen. Taken from (Melton-Witt *et al.*, 2012).

Mouse models infected with *L. monocytogenes* show that Kupffer cells are responsible for activating the first line of defence in the liver (Conlan and North, 1992). These cells destroy more than 95% of the bacteria within 6 h, while bacteria that are not destroyed by Kupffer cells proliferate in surrounding liver cells (Conlan and North, 1992). In the spleen, *L.*

monocytogenes concentrate themselves inside macrophages in the space between the white pulp and the red pulp (Conlan, 1996). These phagocytic cells become infected and they move into the white pulp of the spleen where they eventually infect surrounding cells thereby enabling bacterial spread (Aoshi *et al.,* 2009). A functioning immune system can ward off the invading bacteria, but where the immune system is compromised, chronic bacteraemia may occur (Lecuit, 2007).

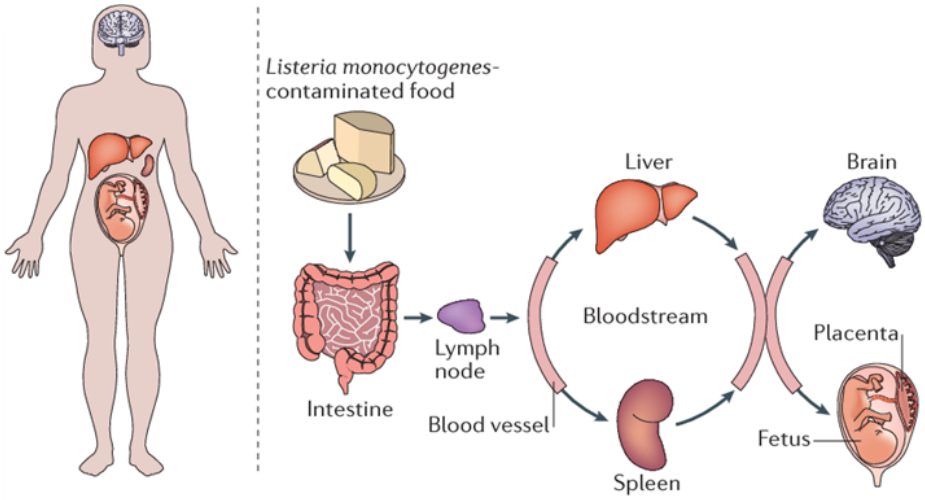

Figure 1.2 Overview of *L. monocytogenes* infection: After ingestion of contaminated food, *L. monocytogenes* (depicted by the arrows) can traverse the intestinal barrier and spread into the bloodstream through the lymph nodes to disseminate to target tissues, such as the liver and spleen. In immunocompromised individuals, *L. monocytogenes* can cross the blood–brain barrier or fetoplacental barrier and cause potentially fatal meningitis, sepsis, premature birth or abortion. Taken from (Radoshevich and Cossart, 2018).

1.5. *L. monocytogenes* life cycle

1.5.1. Internalisation

Two processes needed for *L. monocytogenes* to invade the target cell are attachment to the cell surface and internalization (Mansell *et al*., 2001). It can invade both phagocytic and non-phagocytic cells using two Internalins InlA and InlB (Jones and D'Orazio, 2017). InlA and InlB are members of a large family of proteins termed Internalins and are required for its entry into intestinal epithelial cells; they bind to specific receptors in the case of InlA it is E-cadherin and in the case of InlB it is c-Met hepatocyte growth factor receptor (Jones and D'Orazio, 2017). Expression of cell surface receptors on the host cells determine which internalin will facilitate

entry of *L. monocytogenes,* as well as determining how the bacteria will enter, individually or in concert (Vadia *et al.,* 2011).

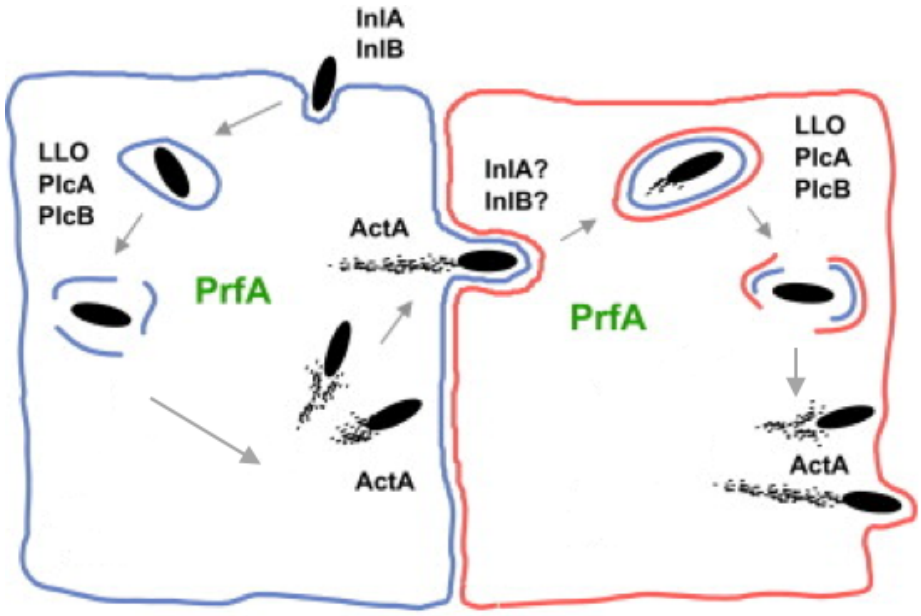

Figure 1.3 Life cycle of *L. monocytogenes* pathogenicity. *L. monocytogenes* can enter into a non-phagocytic cell by using its surface proteins, internalin A (InlA) and internalin B (InlB), to bind with the host receptors. By secretion of two phospholipases (PlcA and PlcB) and listerolysin O (LLO), the phagosomal membrance is degraded and the bacterium escapes from the vacuole. It replicates in the host cytoplasm and polymerizes host actin by using ActA. Then it spreads to neighboring cell through actin-based motility after destroying the first one. Taken from (Scortti *et al.,* 2007).

1.5.1.1. Internalin A (InlA)

InlA is a cell surface protein of *L. monocytogenes* distinguished by the presence of leucine-rich repeats (LRRs) which are involved in protein-protein interactions (Drolia and Bhunia, 2019). InlA is covalently bound to the cell wall of *L. monocytogenes* characterised by the distal motif Leucine-Proline-X-Threonine-Glycine. The cellular receptor of InlA is the transmembrane protein, epithelial-cadherin (E-cadherin) which belongs to the cadherin superfamily. The extracellular domain of E-cadherin is involved in homophilic interactions which result in adherence between epithelial cells (Turner, 2009). Cytoplasmic effector proteins link the intracellular domain of E-cadherin to the actin cytoskeleton, which is crucial

for cell signalling and differentiation (Li *et al.,* 2012). The first ectodomain of E-cadherin interacts with the LLR units of InlA in a calcium dependent manner leading to endocytosis of *L. monocytogenes* (Bierne and Cossart, 2007; McGuckin *et al.,* 2011; Drolia and Bhunia, 2019).

L. monocytogenes invades the host cell by hijacking the molecular machinery of the E-cadherin cytoplasmic tail (Figure 1.4). InlA binds to host E-cadherin which triggers the binding of β-catenins on the cytosolic side to E-cadherin's intracellular domain, leading to the formation of the InlA-E-cadherin-β-catenin complex (Ortega *et al.,* 2017). The monomeric association of α-catenin with β-catenin, and its dimeric association with F-actin, allows cytoskeletal organisation of the host via a molecular switch that depends on α-catenin concentration at the site (Ortega *et al.,* 2017). ARHGAP10 is a Rho-GAP domain protein that allows α-catenin recruitment to the *L. monocytogenes* entry site via interaction with Arf6, a small GTP-binding protein (Drolia and Bhunia, 2019). The Arp2/3 signalling complex recruited at the bacterial entry site directs actin remodelling and *L. monocytogenes* engulfment in host cells. InlA recruitment to E-cadherin allows activation of GTPase Rac1, a Rho family protein at the site of bacterial attachment which stimulates the Arp2/3 independently of the proteins WAVE (WASP-family verprolin-homologous protein) and WASP (Wiskott-Aldrich syndrome protein). Arp2/3 stimulation drives actin assembly that ultimately leads to *L. monocytogenes* uptake. Rac1 further allows regulation of Cortactin, an important protein that can bind to both Arp2/3 and F-actin and regulate actin assembly. Cortactin can also be activated by the Src tyrosine kinase. Additionally, *L. monocytogenes* infections involve InlA-induced triggering of Src-mediated E-cadherin phosphorylation (Drolia and Bhunia, 2019).

However, the presence of glutamate rather than proline at position 16 of murine E-cadherin (mEC1) inhibits E-cadherin dependent internalisation of *L. monocytogenes* in the intestinal epithelial cells of mice (Wollert *et al*., 2007). As a result, murine challenge of *L. monocytogenes* via the oral route was not possible for *in vivo* laboratory procedures (Lecuit *et al.,* 1999). In

2007, strain *EGDe::InlA^m* was generated containing two amino acid substitutions S192N-Y369S that increase the binding and affinity of InlA^m to murine E-cadherin (mEC1) (Wollert *et al*., 2007). The *EGDe::InlA^m* strain circumvents this obstacle of orally administering Listerial infection in mice models and allowed the construction of an oral infection model that more closely resembled that of human infection (Wollert *et al*., 2007).

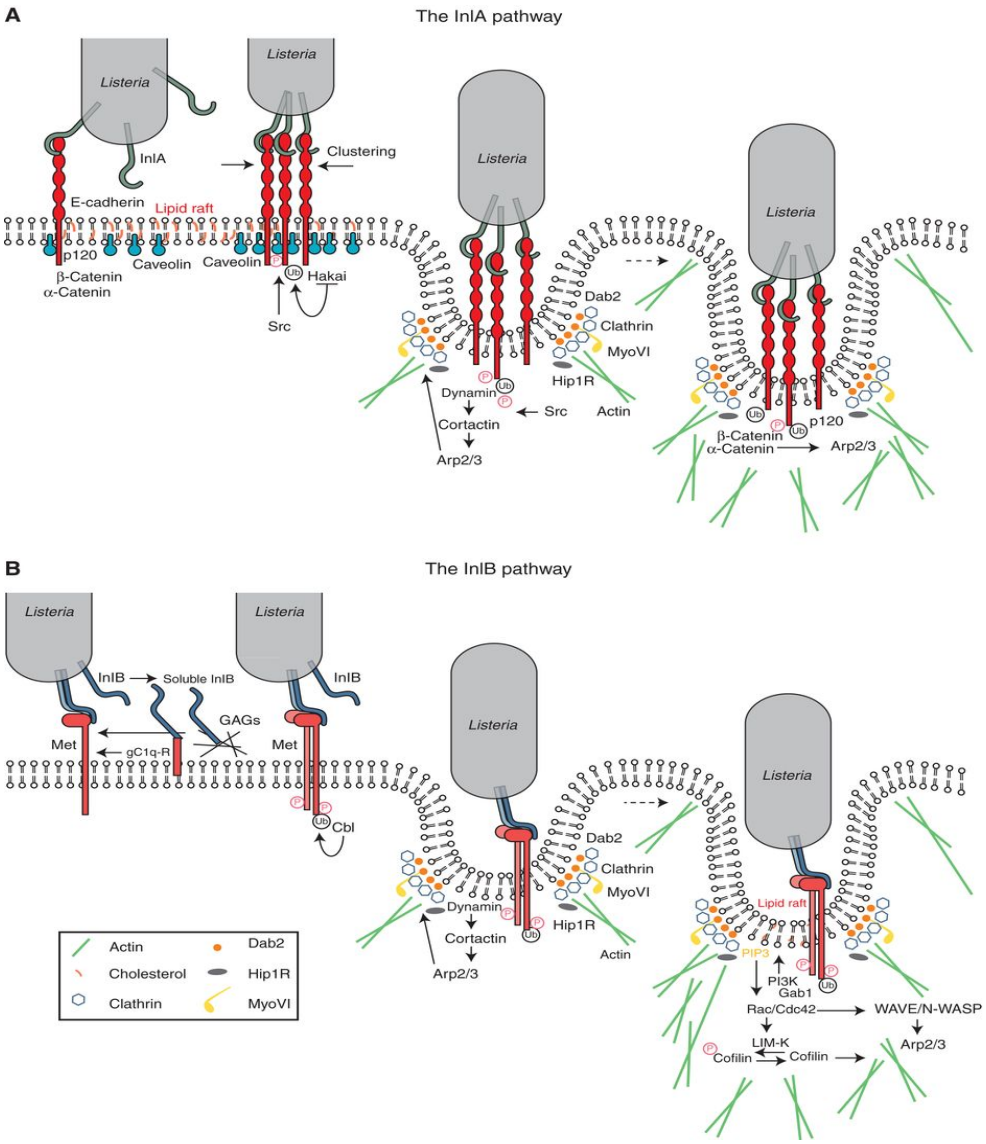

Figure 1.4 Signaling cascades activated via the InlA and InlB pathways of invasion. InlA and InlB required for entry of *Listeria* into the host cell; they bind to specific receptors in the case of InlA it is E-cadherin and in the case of InlB it is Met. The recruitment of clathrin endocytosis machinery (dynamin, Dab2, Hip1R, clathrin, MyoVI) provides an initial platform for actin cytoskeleton polymerisation. Downstream from E-cadherin, this first actin polymerisation wave is activated by Src and cortactin that enhance recruitment of Arp2/3 complex. Association of α and β catenins to the bacterial entry site favors dynamic interactions between the actin cytoskeleton and E-cadherin cytoplasmic tail. In the case of Met, actin polymerisation can be first coordinated by dymamin and cortactin upstream of Arp2/3 complex, and subsequently by a signaling cascade downstream from the IA PI 3-kinase, which involve the small GTPases Rac1 and Cdc42, abi1, WAVE, and N-WASP (cell type-dependent); LIM-K and cofilin essential in the depolymerisation of actin to facilitate the internalisation process. Taken from (Pizarro-Cerdá *et al.,* 2012).

1.5.1.2. Internalin B (InlB)

InlB, is also a part of the internalin family with the *inlB* gene being part of the same operon as the *inlA* gene (Khelef *et al*., 2006). The entry of *L. monocytogenes* into non-phagocytic cells, such as the human epithelial LoVo cell line is mediated by InlB (Khelef *et al*., 2006). The N-terminal domain of InlB contains a signal sequence, there are seven LRR domains, one IR region, and one B repeat (Jung *et al.,* 2009). The dipeptide Gly-Trp (GW) is a conserved tandem repeat presented on the C-terminal GW region, which facilitates non-covalent adhesion to the *L. monocytogenes* cell wall (Figure 1.5) (Cossart *et al.,* 2003).

The receptor of InlB is the hepatocyte growth factor Met and binding occurs through the concave surface of the LRR region (Bierne *et al.,* 2007). This triggers downstream signalling pathways leading to the remodelling of F-actin cytoskeleton. Endocytosis of *L. monocytogenes* leads to the activation of the classical phosphatidylinositol 3-kinase (PI3K) pathway. Firstly, Gab1 and Cbl are recruited which are located on phosphotyrosine residues of the intracytoplasmic region of Met. Gab1 is a multiple-site tyrosine-phosphorylated adaptor protein, which brings together Met to the adaptor protein CrkII and to p85 regulatory subunit of type IA PI3K (See Figure 1.4) with both CrkII and Gab1 eliciting the recruitment of PI3K to the membrane (Ireton, 2007). Moreover, CrkII consists of two SH3 domains, one of which stimulates PI3K activity (Ireton, 2007). This process is required for bacterial uptake. The process by which PI3K activity drives actin remodelling has not yet been fully elucidated and it is thought that this process may occur by directly promoting actin polymerisation via uncapping of the barbed ends of the actin filaments (Hartwig *et al.,* 1995). The PI3K pathway activates the small GTPases, Rac1 and Cdc42, however, this process is not fully understood. These GTPases activate WAVE and/or N-WASP, which result in the activation of the Arp2/3 complex and actin polymerisation of host cells (Ireton, 2007). Furthermore, activation of PI3K also results in the activation of the anti-apoptotic Akt (serine-threonine kinase)/PKB (protein kinase B) pathway and the transcription factor NF-κB (Mansell *et al.,* 2001).

1.5.1.3. Other internalin proteins

Besides InlA and InlB, *L. monocytogenes* has other internalins members which are involved in its invasion. *L. monocytogenes* contains 25 internalins in total that can be grouped into three families (See Figure 1.5) (Radoshevich and Cossart, 2018). Internalins are surface proteins that characterized by the presence of N-terminal domain containing leucine-rich repeats (LLRs). They are divided into three types based on their interaction with the bacterial surface, which are LPXTG, WxL or GW anchored and the

secreted internalins (Bierne *et al*., 2007). Internalins A and B essential for adhesion belong to LPXTG and GW families respectively (Bierne *et al*., 2007). They are important for internalization of *L. monocytogenes* into non-phagocytic cells (Pentecost *et al*., 2010). In addition, Lmo0549 with eight internalins of LPXTG group are also characterized by the presence of PKD repeats (Figure 1.5). The PKD repeat contains around 80 amino acids and was originally identified in the polycystin-1 protein although the precise function of the PKD repeat is unknown, it may mediate protein/protein or protein/carbohydrate interactions (Bierne *et al*., 2007). No function has been assigned to the PKD repeats in *Listerial* internalins (Bierne *et al*., 2007).

Lmo2026 has been reclassified as InlL (Popowska *et al*., 2017). This internalin has been shown to bind to mucin and has two mucin binding domains (MucBP) but is not involved in internalisation. Likewise, Lmo0723, InlI, Lmo0171, InlJ, Lmo0327 and Lmo2396 have been shown to bind mucus (Figure 1.5) (Popowska *et al*., 2017). As such these proteins may be important in attachment to mucosal epithelial layers.

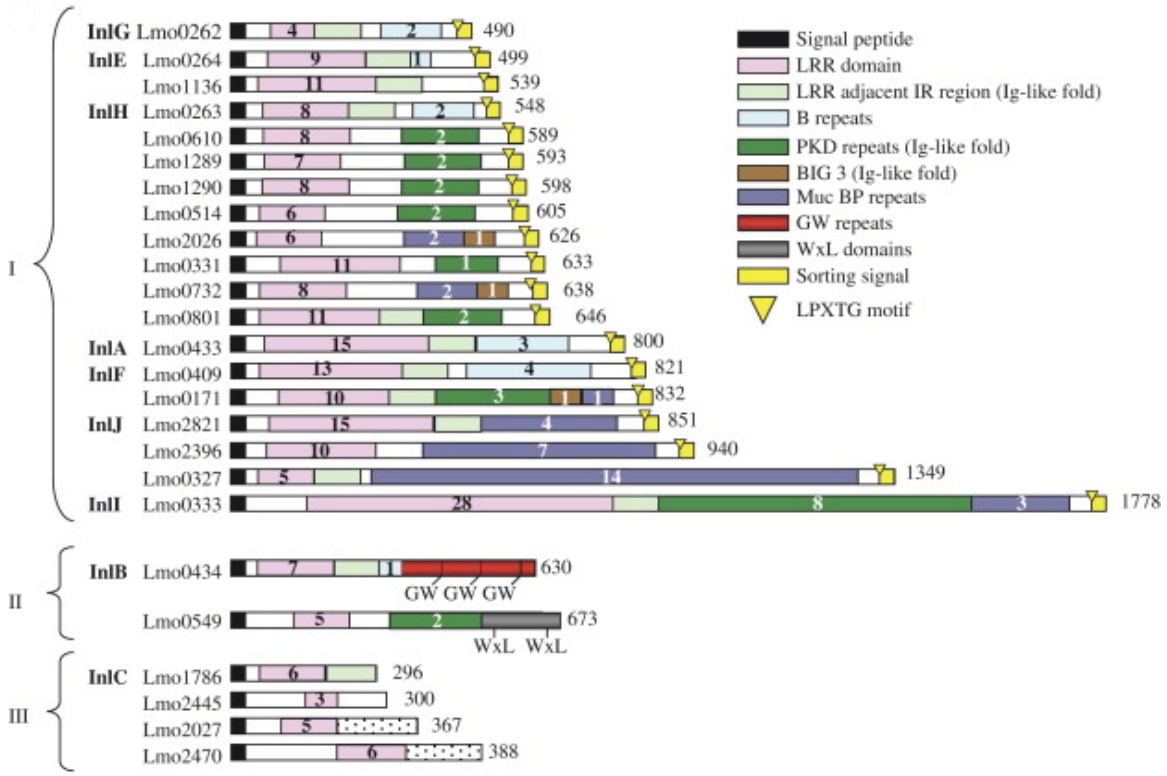

Figure 1.5 Structure of 25 proteins of *L. monocytogenes* EGDe are included in three families of internalns. I: LPXTG, II: WxL or GW anchored and III: secreted internalins. Homologous regions are colour coded with legends provided in boxes on the right. Numbers within different domains indicate the number of repeats. Taken from (Bierne *et al.,* 2007).

Other members of the internalin family may influence *L. monocytogenes* invasion. This process is modulated by numbers of factors. These internalins can act as adhesins, they can indirectly affect the exposure of InlA and/or InlB or they can directly interact with putative novel cellular receptors (Pizarro-Cerdá *et al.,* 2012). For example, InlJ, which is a LPXTG surface protein, is expressed by *L. innocua*. InlJ results in bacterial adhesion to human JEG-3 and HT29 polarized epithelial cells, however the cell ligand to which InlJ binds has yet to be determined. For full invasion of Caco-2 cells by the *L. monocytogenes* EGDe, it is necessary to have the gene cluster *inlGHE*. It has been hypothesized that expression of this gene cluster

may indirectly regulate the organisation of the cell wall of *L. monocytogenes*, therefore, affecting the presentation of InlA (Pizarro-Cerdá *et al.,* 2012).

The LPXTG-containing internalin, InlF does not influence the invasion of Caco-2 and HepG2 cells in-vitro under standard cell culture conditions or *in-vivo* during BALB/c mice infection (Dramsi *et al.,* 1997). However, it has been shown that inhibiting the RhoA/Rho kinase signaling pathway using the drug Y27632 in human HeLa and HEp-2 cells, leads to an increase in bacterial adhesion in an InlF-dependent manner (Kirchner and Higgins, 2008).

There are a number of internalins which are currently not fully understood and the roles of these internalins have not been determined, including InlI (Sabet *et al.,* 2005). InlC2 and InlD in the strain EGD are not involved in the invasion of Caco-2 or S180 cells *in-vitro* or in BALB/c mice *in-vivo* (Dramsi *et al.,* 1997). Surprisingly, along with InlA, these internalins are the main targets of the rabbit humoral response to *L. monocytogenes* (Yu *et al.,* 2007).

Moreover, InlC is included in secreted internalins and it plays an important role for *L. monocytogenes* infection as it enhances InlA function to invade the cell and promotes spread to neighbouring cells by promoting the formation of protrusions containing *L. monocytogenes* that invade into neighbouring cells (Ooi *et al*., 2006; Popowska *et al*., 2017).

Therefore, in summary, the repertoire of Internalins play a major role in the entry of *L. monocytogenes* into host cells. However, additionally, the factor listeriolysin LLO known to play a role in the intracellular life cycle of *L. monocytogenes* (see section 1.5.2.2) is also involved in invasion although it is not involved in bacterial association with host cells (Vadia *et al.,* 2011). The process by which LLO mediates entry is through perforation of the plasma membrane of the host cell, which activates internalisation of *L. monocytogenes* into human hepatocyte HepG2 cells and Hela cells (Vadia *et al.,* 2011). *In-vitro*, with a neutral pH condition, extracellular LLO perforates host cells and induces the formation of internalisation vesicles which can contain large particles, including bacteria or 1 μm beads. This process is modulated by a cholesterol-, dynamin-, and F-actin-dependent pathway, which is independent of the clathrin pathway (Vadia *et al.,* 2011).

1.5.2. Phagosome escape

After invasion, *L. monocytogenes* can persist in the phagosome before moving to the cytoplasm followed by replication (Quereda *et al*., 2016). It secretes two bacterial phospholipases, a specific phosphoinositol-PLC *(*PlcA) and a broad range phosphatidylcholine-PLC (PlcB)*,* both of which are important in acting with LLO to escape from the phagosome (Rabinovich *et al*., 2012; Quereda *et al.,* 2016).

1.5.2.1. Listeriolysin O (LLO)

LLO is secreted by *L. monocytogenes* and is encoded by the *hly* gene (Smith *et al*., 1995). It is a pore-forming toxin that forms a key virulence factor for the pathogenesis of *L. monocytogenes* (Dramsi and Cossart, 2002). LLO is a 58 kDa protein and is a member of the Cholesterol-Dependent Cytolysin (CDC) family that consists of 20 pore forming toxins with expressed by Gram-positive bacteria such as *Streptococcus*, *Clostridium* and *Listeria* (Ruan *et al*., 2016*)*. LLO is the only pore-forming cytolysin synthesised by an intracellular pathogen (Nguyen *et al.,* 2019) and its main capability lies in mediating lysis of the primary phagosome after the bacteria is taken into the cell (Gedde *et al.*, 2000). Moreover, LLO can also degrade the double-membrane secondary vacuole formed when the bacterium spreads from cell to cell (Gedde *et al.*, 2000). This was shown in an elegant study by Henry *et al.* (2006), where LLO was found to delay vacuole maturation and fusion of *L. monocytogenes*-containing vacuoles with LAMP-1 (lysosome-associated membrane protein-1)- positive lysosomes, thus highlighting the essential role of LLO in delaying vacuole-lysosomal fusion and in enabling escape of the pathogen to the cytosol (Henry *et al.,* 2006). The LLO-dependent delay in phagosomal maturation is caused by generation of lesions in the phagosome membrane that perturb the pH and calcium gradients. Induction of delayed vacuole maturation facilitates escape of *L. monocytogenes* and spread to other cells by increasing the amount of time the bacterium can reside inside these penetrable compartments. A vital component of *L. monocytogenes's* intracellular pathogenesis relies on its ability to prevent the lysosomal content from spilling over into the cytoplasm (which can be avoided if the pathogen escapes

prior to lysosomal fusion (Henry *et al.*, 2006). Thus, the maintenance of a habitable cytosolic environment and compartmentalisation of LLO activity to the phagosome plays a key role in preventing host cell cytotoxicity (Henry *et al.*, 2006).

There are two mechanisms through which LLO activity occurs within the endosomal environment to stop host cell lysis after bacteria have escaped from the vacuole into the cytosol. As a first step, it is pH sensitive and most active in low pH environments like those found in endosomes and phagosomes (Bavdek *et al.,* 2012). Secondly, LLO contains a PEST-like sequence near its N-terminus that is enriched in proline (P), glutamic acid (E), serine (S), and threonine (T) which interacts with host cell endocytosis machinery adaptor protein 2 and facilitates the removal of LLO and maintains the integrity of the plasma membrane, preventing premature lysis of the host cell (Chen *et al*., 2018). PEST-like sequences also undergo cysteine glutathionylation in the cytosol, which inhibits the activity of LLO (Portman *et al*., 2017). The presence of oxidoreductases in endosomes and phagosomes prevents cysteine glutathionylation and preserves the activity of LLO (Portman *et al*., 2017). This regulation of LLO is essential for *L. monocytogenes'* virulence because the infection would be recognized by the immune system if the host cell was damaged. During translation, expression of the LLO mRNA in the cytosol is restricted by rare codon usage in the PEST-encoding region and by the development of a ribosomal blocking secondary structure (Chen *et al*., 2018; Peterson *et al*., 2020).

Several studies have also elucidated that LLO carries out more functions before and after cell entry (Hamon *et al*., 2012; Pillich *et al.,* 2012). It contributes to reducing the DNA damage response (DDR) which is induced in the host in response to DNA damage (Samba-Louaka *et al.,* 2014). The inhibition of this response is critical for cytoplamisc replication by *L. monocytogenes* and inhibition of the DDR is achieved through the LLO-mediated degradation of the sensor protein Mre11 which crucial for the DDR (Samba-Louaka *et al.,* 2014). It can increase expression of cytokines and lead to inflammation as a consequence of inducing

histone modifications (Nguyen *et al.,* 2019). LLO participates in modulating the immune response by activating the mitogen-activated protein kinase (MAPK) (Witte *et al*., 2012). It is believed that the activation of the MAPK signalling transduction pathway promotes entry into epithelial cells, which in turn promotes the host immune response (Weiglein *et al.,* 1997). Infection of trophoblast giant cells during infection-associated abortion inhibits the MAPK signalling pathway (Hashino *et al.,* 2015). LLO also modulates the adaptive immune response. It can cause CD4+ T lymphocytes to become unresponsive by activating transcriptional factors that promote negative regulators of T-cell receptor signalling (Gekara *et al.,* 2010). The interaction of LLO with mitochondria causes mitochondria to fragment, resulting in visually punctate mitochondrial structures (Stavru *et al.,* 2013). The morphology of the lysosomes can also be affected by LLO. The infection disrupts the membrane around the lysosome leading to leakage of cathepsin into the intracellular fluid (Malet *et al*., 2017). In addition, it may affect the rate at which bacteria are phagocytosed by macrophages of the host. Treatment of macrophages with recombinant LLO compromised their ability to phagocytose *L. monocytogenes* (Moran *et al.,* 2022). Bacteria use LLO to coordinate their uptake of host cells and reduce internalization at high levels - thereby reducing the probability of replicative invasion by macrophages (Moran *et al.,* 2022).

1.5.2.2. Phospholipase C

L. monocytogenes produces two membrane-damaging phospholipases in addition to LLO that are specific for phosphatidylinositol- and phosphocholine- PI-PLC and PC-PLC respectively (La Pietra *et al.,* 2020). The highly specialised PI-PLC is a phospholipase that specifically cleaves phosphatidylinositol (Goldfine and Knob,1992) and allows *L. monocytogenes* to escape from primary vacuoles (Camilli *et al.,* 1993). On the other hand, PC-PLC is broad-range phospholipase capable of cleaving phosphatidylethanolamine (PE), phosphatidylcholine (PC), sphingomyeline (SM) and phosphatidylserine (PS) and can produce phosphocholine, phosphoethanolamine and phosphoserine (Geoffroy *et al.,* 1991; Goldfine *et al.,* 1993). PC-PLC expression allows cell-to-cell spread via secondary vacuole

escape, leading to spread of *L. monocytogenes* to neighbouring cells (Vazquez-Boland *et al.,* 1992). Produced as a pre-proenzyme, PC-PLC requires removal of its associated signal-peptide to exist as a proenzyme with a residue propeptide extension of 24 amino acids. The propeptide is cleaved with the help of Mpl, the metalloprotease of *L. monocytogenes* (Raveneau *et al*., 1992; Poyart *et al.,* 1993)

Paradoxically, both PI-PLC and PC-PLC have been shown to activate the phagocytic enzyme NADPH oxidase, which helps to kill phagocytosed bacteria. However, this activity is counteracted by the activity of LLO which inhibits the localisation of NADPH-oxidase in the phagosomes LLO (Lam *et al.,* 2011). Finally, bacteria are released from exofacial PS structures stimulated by LLO by phospholipase activity (La Pietra *et al.,* 2020). In this way, PC-PLC seems to both enhance LLO activity and inhibit membrane repair.

1.5.3. Cytoplasmic growth

Following the escape from the vacuole, *L. monocytogenes* reaches the cytoplasm and starts to multiply there. The cytosol is considered a suitable environment for the growth of bacteria. The LLO expressing *Bacillus subtilis* or *Escherichia coli* which is precoated with LLO can escape from vacuoles and survive in the cytoplasm of macrophage J774 cells or epithelial cells respectively (Bielecki *et al.,* 1990; Monack and Theriot 2001). However, they fail to replicate to the same level as cytosolic bacterial pathogens, which indicates that intracellular bacterial pathogens have specific metabolic adaptations for maximum bacterial growth inside the cell (O'Riordan and Portnoy, 2002).

L. monocytogenes is greatly adapted to the cytoplasm of host cells in mammals, where the major carbon sources used during intracellular growth are di-hydroxyacetone, glycerol and phosphorylated carbohydrates (Fuchs *et al*., 2012; Lobel *et al*., 2012). Using these substrates as a carbon source is due to their availability in the cytosolic niche (Lobel *et al*., 2012). *L. monocytogenes* can use ethanolamine, ammonium or/and arginine as sources of nitrogen for intracellular replication while it uses intracellular peptides as a source of amino acids (Fuchs *et al*., 2012). During growth in the host cell cytosol there is increased expression of the PrfA

regulon a consequence of which is the increased expresson of Hpt a glucose 6 phosphate (G6P) transporter, loss of which, impairs intracellular growth indicating the importance of G6P as intracellular carbohydrate source (Joseph *et al.,* 2006).

1.5.4. Cell to cell spread

ActA is a dimeric envelope protein located at the pole of the cell comprising 639 amino acids with a C-terminal transmembrane motif that acts as an anchor to the bacterial cell wall (Cossart and Lecuit, 1998). The N-terminal, on the other hand, contains necessary information to initiate F-actin assembly and Listerial intracellular movement within the host cell cytoplasm (Cossart and Lecuit, 1998; Shetron-Rama *et al.,* 2002; Travier and Lecuit, 2014).

The ActA protein mimics the actin-nucleating function of Wiskott-Aldrich syndrome protein (WASP), with both proteins containing a VCA (verprolin homology, cofilin homology and acidic) region. Both ActA and WASP proteins are capable of recruiting and activating the multimeric Arp2/3-complex. The VCA region of the ActA N-terminal activates the Arp2/3 complex by allowing the complex to bind to ActA via the cofilin homology region (Pizarro-Cerdá and Cossart, 2006).

The acidic region enhances actin nucleation efficiency, motility rate and has also been suggested to form a second Arp2/3 binding site. Furthermore, ActA interacts with ATP-G actin through the actin-binding region, although this interaction is not essential for infected cell motility (Lambrechts *et al,* 2008). The central ActA region has four proline-rich repeats containing FPPIP or FPPPP motifs capable of mimicking proteins such as vinculin, paladin and zyxin found in the cytoskeleton of the host cell. These proteins are further associated with focal adhesions and stress fibres (Reviewed by Lambrechts *et al,* 2008).

ActA binds to a domain of VASP protein (Vasodilator-stimulated phosphoprotein) called the EVH1 (Ena/VASP homology domain 1) through this central region to control the geometry of the network via the Arp2/3 complex (Figure 1.6) (Samarin *et al.,* 2003; Trichet *et al*., 2007).

VASP protein is found at sites of actin polymerisation and can recruit profilin and actin monomers to the Act-A N-terminal. VASP can also interact with F-actin through its EVH2 domain at the C-terminal, thereby linking *L. monocytogenes* to the actin tail (Cossart and Bierne, 2001).

Actin comet tail formation and motility of *L. monocytogenes* depends upon the polarized distribution of ActA. ActA becomes localised at one distal end and partly to the sides of the bacterium due to a combination of non-polarized secretion and continuous septal cell wall growth (Rafelski and Theriot, 2006). As a result of this polarisation, the actin cloud's symmetry breaks owing to the accumulation of F-actin along the sides of the bacterium that eventually move to the pole during tail-formation (Rafelski and Theriot, 2005).

The *actA* knockout mutant (*ΔactA)* of *L. monocytogenes* can escape from the vacuole, growing in the cytosol in the form of microcolonies in the perinuclear area, with this growth not involving intracellular movement or spread to neighbouring cells (Vázquez-Boland *et al.,* 2001). The role of ActA on *L. monocytogenes* is not only exclusive in the motility of the pathogen inside the host cell but also it includes a role in helping intracellular *L. monocytogenes* avoid the autophagic pathway (Dortet *et al*., 2012). The same study reported that mutants lacking ActA produced faster autophagic identification and lysis for the bacterium by selective receptor p62; this led to decreasing of the pathogen survival compared with wild-type bacteria (Dortet *et al*., 2012). Also, the recruitment of the Arp2/3 complex, Ena/VASP and actin proteins to the surface of the bacterium allow it to be camouflaged against the host's autophagy recognition and killing pathways (Yoshikawa *et al.,* 2009).

ActA has also been shown to play critical role in mediating aggregation and biofilm formation through ActA-ActA interactions directly. It is belived to be important in the lumen of the intestine to promote persistence in the cecum, the colon and fecal shedding (Travier and Lecuit, 2014). ActA is also implicated in invasion of host cells through actin cytoskeleton

rearrangement and the formation of pseudopods that facilitate effective invasion of host cells (Suárez *et al.,* 2001).

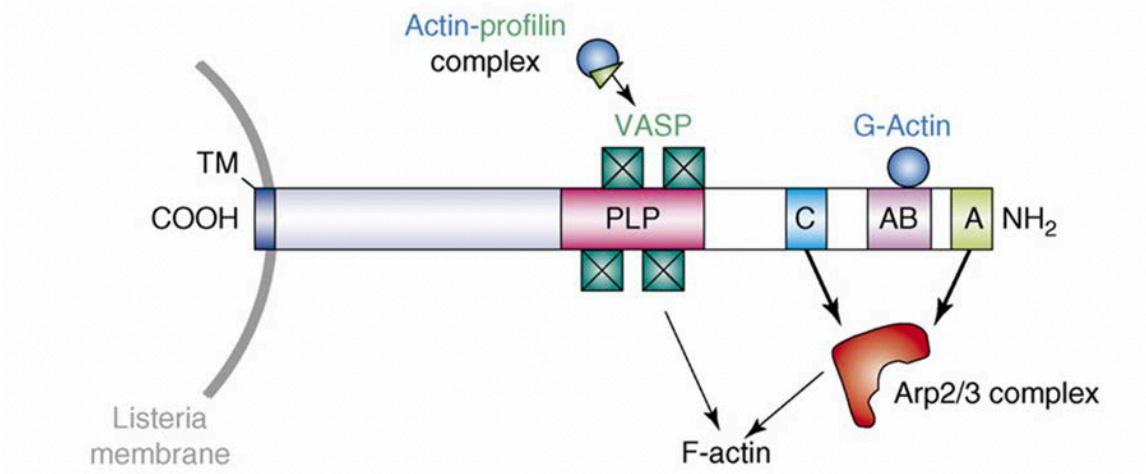

Figure 1.6 Domain organization of the ActA protein, its presentation on the bacterium, and the target sites for host cell proteins. The N-terminal part (residues 1–293) of bacterially presented ActA contains the following domains: A, acidic region; AB, actin-binding region, C, cofilin homology region. The central region (residues 293–390) is the polyproline region (PLP). The transmembrane domain (TM) spans residues 614–639. Taken from (Lambrechts *et al,* 2008).

1.6. Regulators important in infection and response to stress

1.6.1. PrfA Regulon

PrfA belongs to Crp/Fnr family of bacterial transcription activators (Freitag and Portnoy, 1994). It is a 27 kDa homodimeric protein with each individual protein having a substrate binding domain at the N-terminus and a DNA binding domain at the C-terminus (Scortti *et al*., 2007). Activation of transcription by PrfA is achieved by the binding of PrfA to a 14 bp nucleotide sequences (PrfA box) which is located at 40 bp upstream from the transcription start site of PrfA regulated genes (de las Heras *et al*., 2011).

PrfA is the master regulator of virulence gene expression in *L. monocytogenes* with a number of genes essential for virulence being part of the PrfA regulon (*inlA, inlB, inlC, hly, plcA, plcB, actA* and *hpt*) (See figure 1.7) (Milohanic *et al.,* 2003). Therefore, *L. monocytogenes prfA* mutants are avirulent (Rolhion and Cossart, 2017). In order for *L. monocytogenes* to

successfully infect the host, it needs to ensure that expression of each gene regulated by PrfA is adequately controlled. Failure to do so can affect the viability of the bacteria (Bruno and Freitag, 2010).

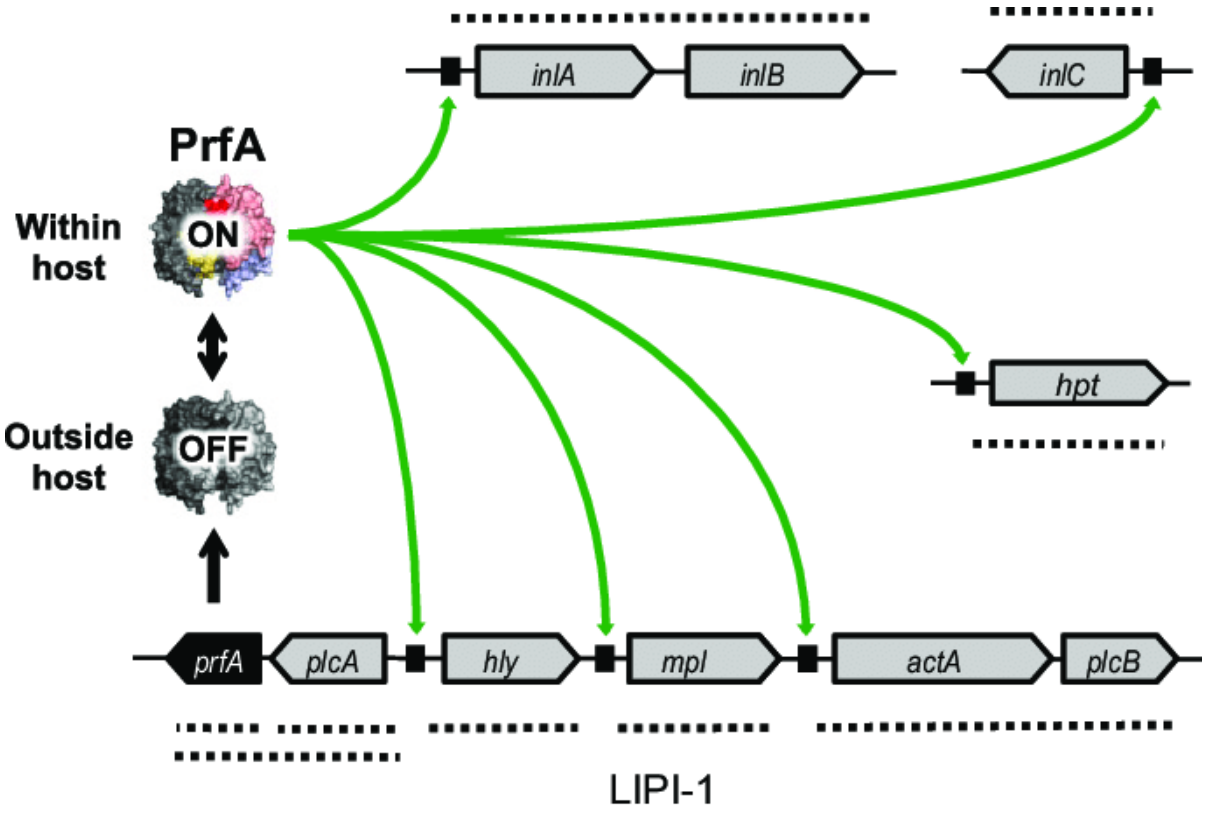

Figure 1.7 Schematic of *L. monocytogenes* PrfA virulence regulon and ON–OFF PrfA switching. Dotted lines indicate relevant transcriptional units. The filled black boxes denote the PrfA binding sites and LIPI-1 is the listeria pathogenicity island. Taken from (Vasanthakrishnan *et al.,* 2015).

Proteins encoded by the PrfA regulon function to facilitate survival and proliferation within cells and between cells. The majority of PrfA-dependent genes responsible for the functions are encoded within a pathogenicity island known as PrfA island or listeria pathogenicity island 1 [LIPI-1] (Camejo *et al*., 2011). Genes regulated by PrfA all have a PrfA box and are each expressed at different times and in different intracellular niches (Shetron-Rama *et al.,* 2002; Gaballa *et al.,* 2019). For an example, *hly, plcA, and plcB* are the genes responsible for enabling escape from the phagosome and they are expressed inside the vacuole of the host

while the gene responsible for actin-dependent motility, *actA,* is predominantly expressed in the cytoplasm. The regulation of transcription of genes by PrfA depends on the following: i) PrfA protein levels ii) PrfA activity iii) the conservation of the PrfA box in the promoter region of PrfA regulated genes (Shetron-Rama *et al.,* 2002; Gaballa *et al.,* 2019). The PrfA binding site plays an important role in the expression of PrfA regulon because when the PrfA box has greater identity to the canonical consensus sequence, PrfA mediated activation may occur at lower levels of PrfA (Scortti *et al*., 2007). For the *L. monocytogenes* infection process to be efficient, it is particularly important that the genes for virulence be tightly controlled, at different times and in different spaces (Bruno and Freitag, 2010; Vasanthakrishnan, 2015). Regulation of PrfA activity is composed of three levels: transcriptional, post-transcriptional and post-translational control.

1.6.1.1. Transcriptional regulation of the *prfA* gene.

Transcriptional regulation of *prfA* expression occurs via three separate promoter elements: two are located close to *prfA* (*P1prfA* and *P2prfA*), one is located relatively far from the *prfA* gene *(P3prfA)* (Gaballa *et al.,* 2019). *P1prfA* is regulated by sigma factor σ^A whereas *P2prfA* is regulated by both σ^A and the stress sigma factor σ^B; *P3prfA*, which is the only promoter upstream from *plcA*, represents a σ^A-dependent promoter with an upstream canonical perfect PrfA box (de las Heras *et al.,* 2011). Evidence from *in-vivo* models suggests that both the σ^A and σ^B-dependent *P1prfA* and *P2prfA* promoters are not required for full virulence. For example, mice infected with *L. monocytogenes* strains containing deletions of either *P1prfA* or *P2prfA* are still fully virulent. The presence of at least one of the promoters is required for full bacterial virulence (Freitag and Portnoy,1994).

The *P1prfA* and *P2prfA* promoters regulate the expression of a monocistronic *prfA* transcript which leads to the synthesis of enough PrfA protein to activate the expression of *hly* and *plcA* promoters (Gaballa *et al.,* 2019). The gene products of *hly* and *plcA* are required for the movement of *L. monocytogenes* from host cell phagosomes (Freitag and Portnoy,1994). PrfA

activates the promoter *P3prfA* which controls the production of the *plcA–prfA* transcripts which results in an increase in PrfA synthesis which is critical for the expression of *actA* (Gaballa *et al.,* 2019). The expression of *actA* is important for actin-based intracellular motility of *L. monocytogenes,* (see section 4.5) therefore, the cell-to-cell transmission of this bacteria (Freitag and Portnoy,1994).

1.6.1.2. Post-transcription regulation of PrfA

After transcription, expression of PrfA, depends on an RNA-based mechanism such as siRNA and a riboswitch that play a role in regulating the post-transcriptional expression of PrfA. The 5'-UTR region of the *P1prfA* -directed mRNA is a thermosensor riboswitch which forms a stem-loop structure at temperatures of 30°C or lower. This riboswitch masks the Shine-Dalgarno (SD) sequence necessary for translation of the *prfA* transcript thereby inhibiting translation (Johansson *et al*., 2002). At temperatures of equal to or above 37°C, the stem-loop becomes unstable and undergoes a conformational change exposing the SD sequence and allowing efficient translation (NicAogáin and O'Byrne, 2016).

It has been shown that S-adenosylmethionine responsive riboswitches are also critical in post transcription regulation with both SreB and SreA contributing to the regulation of *prfA* (Loh *et al*., 2009). Binding of S-adenosylmethionine to a riboswitch leads to early transcriptional termination and the creation of small RNAs 100-250 nucleotides long. The interaction between SreA with *prfA* 5′-UTR reduces *P1prfA*-directed mRNA translation through unknown mechanism. However, this can happen only when the thermosensor is in a melted state and the ribosomal binding site is exposed (Loh *et al*., 2009). Therefore, the 5′ UTR of p*rfA* appears to function as both a thermometer and a metabolism sensor, both of which are integrated through S-adenosylmethionine signalling (Johansson and Freitag, 2019).

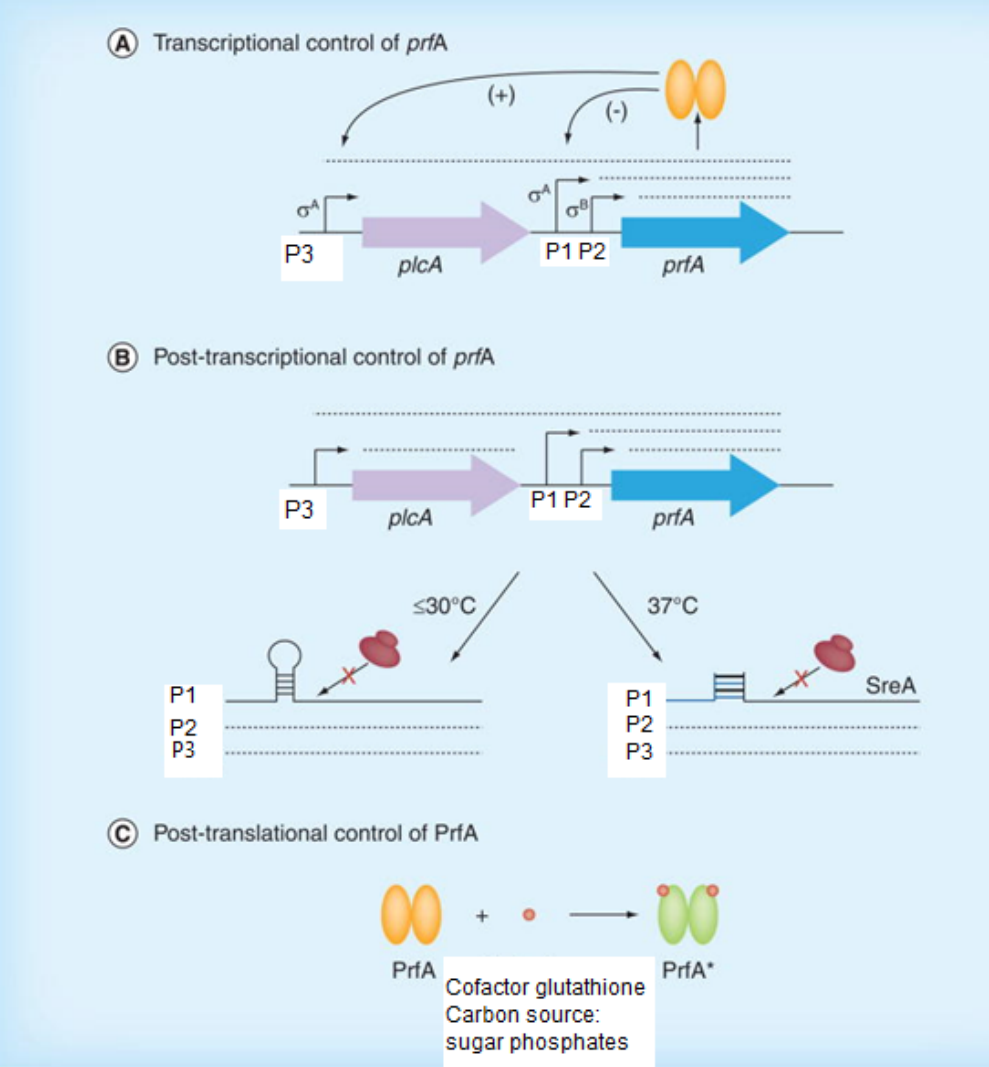

Figure 1.8 Multiple regulatory check-points control *prfA* expression and protein activity. Regulation of PrfA activity in facilitating *L. monocytogenes* survival within host cells is composed of three levels: transcriptional, post-transcriptional and post-translational control. **(A)** Transcriptional control of *prfA* expression is mediated by the presence of three separate promoter elements. *prfA*P1 (P1) and *prfA*P2 (P2) are located immediately upstream of *prfA*, and both direct monocistronic transcripts of *prfA*. The *prfAP3 (P3)* promoter is located upstream of *plcA* and directs both a monocistronic *plcA* transcript and a bicistronic *plcA* and *prfA* transcript. *prfA*P1 and *prfA*P2 are responsible for maintaining basal levels of PrfA protein, but both promoters are negatively (-) influenced by high levels of PrfA, whereas *prfAP3* is positively (+) influenced, resulting in the production of the bicistronic mRNA to generate the high levels of PrfA required for intracellular growth and spread. **(B)** Post-transcriptional control of *prfA* expression involves the presence of a thermosensor riboswitch in the 5′ untranslated region of the *prfA*P1-directed mRNA promoter region that forms a stem-loop structure at temperatures of 30°C or lower. This stem-loop structure effectively masks the *prfA* mRNA

ribosome-binding site to inhibit PrfA protein synthesis. At higher temperatures (37°C), the thermosensor stem-loop is destabilized; however, a *trans*-acting S-adenosyl methionine-responsive riboswitch (SreA) is then able to bind to a complementary region in the *prfA* transcript in the *prfA*P1 promoter region to inhibit translation and reduce PrfA protein synthesis. **(C)** Post-translational modification of PrfA is required to fully activate PrfA within the host. Binding of a small-molecule cofactor glutathione which induces structural changes that activate PrfA and that are associated with the high levels of PrfA-dependent virulence gene expression required for survival within the host. Adapted from (Xayarath, and Freitag, 2012).

1.6.1.3. Post-translational regulation of PrfA expression

The post-translational activation of PrfA occurs when it binds to the cofactor glutathione, which stabilizes the DNA-binding HTH motif (Reniere *et al*., 2015; Hall *et al*., 2016). This stabilization creates a confirmation of the protein which is compatible with DNA-binding, therefore, PrfA-regulated virulence factors can be expressed (Hall *et al*., 2016). The expression of PrfA regulated genes are also affected by the carbon source. When *L. monocytogenes* is grown in media containing sugars that are taken into the cell via the phosphoenolpyruvate phosphotransferase system (PTS) such as cellobiose and glucose, the expression of PrfA-regulated genes is inhibited (Hansen *et al*., 2020). It was reported that in PTS-dependent sugar transport, phosphoryl groups are transferred from Enzyme IIA (EIIA) to EIIB, leaving EIIA unphosphorylated. Through an unknown interaction with PrfA, EIIA sequesters its activity in its unphosphorylated state (Freitag *et al.,* 2009). In contrast, when *L. monocytogenes* are grown in LB medium supplemented with non-PTS sugars carrying a phosphate group, such as sugar phosphates, PrfA-regulated gene products are not repressed (Ripio *et al.,* 1997; Chico-Calero *et al*., 2002). Examples of sugar phosphates include: glucose-1-phosphate (G-1-P), mannose-6-phosphate (M-6-P), glucose-6-phosphate (G-6-P), and fructose-6-phosphate (F-6-P). Uptake of sugar phosphates occurs through the Hpt transporter, while uptake of glucose and cellobiose occurs through the PTS. It is thought that activated PTS represses PrfA activity, however, how this occurs is not fully understood (Chico-Calero *et al*.,

2002). It is therefore critical for bacteria because they use it to sense their environment via the availability of different sugars.

1.6.2. SigmaB factor (SigB)

Sigma factors are proteins that recognize the promoter sequence where RNA polymerase will attach to in order to start transcription. There are several types of sigma factors that are responsible for the transcription of different genes. One of them is the SigB factor. SigB factor is an alternative sigma factor that works in the transcription of genes necessary to regulate the stress response of many Gram-positive bacteria (Tuchscherr *et al.,* 2015). It is important in bacterial survival since it enables them to become resilient in stressful environments (Tuchscherr *et al.,* 2015). Examples of environmental stresses that might trigger the activity of the SigB factor are oxidative, antibiotic, and heat stresses (Tuchscherr *et al.,* 2015). When subjected to these stresses, the activity of the SigB factor increases (see below).

The SigB factor operon is composed of the *sigB* gene, which encodes the SigB protein, and several *rsb* genes, which encodes Rsb proteins that are involved in the regulation of the SigB factor activity (Kazmierczak *et al*., 2005). The number and kinds of Rsb proteins are different in every bacterium; however, RsbV and RsbW proteins are present in all the bacterial species with SigB factor (Kazmierczak *et al*., 2005). The binding of RsbV to the RsbW protein determines whether SigB protein will be active or not and whether transcription of the *sigB* gene will occur. When a cell is not in a stressed state, the RsbV protein, an anti-anti-sigma factor, is in a phosphorylated state; thus, it cannot bind to the RsbW protein. In this case, the RsbW protein, which is an anti-sigma factor, binds to the SigB protein, preventing its attachment to the RNA polymerase, and inhibiting the transcription of the sigB regulon. When the cell becomes stressed, the RsbV protein is dephosphorylated by a phosphatase, allowing it to bind to the anti-sigma factor, RsbW. When this happens, RsbW will not be able to bind to the SigB protein. Since the SigB protein becomes unrestricted, it becomes available for the attachment of RNA polymerase, allowing the transcription of the sigB regulon to take place (Dorey *et al*., 2019).

In addition, the sigB operon of *L. monocytogenes* consists of a stressosome containing the *rsbR*, *rsbS* and *rsbT,* and a downstream signaling pathway containing the *rsbU, sigB,* and *rsbX* genes (Dorey *et al*., 2019). The stressosome senses stress signals through the N-terminal part of the RsbR protein, which extends out into the cell (Dorey *et al*., 2019). This protein has four paralogues: Lmo0161, Lmo0799, Lmo1642, and Lmo1842; however, the roles of these paralogues are not yet clear except for Lmo0799, which works in blue light sensing (Dorey *et al*., 2019).

L. monocytogenes is known to have extreme resistance to harsh environments. It can tolerate high osmotic pressure, intense acidity, oxidative stress, hydrostatic pressure, and low temperature (Liu *et al.,* 2017). To add to that, it is resistant to the activity of bile and some antibiotics (Liu *et al.,* 2017). These characteristics of the bacterium involve the action of the SigB factor which has the largest set of genes in its regulon for mounting the stress response of *L. monocytogenes* (Liu *et al.,* 2017). There are 105 transcription units that are dependent on the SigB and these transcription units that include 201 genes most of which are necessary for the homeostasis, repair, and defence of the cell (Liu *et al.,* 2017).

One of the environmental stresses that *L. monocytogenes* encounters is osmotic pressure. Osmotic inhibition is a method used in food processing as a means of preservation; however, *L. monocytogenes* can tolerate as much as 18 % (w/v) salt concentration (O'Byrne *et al.,* 2008). One of the mechanisms involved in the osmotic regulation within the bacterium is the uptake of compatible solutes such as betaine and carnitine. The occurrence of the carnitine transport system is dependent on the activity of a transporter called OpuC, which is encoded by an operon containing the *opuCA, opuCB, opuCC*, and *opuCD* genes (O'Byrne *et al.,* 2008). SigB plays a role in osmotic response by initiating the transcription of the *opuCA* gene (O'Byrne *et al.,* 2008). Likewise, *gbuAP2* gene, which is involved in betaine transport, is also dependent on the SigB (O'Byrne *et al.,* 2008). Aside from osmotic pressure, an acidic environment is also often encountered by *L. monocytogenes,* especially as it enters the human digestive tract. Among its numerous stress response mechanisms against acid-induced

stress, three systems necessitate the use of SigB factor – the glutamate decarboxylase (GAD) system, the arginine deaminase system, and the adaptive acid tolerance response (ATR) (Dorey *et al*., 2019). SigB regulates the GAD system by promoting the transcription of the *gadB*, *gadC,* and *gadD* genes, which are important players in the accumulation of glutamate-γ-aminobutyrate (GABA) antiporter, reducing the acidity inside the cell (Dorey *et al*., 2019). In the arginine deiminase (ADI) system, SigB is involved in the transcription of the *arcA* and the *argR* genes (Ryan *et al.,* 2009). The *argR* gene encodes for ArgR, which is a putative transcriptional regulator of ADI, while the *arcA* gene is part of ADI operon (Ryan *et al.,* 2009). SigB factor also acts to promote transcription of *lmo0515, lmo1580,* and *lmo2673* genes, that encode three universal stress proteins which are involved in resistance to oxidative stress (Seifart Gomes *et al.,* 2011). There was an impaired ability of *L. monocytogenes* deletion mutations of these genes to tolerate H_2O_2 (Seifart Gomes *et al.,* 2011). Other stress responses that involve the activity of SigB are thermal stress, where it promotes the activation of the Class II heat shock response and cold stress (Bucur *et al*., 2018). Its activity also affects hydrostatic pressure by regulating the production of ClpP and Csp1 proteins. In antibiotic resistance (bacteriocin, ampicillin, and penicillin), SigB controls the transcription of *htrA (lmo0292)* gene involved in penicillin G tolerance and *mdrL (lmo1409)* gene involved in antibiotic efflux (Gaballa *et al.,* 2019). Lastly, it regulates the expression of the *bile* operon that acts in bile transport, *bhs* gene that encodes for bile salt hydrolase, and *pva* gene that also contributes to bile tolerance essential for successful transit in the host's small intestine (Wemekamp-Kamphuis *et al*., 2004; O'Byrne *et al*., 2008; Bucur *et al*., 2018).

As such, mutations in the *sigB* gene affect the activity of the above-mentioned response systems. For example, *L. monocytogenes* with *ΔsigB* mutation showed impairment in betaine accumulation important in osmotic shock response (Dorey *et al*., 2019). The same mutation also displayed a lack of Lmo0913 protein resulting in obstruction to GABA accumulation as well as inhibited induction of GalE, ClpP, and Lmo1580 proteins, all of which play a role in acid-induced stress response (Dorey *et al*., 2019). Likewise, *L. monocytogenes* with

ΔsigB mutation exhibited sensitivity to oxidative stress, cold environment, and hydrostatic pressure (Dorey *et al*., 2019). Aside from that, a *ΔsigB,* mutation resulted in increased sensitivity to penicillin G, tetracycline HCl, erythromycin, rifampicin, and gentamicin sulfate compared to the wild type strain (Wang *et al*., 2014). Lastly, a mutation in *sigB* causes a considerable reduction in transcription of the *bilE* operon resulting in intracellular accumulation of bile (O'Byrne *et al*., 2008). Therefore, *L. monocytogenes* cannot survive and spread in the gastrointestinal tract without SigB.

1.7. *L. monocytogenes* in transit in the gut

1.7.1. Short Chain Fatty Acid (SCFA)

1.7.1.1. Mechanisms of SCFAs production

Microorganisms found in the gut are capable of producing metabolites such as SCFAs by breaking down fibre and carbohydrates that are not digestible such as resistant starch, cellulose, inulins and xylans and this fermentation process is performed by anaerobic bacteria found in the colon thus yielding SCFAs and gas (Cummings *et al.,* 1987). This means that the quantity of substrate available for fermentation is a factor that can affect yield of SCFAs.

For illustration, when 50-60 g of carbohydrates are fermented in the large intestine, an average of 500-600 mM SCFAs are produced *ex vivo* and constituting 10 % of host's energy source (McNeil, 1984). The foremost SCFAs produced are propionate, acetate and butyrate with 3 carbon, 2 carbon and 4 carbon respectively accounting for up to 95 % of all SCFAs in the gut (Rinehart, 2020). They are in acid form and serve as electron acceptors in the large intestine (Rinehart, 2020) and are believed to play roles in the maintenance and normal functioning of the digestive system and the overall health condition (Ríos-Covián *et al.,* 2016).

SCFA are not just produced in the large intestine, but also in the human distal ileum where the concentrations of propionate, acetate and butyrate are 2.25, 25.5 and 2.25 mM respectively, although lower than found in the colon where the levels of propionate, acetate and butyrate are 70, 110, and 20 mM respectively (Neanover, 2020). A variety of animal

species and diets can affect these concentrations (Neanover, 2020). Elevated levels of SCFAs reduce the growth and colonization of *Salmonella. typhimurium* in the gastrointestinal tract, whilst low levels of SCFAs enhance the expression of *S. typhimurium hilA* gene which increases invasion and host susceptibility (Lawhon *et al*., 2002). Therefore, SCFA may affect bacterial pathogenesis.

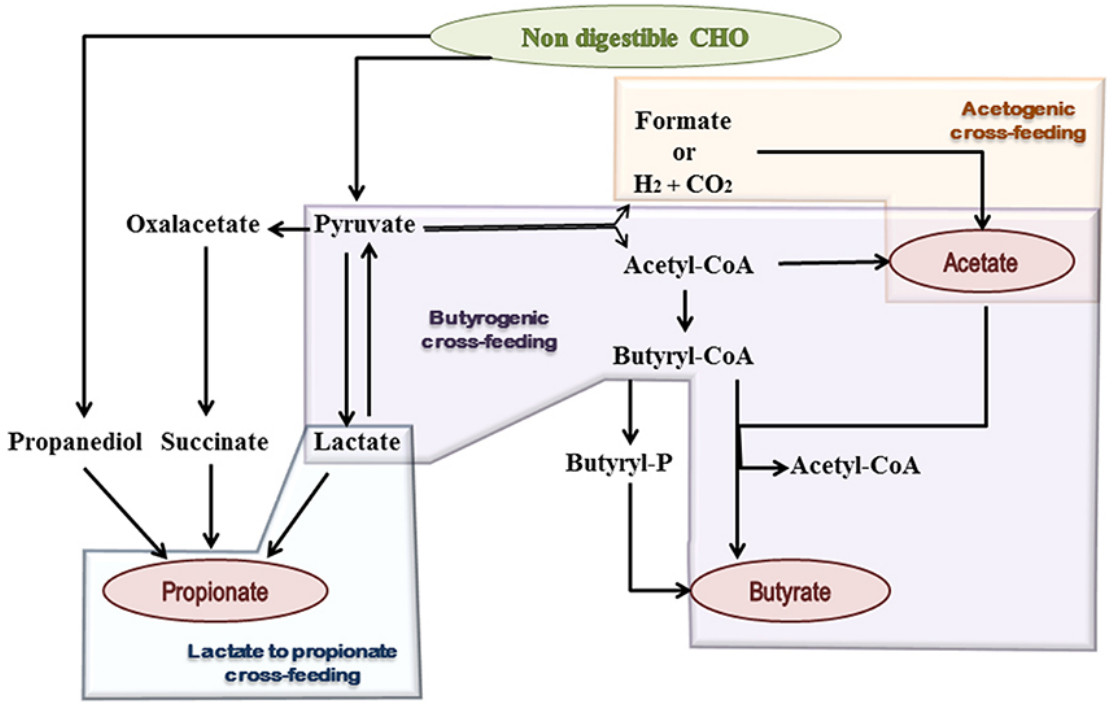

Figure 1.9 Schematic representation of microbial metabolic pathways and cross-feeding mechanisms, contributing to SCFA formation in the human gut. Shaded geometric shapes summarise routes of SCFAs production for each one butyrate, propionate and acetate. Taken from (Ríos-Covián *et al.,* 2016).

1.7.1.2. Biological effects of SCFAs in the host organism

When SCFA is produced, the environment within the small intestine becomes acidic. This helps to impede disease-causing microorganisms and allow nutrients to be absorbed (Macfarlane and Macfarlane, 2012). Bifidobacterium produces acetate which plays a major role in inhibiting pathogens in the small intestine (Fukuda *et al.,* 2011). The actions of butyrate on epithelial cells help to hinder bacterial attachment and foster the cohesion between cells and maintain integrity (Peng *et al*., 2009; Jung *et al*., 2015). It has been shown that butyrate

treatment led to an increase in mucin protein production in LS174T cells in a dose-dependent manner with the peak increase between 6 to 9 mM of treatment (Jung *et al*., 2015). Moreover, butyrate treatment resulted in higher levels of MUC3, MUC4, and MUC12 transcriptional levels, accompanied by higher gene expression of signaling kinases and transcription factors (Jung *et al*., 2015). The increase in mucus and mucin protein will effectively increase the coating of epithelial cells making it harder for pathogens to adhere. In addition, this increase in mucus resulted in elevated adherence of probiotics, which subsequently reduced the adherent ability of *E. coli* (Jung *et al*., 2015).

Furthermore, butyrate and propionate play a role in regulating the host immune system. Butyrate and propionate enter immune cells through the sodium transporter SLC5A8 (Singh *et al.,* 2010; Zimmerman *et al.,* 2012). These SCFAs have immunomodulatory effects by blocking dendritic cell development and by activating Fas to induce apoptosis of T cells (Sun and O'Riordan, 2013). This occurs through Fas-FasL interactions such that an immune response is terminated after clearing pathogen-infected or diseased cells (Zimmerman *et al.,* 2012). Butyrate also affects expression of certain interleukins, for example, butyrate decreases the production of interleukin-12 (IL-12) and increases the production of interleukin-23 (IL-23) due to the activation of dendritic cells (Berndt *et al.,* 2012). This demonstrates the potential importance of the SCFA synthesised by the gut microbiota (Berndt *et al.,* 2012).

The production of SCFAs by endogenous gut microbiota stimulates the synthesis of host antimicrobial peptides (AMPs) which prevent enteric pathogens attaching to and invading the intestinal epithelium (Gallo and Hooper, 2012). One example of this is the induction of the expression of the AMP, LL-37, which is induced by microbiota derived SCFAs (Termén *et al.,* 2008; Gallo and Hooper, 2012). Generally, antibiotics are used in animal feed to reduce the spread of infection and reduce colonization by human pathogens (Sun and O'Riordan, 2013). Studies have shown that introducing exogenous SCFAs in feed led to a reduction in Salmonella in the cecum of the large intestine (Sunkara *et al.,* 2011; Sunkara *et al.,* 2012).

Therefore, including exogenous SCFAs in animal feed or pre-biotics which induce SCFA production through the microbiota, may be a suitable alternative to antibiotics.

Furthermore, investigations have shown that butyrate can reduce the incidence of cancer, with diets high in fibre reducing the risk of colonic cancer (Tang *et al*., 2011). A study using murine models showed that a high-fibre diet led to a decrease in tumours by 75 % and this effect was seen in gut produced butyrate (Neanover, 2020). A combination of butyrate and gut microbiota effectively reduced tumour formation, whereas using them individually could not suppress tumour formation (Donohoe *et al*., 2014). The anti-inflammatory properties of the SCFAs: butyrate, propionate, and acetate mean that they are utilised as treatments for inflammatory disorders of the digestive system (Neanover, 2020). Patients treated with SCFA supplements such as acetate and butyrate showed improved symptoms of the following disorders: diarrhoea, Cron's disease, and ulcerative colitis. Moreover, patients with reduced SCFAs described having worse ulcerative colitis symptoms (Vieira *et al.,* 2012).

1.7.1.3. Biological activities of SCFA in bacteria

In addition to affecting host function, SCFAs are also a carbon source for endogenous gut microbiota (Fischbach and Sonnenburg, 2011). High levels of SCFAs can induce toxic effects on bacteria. This toxicity has been attributed to the non-ionized forms of these acids, that exist primarily at a low pH (Sun and O'Riordan, 2013). Non-ionized acids are uncharged and small and therefore are able to diffuse freely across the bacterial membrane and it is the entry of non-ionized acids into the bacteria cytoplasm that is the mechanism by which SCFAs elicit toxicity. Bacterial cytoplasm has a circumneutral pH, however, upon entry of non-ionized acids into the cytoplasm these acids dissociate into protons and SCFA anions (Sun and O'Riordan, 2013). This accumulation of protons acidifies the cytoplasm and dissipates proton motive force (Axe and Bailey, 1995). The effects of this include altering metabolic reactions and energy conservation (Roe *et al.,* 2002). The increase of SCFA anions, significantly affects the cellular physiology, by altering processes such as osmotic homeostasis (Roe *et al.,* 2002).

Diffusion of SCFAs into bacteria and their subsequent toxicity are strongly determined by the external pH, which indicates the amount of non-ionized SCFA which are present (Raven and Beardall, 1981). Consequently, the toxicity of SCFAs increases in acidic conditions, during which the pKa value for the SCFA acetate 4.76, butyrate 4.82 and propionate 4.87 are equal to or higher than the external pH. Internal pH also influences SCFA-mediated toxicity by affecting the transmembrane pH gradient which leads to the influx of acid (Sun and O'Riordan, 2013). The intrinsic impermeability of the bacterial membrane to protons, results in a fairly resistant bacterial cytoplasm to pH perturbation (Raven and Beardall, 1981). In addition, the buffering capacity of ionizable moieties such as amino acid side chains also help to protect the cytoplasmic pH (Booth, 1985; Slonczewski *et al.,* 2009). Despite this, there are several adaptive mechanisms which actively maintain the intracellular pH, one such example being proton transporters (Booth, 1985). Some organisms maintain a neutral pH, therefore, when their external pH is low, this leads to a high transmembrane pH gradient. This enhances acid influx and increases the chances of experiencing SCFA toxicity compared with organisms which can tolerate lower intracellular pH (Russell, 1991; Diez-Gonzalez and Russell, 1997).

SCFA-induced toxicity generally leads to growth inhibition due to pleiotropic effects on cellular processes (Cherrington *et al*., 1990). Growth inhibition is likely to differ depending on the metabolic pathway, organism and the environmental conditions. Examples of this include the synthesis of DNA, which is more susceptible to toxicity by propionate than synthesis of RNA, proteins, lipids and cell walls in *E. coli* (Cherrington *et al*., 1990). Another example is the uptake of amino acids in *B. subtilis*, which is inhibited following acetate and propionate treatment (Freese *et al.,* 1973). In contrast with this, after acetate treatment, some amino acid transporters were found to be more abundant in *E. coli* (Kirkpatrick *et al.,* 2001). This implies that cellular and metabolic responses to SCFAs may differ between organisms. The same study showed a different proteomic response following acetate treatment when the environmental condition was minimal medium instead of rich medium. Again, suggesting the environmental condition plays a role in determining the proteomic response to SCFAs in bacteria (Kirkpatrick *et al.,* 2001).

1.7.1.4. Virulence regulation of *L. monocytogenes* by SCFA

There is very little knowledge about the role of the level of SCFAs and what effects SCFAs may play in individual susceptibility to *L. monocytogenes* infections. Butyrate, propionate and acetate have been shown to inhibit the expression of LLO by *L. monocytogenes*, an activity mediated due to the loss of branched chain fatty acids (BCFAs) in the cell membrane (Sun *et al*., 2012). The membrane fatty acid of *L. monocytogenes* is composed of almost 90 % anteiso-BCFAs, in specific anteiso-$C_{15:0}$ and $C_{17:0}$ when it is produced under standard conditions at 37 ºC in the laboratory (Rinehart *et al*., 2020). The branched chain alpha-keto acid dehydrogenase complex (BKD) acts as a catalyst in the synthesis of BCFAs. It is an enzyme complex dependent on lipoic acid-and responsible for formation of the branched chain amino acid-derived substrates for the synthesis of BCFA (Kaneda,1991). Transposon insertion mutants of BKD lead to a decrease in the levels of BCFAs and showed extremely compromised in fitness phenotypes and the production of LLO (Rinehart *et al*., 2020).

Another study analyzing the effects of propionate on *L. monocytogenes* under both aerobic and anaerobic conditions showed that LLO production is sensitive to regulation by exogenous propionate such that aerobic propionate exposure caused dose-dependent decrease in the production of LLO while in contrast anaerobic propionate exposure resulted in a dose-dependent increase in the production of LLO (Rinehart *et al*., 2018). In addition, overall BCFA levels decreased *when L. monocytogenes* are treated with propionate under both aerobic and anaerobic conditions. Supplementations of SCFA mixtures under aerobic conditions do not cause a significant decrease in *hly* transcription whereas SCFA supplementations at the low levels (2.25 mM butyrate, 2.25 mM propionate, 25.5 mM acetate) under anaerobic conditions lead to a significant increase in *hly* transcription (Rinehart *et al*., 2020). Moreover, supplementations of individual SCFAs under anaerobic conditions caused a significant increase in *hly* transcription. It clearly shows that the general loss of BCFAs upon exposure to butyrate or propionate is not the only system that mediates the regulation of LLO production (Rinehart *et al*., 2020). Furthermore, these findings show a potential opposing effect of

individual SCFAs on the production of LLO. Future investigation needed about the adaptation of *L. monocytogenes* with mixtures or individual components of SCFAs to identify potential interactions.

1.7.2. Serotonin (5-HT)

Serotonin is a key neurotransmitter that modulates brain behaviour that is synthesised predominantly by enterochromaffin cells (EC) in the gut mucosa that secrete serotonin into the gut where is acts to control gut motility, secretion and vasodilation (Spohn and Mawe, 2017). Serotonin was isolated by Page and Rapport in 1984 and has been known as 5-hydroxytryptamine (5-HT) (Page *et al*., 1984). 5-HT is similar to norepinephrine, histamine, epinephrine and dopamine, all are biogenic monoamines. 5-HT can be produced in two steps, first tryptophan hydroxylase alters the amino acid tryptophan to 5-hydroxytryptophan (5-HTP), then 5-HTP is decarboxylated to form 5-HT (Mohammad-Zadeh *et al*., 2008).

1.7.2.1. The function of 5-HT in GI tract

1.7.2.1.1. Pro-inflammatory actions of 5-HT in the gut

There is evidence that in the intestinal mucosal layer, serotonin can function as both a pro- and anti-inflammatory signaling molecule as well as a trophic factor. Evidence also shows that 5-HT released from EC cells functions as a pro-inflammatory molecule (see Figure 1.10) (Spohn *et al.,* 2016). A study found that experimental colitis is augmented in mice lacking the serotonin re-uptake transporter (SERT), increasing availability of serotonin released from EC cells (Bischoff *et al.,* 2009). Another study also showed that mice were protected from colitis when mucosal serotonin synthesis was ended by use of the *Tryptophan hydroxylase* (TpH) inhibitor parachlorophenylalanine, and in TpH1 knockout mice (Ghia, *et al.,* 2009). Several studies show that there is protective effect in models of colitis if mice are treated with a TpH1 inhibitor (Margolis *et al.,* 2014; Kim *et al.,* 2015). Dendritic cells are vital in the serotonin-mediated pro-inflammatory response (Li *et al.,* 2011). The 5-HT_7 receptor is expressed on dendritic cells, and after pharmacological inhibition of this receptor, experimentally induced

colitis is increased, showing that mucosal serotonin plays an important role by acting on body immunity to produce gut inflammation (Kim *et al.,* 2013*)*. In this regard serotonin is like a "sword and a shield" in the gut, and in this model, the pro-inflammatory actions of serotonin serve as the sword by activating an immune response for the protection of gut from attack (Gershon, 2012).

Serotonin does not just affect immune cells and cause inflammation, but immune cells can also affect mucosal serotonin handling and alter EC cell biology (Motomura *et al.,* 2008). It is possible that immune cells can release cytokines that can promote the formation, synthesis, and secretion of EC cells, which is why SERT levels are decreased in inflammation (Mawe and Hoffman 2013). Therefore, an increase in the availability of serotonin in the inflamed gut can be described as a feed-forward pro-inflammatory factor in GI pathophysiology.

1.7.2.1.2. Anti-inflammatory actions of 5-HT in the gut

Serotonin also can cause an anti-inflammation in the intestinal mucosa through activation of epithelial 5-HT_4 receptors as shown in Figure 1.10. In dextran sulfate, sodium DSS and 2,4,6-trinitrobenzene sulfonic acid TNBS colitis, activation of epithelial 5-HT_4 receptors leads to anti-inflammation in both protection and recovery paradigms (Spohn *et al.,* 2016). There are various mechanisms that seem to help in the protective effect of 5-HT_4 receptor activation, which include more epithelial proliferation, increased healing of wound, and enhanced resistance to oxidative stress-induced apoptosis (Spohn *et al.,* 2016). In addition, in normal animals, inhibition of 5-HT4 receptor activity causes inflammation and disrupts motor function. The epithelial 5-HT4 receptor serves an invaluable physiological function that helps maintain mucosal integrity (Spohn *et al.,* 2016). Furthermore, 5-HT_4 knockout mice have a higher histological damage score as compared to wild type littermates. These show that a luminally restricted 5-HT_4 agonist may prove effective in treatment of inflammatory bowel syndrome (Spohn *et al.,* 2016).

Therefore, there is compelling evidence that 5-HT can act as both a pro-inflammatory molecule and it has been shown that it can also has anti-inflammatory properties, what is clear is that 5-HT is a critical molecule in homeostasis of the gut.

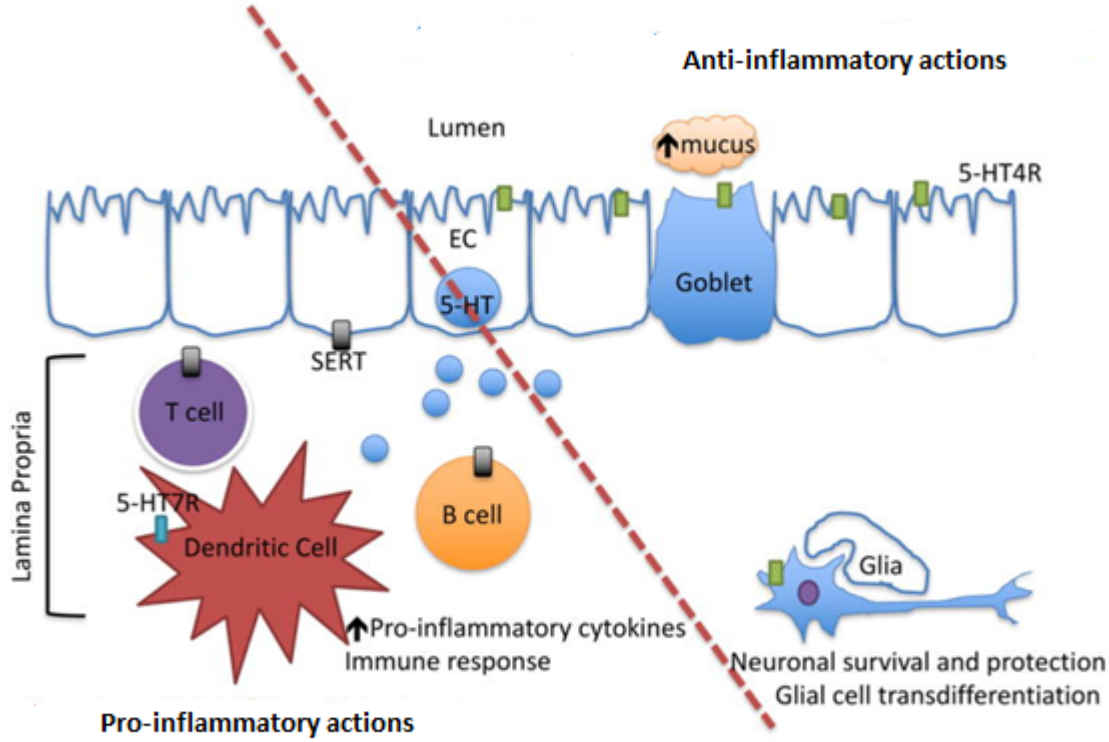

Figure 1.10 5-HT can act as both a pro-inflammatory molecule and anti-inflammatory properties. On the proinflammatory side (lower left), 5-HT released from EC cells can act on 5-HT7 receptors on dendritic cells in the lamina propria (blue rectangle) to set off proinflammatory cascades. Furthermore, 5-HT in the lamina propria can be taken up by SERT-containing cells (grey rectangles) like T and B cells, which also activate the immune response. On the anti-inflammatory side (upper right), 5-HT released from EC cells acts on 5-HT_4 receptors (green rectangles) to increase mucus secretion, improve barrier function, improve epithelial cell wound healing, and it can also potentially promote and protect enteric neuronal survival. Adapted from Spohn *et al.,* 2017.

1.7.2.1.3. Neuroprotective and trophic factor actions of 5-HT

Enteric serotonergic neurons synthesise 5-HT, and this process is dependent on TpH2 (Spohn *et al.,* 2016). 5-HT is crucial for the development and survival of enteric neurons (Gross *et al*.,

2012). The role of neuronal 5-HT in the bowel has been investigated in TpH2 deficient mice. These mice show decreased levels of myenteric neurons, particularly dopaminergic and GABAergic nerve cells (Gross *et al*., 2012). Enteric neuronal expansion, particularly in the developing gut, is affected by the actions of 5-HT which is thought to be associated with the 5-HT_{2B} receptor (Fiorica-Howells *et al.,* 2000). Dissociated cultures of mixed fetal gut cells and in cultures of neural crest-derived cells isolated from the gut show enhanced differentiation of enteric neurons following stimulation of the 5-HT_{2B} receptors (Fiorica-Howells *et al.,* 2000). This suggests that the action of 5-HT on 5-HT_{2B} receptors may impact the development of enteric neurons (Fiorica-Howells *et al.,* 2000).

Other 5-HT receptors impact the development and survival of enteric neurons, such as the 5-HT_4 receptor. 5-HT_4 deficient mice show normal development of neurons at birth, however, after birth the density of enteric neurons reduces drastically. This phenomenon can be treated in adult mice using 5-HT_4 agonists which stimulate the production of new enteric neurons (Gershon and Liu, 2007; Liu *et al*., 2009). Enteric neurons studied in culture show enhanced survival and proliferation following stimulation of 5-HT_4 receptors, as well as enhanced neurite outgrowth (Gershon and Liu, 2007; Liu *et al*., 2009). Stimulation of 5-HT_4 receptors leads to an increase in the formation of neural networks in an embryoid body culture system (Takaki *et al*., 2011). Moreover, stimulation of this receptor also leads to an improvement in the regeneration of enteric reflexes and enhances recovery of a defecation reflex, which is disrupted by colonic resection (Katsui *et al.,* 2008; Matsuyoshi *et al.,* 2010).

The intestinal transit in TpH2 deficient mice does not function as it should normally although it is not known if this disruption is due to changes in serotonergic neurotransmission or due to alterations in the circuitry caused by the loss of neurons (Li *et al*., 2011). It is clear that 5-HT demonstrates protective and trophic effects on integrity of the mysenteric plexus.

1.7.2.2. Interaction between 5-HT and enteric pathogens.

In the case of Gram-negative enteric pathogens there are some data demonstrating a protective role for 5-HT. In the case Enterohemorrhagic *Escherichia coli* (EHEC) it has been shown that 5-HT reduces expression of virulence genes in the locus of enterocyte effacement and reduces the load of *Citrobacter rodentium* in the gut (Kumar *et al.,* 2020). Likewise, 5-HT has been shown to reduce the expression of adhesins in *Campylobacter jejuni* and the attachment and invasion of colonic epithelial cells *in vitro* (Lyte *et al.,* 2021). To date little is known about the interaction between 5-HT and *L. monocytogenes* apart from a single report detailing how *L. monocytogenes* inhibits expression of the 5-HT uptake transporter SERT in enterocytes (Latorre *et al*., 2016). This inhibition of 5-HT uptake will locally increase the levels of 5-HT thereby affecting both *L. monocytogenes* and the physiology of epithelial cells at the site of invasion, potentially facilitating the invasion by *L. monocytogenes*.

In-vivo L. monocytogenes cells causes a drastic reduction in the uptake of 5-HT during the first hour of infection, with this effect being dependent on the multiplicity of infection (MOI) peaking at a high MOI 200 (Latorre *et al*., 2016). The actions of *L. monocytogenes* on the uptake of 5-HT in the intestine seems to occur when there is direct contact between living *L. monocytogenes* cells and intestinal epithelial cells (Latorre *et al*., 2016). Uptake of 5-HT is unaffected in the presence of inactivated *L. monocytogenes* cells and bacterial supernatants (Latorre *et al*., 2016). Overall, *L. monocytogenes* inhibit the action of SERT and this implies the availability of extracellular 5-HT in the intestinal lumen. Consequently, possible feedback on *L. monocytogenes* may occur such as the changes in 5-HT may have a consequence that effect the PrfA regulon.

1.7.3. Low Oxygen (Microaerobic)

In the case of a number of enteric pathogens it has been shown that the microaerobic conditions encountered in the host intestine can act to stimulate virulence gene expression. Microaerobic conditions in the gut have been shown to promote EHEC to phenotypically

express the Type III secretion (T3SS) system and bacterial adherence structures critical for the injection of effector proteins into host cells (Schüller and Phillips, 2010). The number of adherent bacteria at infection sites was significantly higher under microaerobic conditions than aerobic conditions (Schüller and Phillips, 2010).

Shigella flexneri, the causative agent of dysentery, inhabits the gastrointestinal tract where it is challenged by varying oxygen levels (Marteyn *et al*., 2010). These varying oxygen levels control the expression of the bacterium's T3SS which is important in entry and virulence (Phalipon and Sansonetti, 2007). In oxygen-deprived environments such as the gut lumen, the T3SS are not activated with low levels of secretion of the Invasion plasmid antigen Ipa effector (Marteyn *et al*., 2010). This is controlled by FNR a regulator of anaerobic metabolism through the expression of *spa23* and *spa33* virulence genes (Marteyn *et al*., 2010). However close proximity to the intestinal epithelium exposes *S. flexneri* to a microaerobic environment with increased levels of oxygen which leads to activation of T3SS (Tinevez *et al.,* 2019). Subsequently, to promote effective colonisation respiration by *S. flexneri* lowers the adjacent oxygen levels leading to hypoxic infection foci and a decrease in T3SS expression (Tinevez *et al.,* 2019).

In the case of *L. monocytogenes,* it must adapt to varying oxygen levels in the different ecosystems it inhabits from soil, silage and sludges to survival in the mammalian host. In the host across the intestinal wall, there is a high oxygen gradient, where the apical mucosa near the lumen maintains concentrations of 0.1–1 % oxygen. Near the vascularized submucosa, the oxygen concentration is around 6 %. The most oxygenated region is the colonic muscle wall, with 7–10 % oxygen concentrations (Schwerdtfeger *et al*., 2019). As such, *L. monocytogenes* will be exposed to these changes in oxygen availability and have to adapt its metabolism accordingly. My hypothesis is that exposure to microaerobic conditions in the intestine induces the PrfA regulon thereby increasing the likelihood of successful colonisation and subsequent invasion.

It is known that when *L. monocytogenes* is grown anaerobically, it shows increasing adherence and invasion (Wallace *et al.,* 2016). Firstly, internalins; surface proteins involved in adherence to host cells, were upregulated in suboxic conditions (Wallace *et al.,* 2016). Secondly, in both cell culture and animal infection models, anaerobically grown *L. monocytogenes* showed an increased adhesion and invasion phenotype (Wallace *et al.,* 2016). At least one virulence factor, *Listeria* adhesion protein, is upregulated under anaerobic conditions and is needed for the induced adhesion to cultured Caco-2 and HCT-8 cells by bacteria grown anaerobically (Burkholder *et al.,* 2009).

L. monocytogenes infection requires appropriate expression of virulence factors, adhesion factors as well as proteins essential for invasion, replication and survival during pathogenesis. Evidence suggests that *L. monocytogenes* can survive in harsh conditions such as in the human gut, indicating that anaerobic environments may play a role in enhancing *L. monocytogenes* infectivity (Andersen *et al*., 2007). To determine the effects of anaerobic growth on the infectivity of *L. monocytogenes, L. monocytogenes* was cultivated anaerobically prior to infecting Caco-2 cells. It was found that anaerobic cultivation enhanced infectivity by 100-fold (Roberts *et al*., 2020). Animal studies validated these findings, for example the same results were shown in guinea pigs (Roberts *et al*., 2020). The pigs infected with *L. monocytogenes* cultured in anaerobic conditions showed a higher number of bacteria in the intestines compared with animals infected with *L. monocytogenes* cultured in aerobic conditions. Further investigation showed that bacteria concentration was high in the faeces of pigs infected with *L. monocytogenes* cultivated *in vitro* anaerobically prior to infection (Roberts *et al*., 2020). On the other hand, the faeces of pigs infected with *L. monocytogenes* cultivated *in vitro* aerobically prior to infection, showed a lower concentration of bacteria which continued to decrease until the concentration of bacteria was undetectable (Roberts *et al*., 2020). However, *L. monocytogenes* were present between one and three logs greater in the animals given anaerobically grown *L. monocytogenes* (Andersen *et al*., 2007). In the same study, anaerobically cultivated *L. monocytogenes* were also shown to be more virulent in a gerbils

(Roberts *et al.*, 2020). In conclusion this paper has indicated that cultivation of *L. monocytogenes* anaerobically prior to infection increases virulence.

Transcription and post-transcription of LLO are affected by anaerobic conditions, thus affecting the production of LLO. Aerobic conditions and low levels of SCFAs resulted in a decrease in transcription which unexpectedly led to increased supernatant activity (Rinehart, 2020). On the other hand, anaerobic conditions and low levels of SCFAs lead to an increase in transcription, without an increase in supernatant activity (Rinehart, 2020). In summary, these results suggest that LLO production is dependent on the presence of oxygen. The results may also imply that under anaerobic conditions there are inhibitory signals on LLO. Research on how *L. monocytogenes* adapts to low oxygen levels is lacking. Therefore, further investigation is needed to cover the effect of low oxygen on *L. monocytogenes* and changes that may occur on virulence factor.

1.8. Hypotheses, Aims and Objectives

The hypotheses are that *L. monocytogenes* is exposed to environmental signals in the host intestine that activate the PrfA virulence regulon thereby preparing *L. monocytogenes* for infection. The first stimulus to be investigated was the role of short chain fatty acids synthesized by the gut microbiota since these have been shown to be protective and modify gene expression in pathogenic bacteria. In addition, the role of serotonin, a neurotransmitter that modulates brain behaviour secreted predominantly by EC cells and which has been shown to regulate bacterial gene expression was investigated. The last signal to be investigated was the role of oxygen. In the intestine there is a gradient of oxygen from the epithelial surface (microaerobic) to the lumen that is anerobic. To date little is know how *L. monocytogenes* adapts to these microaerobic conditions and whether such changes in oxygen level induces the PrfA regulon. The prediction is that low oxygen levels will induce the PrfA regulon and "pump prime" *L. moncytogenes* for infection.

To address experimentally these hypotheses, I used transcriptional gene fusions to PrfA regulated genes, investigated the role of SigmaB and used RNA seq to look at global changes in gene expression as a consequence of growth in microaerophilic versus aerobic conditions.

Chapter 2 Materials and methods

2.1. Bacterial strains and plasmids

Strain name	Feature	References
Listeria monocytogenes EGDe::InlA^{m}	Serotype 1/2a containing a site directed mutation in the InlA gene to promote interaction with murine E-cadherin / wild type	Wollert *et al*., 2007
Listeria monocytogenes EGDe::InlA Δ*sigB*	Deletion of *sigB* gene in InlA strain	Marie Goldrick, University of Manchester
Listeria monocytogenes EGDe::InlA *phly*:: eGFP	Chromosomal fusion of single copy pCG8 inserted in the InlA strain	This study
Listeria monocytogenes EGDe::InlA *pactA ::eGFP*	Chromosomal fusion of single copy pAD3 inserted in the InlA strain	This study
Listeria monocytogenes EGDe::InlA Δ*sigB phly* ::eGFP	Chromosomal fusion of single copy pCG8 inserted in the InlA Δ*sigB* mutant strain	This study
Listeria monocytogenes EGDe::InlA Δ*sigB pactA* ::eGFP	Chromosomal fusion of single copy pAD3 inserted in the InlA Δ*sigB* mutant strain strain	This study
Listeria monocytogenes EGDe::InlA Δ*prfA*	EGDe::InlA with *prfA* deletion	Marie Goldrick, University of Manchester
Listeria monocytogenes EGDe::InlA Δ*prfA phly* ::eGFP	Chromosomal fusion of single copy pCG8 inserted in the InlA Δ*prfA* mutant strain	This study
Listeria monocytogenes EGDe::InlA ΔPrfA *pactA* ::eGFP	Chromosomal fusion of single copy pAD3 inserted in the InlA Δ*prfA* mutant strain	This study

Listeria monocytogenes EGDe::InlA *p/prfA ::eGFP*	Chromosomal fusion of single copy *p/prfA ::eGFP* inserted in the InlA strain	Liz Lord, University of Manchester
Listeria monocytogenes EGDe::InlA *p/plcA ::eGFP*	Chromosomal fusion of single copy p/plcA:: eGFP inserted in the InlA strain	Liz Lord, University of Manchester
Escherichia coli DH5α	*80dlacZΔM1*, *recA1*, *endA1*, *gyrA96*, *thi-1*, *hsdR17*, (rk-mk+), *supE44*, *relA1*, *deoR*, Δ(*lacYZA -argF*) U169, *phoA*	(Hanahan, 1983)

Table 2.1: Bacterial strains used in this study.

Plasmids	Feature	Antibiotics	References
pCG8	Integrative plasmid that integrates at the $tRNA^{Arg}$-*attBB* site expressing GFP under control of *phly*	Cm	Guldimann *et al*., 2017
pAD3	Integrative plasmid that integrates at the $tRNA^{Arg}$-*attBB* site expressing GFP under control of *pactA*	Cm	Balestrino *et al*., 2010
pLL1	Integrative plasmid that integrates at the $tRNA^{Arg}$-*attBB* site expressing GFP under control of *p/prfA*	Cm	Liz Lord, University of Manchester
pLL2	Integrative plasmid that integrates at the $tRNA^{Arg}$-*attBB* site expressing GFP under control of *p/plcA*	Cm	Liz Lord, University of Manchester

Table 2.2: Plasmids used in this study.

2.2. Media and growth conditions

Unless otherwise stated, all chemicals and reagents were obtained from Sigma-Aldrich.

L. monocytogenes were routinely grown at 37 °C shaking 200 rpm in Tryptone Soya Broth (TSB) (Oxoid) or on TSB plates with additional 1.5% (w/v) agar (Oxoid). For growth in defined media, *L. monocytogenes* were grown in MD10 medium (Corbett *et al.,* 2011). MD10 consists of 49 mM K_2HPO_4, 11 mM NaH_2PO_4, 1.7 mM $MgSO_4$, 187 µM ferric ammonium citrate, 9.3 mM NH_4Cl, 49.5 mM glucose or glycerol, 2.96 µM thiamine-HCl, 1.33 µM riboflavin, 2.05 µM biotin, 24 µM lipoic acid, 0.1 g l^{-1}l-cysteine and l-leucine, 0.2 g l^{-1}l-arginine, l-histidine, l-methionine, l-valine and l-isoleucine. Additionally, the medium was supplemented with 0.1 % w/v case-amino acids. Where required medium was supplemented with antibiotic (Erythromycin 5 µg / ml, Chloramphenicol 7 µg/ml). For microaerobic growth (oxygen 5.5 %-6 % v/v, carbon dioxide 10 % v/v and nitrogen 85 % v/v) *L. monocytogenes* were grown in a VAIN incubator (Don Whitley) in 6 well plates (Costar®) shaking at 140 rpm respectively at 37 °C. The OD_{600} of the culture was measured by placing 1 ml for aerobic conditions or 1:5 dilution for microaerobic conditions into a cuvette and analysing the OD_{600} in a spectrophotometer (Jenway).

Escherichia coli were routinely cultured at 37 ºC shaking 200 rpm in Luria Bertani (LB) broth which consists of 1% (w/v) tryptone, 1% (w/v) NaCl, 0.5% (w/v) Yeast Extract and on LB plates solidified with 1.5% (w/v) agar (Oxoid). Where required medium was supplemented with antibiotic (Erythromycin 300 µg/ml, Chloramphenicol 35 µg/ml).

Stock cultures of all strains were stored at -80 ºC in LB for *E. coli* and TSB for *L. monocytogenes* with 25 % (v/v) glycerol.

2.3. Green fluorescence protein expression

L. monocytogenes Gfp-reporter strains were grown in MD10 or TSB media, where appropriate, final concentration of 5 mM butyrate, 100 µM serotonin or combination of both butyrate and serotonin were used, shaking at 37 °C for 20 hours under aerobic in 50 ml flask

or microaerobic in 6 well plate. Cells were then centrifuged and suspended in phosphate buffered saline (PBS) to an OD_{600} of 1.0. From the PBS cell suspension, 200 µl was transferred into a black-walled 96-well plate with a transparent base in triplicate. Using the Bio-Tek Synergy HT plate reader, both the relative fluorescence units (RFU) (excitation at 485/20 nm and emission at 528/20 nm) and the OD_{600} were measured. The results were interpreted by dividing the RFU by the relative OD_{600}.

2.4. Transformation DNA into *L. monocytogenes*

2.4.1. Preparation of electrocompetent *L. monocytogenes* cells

A 100 µl of a fresh 10 ml overnight (O/N) culture of *L. monocytogenes* grown in TSB was inoculated into a 100 ml fresh TSB containing 0.5 M sucrose and incubated at 37 ºC with shaking for 4 hours, until OD_{600} of 0.2. Then 100 µl of a stock solution of Penicillin G (10 µg/ml) was added to the solution and incubated for 2 hours. Subsequently the cells were harvested by centrifugation at 4 ºC for 20 mins at 3660 x g. The cells were washed once using sterile 50 ml ice-cold 1 mM Hepes pH 7.5, 0.5 M sucrose (Hepes-Sucrose solution) and then twice using 25 ml of Hepes-Sucrose solution. This was followed by resuspending the pellet in a total of 300 µl Hepes-Sucrose solution and this can be kept in cold room until needed for up to a week (Park and Steward, 1990).

2.4.2. Transformation of plasmid DNA into electrocompetent *L. monocytogenes*

Transformation of *L. monocytogenes* was performed as described (Park and Steward, 1990). Briefly, in ice-cold electroporation cuvettes (0.2 mm gap) (Bio-Rad Laboratories), 1 µg of the plasmid DNA was mixed with100 µl of competent cells. The mixtures were electroporated at 200 Ω, 25 µF and 2.5 kV using a Gene Pulser apparatus (Bio-Rad Laboratories). Immediately after electroporation, fresh 900 µl TSB was added to the mixture and the tube incubated at 37

°C for 1 hour without shaking. Then the cells were plated out on TSB with the appropriate antibiotics.

2.5. DNA MANIPULATION

2.5.1. Extraction of the plasmid from *E. coli*

Plasmid DNA samples of high purity were extracted from *E. coli* using the QIAprep Spin Miniprep Kit (Qiagen) as per the manufacturer's instructions. The bacterial overnight culture (10 ml) was pelleted by centrifugation at 4 ºC for 10 mins at 3660 x g, followed by resuspension in RNase A-containing buffer P1, lysis with the NaOH/SDS-containing buffer P2 for <5 min, neutralisation and adjustment to high-salt binding conditions with the N3 buffer solution. Vigorous vortexing was avoided to prevent chromosomal DNA contamination during lysis. After centrifugation of the lysates on a bench-top centrifuge (Eppendorf) at 13000 x g for 10 min, the supernatant (protein- and chromosomal DNA-free) was transferred to spin columns and centrifuged again at 13000 x g for 1 min, during which the plasmid DNA was bound to the column membrane. The spin columns were washed with ethanol-containing washing buffer after removal of the elutant and the ethanol traces were then removed as well. Finally, the plasmid DNA was eluted with 30 µl of water.

2.5.2. Agarose gel electrophoresis

The agarose percentage used was defined according to the expected size of the linear DNA. To visualize the 1 kb fragment or greater, 1 % w/v agarose was prepared in TAE buffer (0.5 M Tris, 5.7% acetic acid v/v, 10 mM EDTA, pH 8). D

NA samples were mixed with 5x DNA loading buffer blue (Bioline) and loaded onto the gels along with 1 kb markers (Bioline). Gels were run at 110 V in TAE buffer containing 0.5 µg/ml ethidium bromide followed by gel visualisation under UV light exposure using an ultraviolet transilluminator (GelDoc).

2.5.3. Polymerase Chain Reaction (PCR)

DNA amplification was carried out as per manufacturer instructions for the My Taq HS Red Mix 2x (Bioline). For sequencing or cloning, Pwo DNA polymerase (Roche) with proofreading activity was added to the reaction mixture. The reaction mixture consisted of 25 µl of My Taq HS Red Mix 2x, 1 µl of each primer (20 µM), 200 ng of template DNA and 0.25 µl of Pwo DNA polymerase (5 U/µl) made up a final volume of 50 µl with sterile distilled water Using a Hybaid thermal cycler, the following PCR protocol was performed: initial denaturation at 95 ºC for 1 min, followed by 30 cycles where each cycle was: denaturation at 95 ºC for 30 sec, annealing at T for 30 sec and extension at 72 ºC for N, with a final extension period of 10 min at 72 ºC (T is obtained by reducing the lower melting temperature (Tm) of the two primers by 5 ºC; N is defined as per the estimated length (kb) of the fragment being amplified with a recommendation of 30 sec/kb).

The colony PCR was performed with the same protocol as above but the DNA template in the reaction mixture was substituted by a single colony of *L. monocytogenes* or *E. coli* for cloning or sequencing purposes. For screening colonies by PCR, no Pwo was added to the 50 µl mixture. The mixture was aliquoted into five PCR tubes with 10 µl each and a single colony was then added to each of the 10 µl reaction mixtures, followed by the PCR run as described above. PCR products were examined by agarose gel electrophoresis and purified by using QIAquick PCR purification kits (Qiagen) according to the manufacturer's recommendations. The primers used in this study are listed as follows:

Primers	Sequence (5'-3')	References	Description
F-phly	ATGCGGATCCAAGTTACT	This study	These primers amplify a 870 bp starting from hly promotor and ending with GFP.
eGFP-1R	CATCCATTCCTAAAGTGATTC	This study	
PL102	TATCAGACCTAACCCAAACCT T CC	Lauer *et al*., 2002	These primers amplify a 533 bp PCR product at $tRNA^{Arg}$-*attBB* attachment site in strains that have no integration.
PL103	AATCGCAAAATAAAAATCTTC TCG	Lauer *et al*., 2002	
NC16	GTCAAAACATACGCTCTTATC	Lauer *et al*., 2002	These primers amplify a 499 bp PCR product in strains contains an integration into $tRNA^{Arg}$-*attBB* attachment site
PL95	ACATAATCAGTCCAAAGTAGA TGC	Lauer *et al*., 2002	
F-PrfA	ATGAACGCTCAAGCAGAAG	This study	These primers amplify a 710 bp of *prfA.*
R-PrfA	TTTAATTTTCCCCAAGTAGCA G	This study	
F-rpoB	GTTGTGGTGTAATTGTAGTCA TATCTTG	This study	These primers amplify a 120 bp of *rpoB* constant gene.
R-rpoB	GTCGTCTTCGTTCTGTTGGTG	This study	
PrfA1F	CCTATGTGTATGGTAAAGAAA CTCCTG	This study	These primers amplify a 98 bp of *prfA.*
PrfA1R	GCTATGTGCGATGCCACTTG	This study	

Table 2.3: List of primers used in this study.

2.6. RNA extraction

RNA extraction was carried out using Invitrogen's Purelink RNA Extraction Kit and Lysing Matrix E tubes (MP Biomedicals). Prior to starting the extraction, fresh lysozyme solution (consisting of 10 mg/ml lysozyme, 10 mM Tris-HCl pH 8.0 and 0.1 mM EDTA,) and a solution of 10% SDS (w/v) were prepared in RNAse-free water and the kit lysis buffer was supplemented with 10 µl of 2-mercaptoethanol per 1 ml of lysis buffer. Bacterial cells were harvested by centrifugation at 13000 x *g* for 3 mins. The supernatant was discarded and 100 µl of lysozyme solution was added to the pellet for cell resuspension. Next, 0.5 µl of SDS

solution (10% v/v) and 350 µl of lysis buffer was added and vortexed sequentially. The lysate, added to a Lysing Matrix E tube, was homogenised in a rotor stator homogeniser (FastPrep FP120, 6.5 speed) for 45 secs. The tube was centrifuged for 5 mins at 2600 x *g* followed by transfer of the supernatant to a microcentrifuge tube (RNAse-free) and addition of 250 µl of absolute ethanol (100% v/v) to the tube. The solution mixture was vortexed to remove precipitate. The sample was then transferred to a spin cartridge and centrifuged at 12000 x *g* for 15 secs allowing RNA to bind to the spin column. The subsequent flow-through was discarded and 700 µl of Wash Buffer 1 was added to the column. This was then centrifuged again for 15 secs at 12000 x *g*, followed by discarding both the flow through and the collection tube. The column was then placed in a new collection tube. Wash Buffer 2 (500 µl) was added to the column and centrifuged at 12000 x *g* for 15 secs, again discarding the subsequent flow-through. The wash step was repeated with Wash Buffer 2 and flow-through was discarded again. The column was centrifuged at 12000 x *g* to remove any residual wash buffer. The collection tube was discarded and the column was transferred to a RNAse-free recovery tube; 50 µl of RNAse-free water was carefully added to the column membrane. RNA was eluted in this 1.5 ml tube with 1 min incubation at room followed by centrifugation at 12000 x *g* for 2 mins. All further experiments involving RNA were performed on ice. The Nanodrop spectrophotometer (ND-1000) was used for RNA quantification using 1 µl of the sample. Additionally, the Super RNAse Inhibitor (Invitrogen) was added to the samples at 1U/µl to inhibit RNAse activity.

2.7. Removing genomic DNA from RNA samples

Genomic DNA (gDNA) was removed using DNAse free kit reagents (Ambion) (0.1 volume of 10x TURBO DNAse buffer and 1 µl of TURBO DNAse) which were added to the RNA samples and gently mixed. The samples were incubated for 30 mins in a 37 ºC heat block, then vortexed and followed by addition of 2 µl of the kit DNAse inactivation reagent. The sample was incubated at room temperature for 5 mins and flicked a few times during incubation to ensure suspension of the inactivation reagent evenly throughout the mixture. Next, the sample

was centrifuged at 10,000 x *g* for 90 secs and the supernatant was collected in a fresh collection tube (RNAse free). Samples were kept frozen at -80 ºC until they were taken for sequencing.

2.8. Quality Control of RNA samples

Prior to sample freezing at -80 ºC, small aliquots of each sample were taken to analyse for RNA integrity and concentration alongside testing for the presence of gDNA using a Tapestation System (Agilent). Agilent's gel supplied loading dye (5 µl) was added to 1 µl of the RNA sample in a 200 µl PCR tube. The mixture was briefly centrifuged and the samples were heated for 3 mins at 72 ºC then placed on ice for a subsequent duration of 3 mins. Once cooled, the tubes were briefly vortexed and centrifuged again to remove condensation from the tube lids. The samples were transferred to the Tape Station System and analysed using the 'Prokaryotic RNA' and 'No Ladder' user settings. The RIN value data and associated gels were shared with the sequencing facility to ensure high-quality of samples prior to RNA-sequencing.

2.9. Rapid Amplification of 5' cDNA ends

Rapid amplification of 5' cDNA ends (5' RACE) was performed using the 5'/3' RACE assay (Roche, gen 2) as per the kit instructions (See figure 2.1). After RNA extraction from bacterial strains as described above, cDNA synthesis for the first strand was carried out using kit reagents comprising a gene-specific primer SP1, Transcriptor Reverse Transcriptase and a mixture of deoxynucleotides. The first-strand cDNA was purified using the High Pure PCR Product Purification kit (Roche). dATP and recombinant terminal transferase were used for the A-tailing to the 3´ end of first-strand cDNA. The A-tailed cDNA was then amplified by PCR using a gene-specific primer SP2 and oligo dT-anchor primer. The product was cloned in pGEM-T Easy Vector and taken for colony PCR which was followed by DNA sequencing.

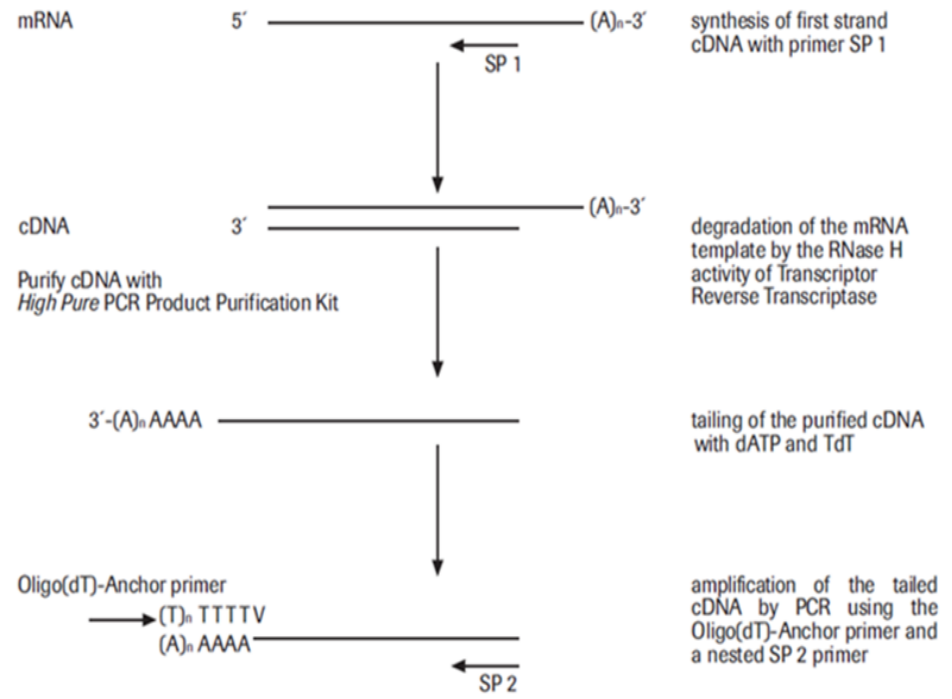

Figure 2.1: Schematic representation of Rapid Amplification of 5' cDNA. (Taken from RACE kit Roche gen 2)

2.10. Quantitative Real-Time Polymerase Chain Reaction (qRTPCR)

Reverse transcription was carried out on extracted RNA (500 ng) using the QuantiTect Reverse Transcription Kit (Qiagen). The quantitative polymerase chain reaction (qRTPCR) was performed using the ABI Prism sequence detector (Applied Biosystems) followed by cDNA measurement with a Qubit 2.0 Fluorometer. The final master mix (total volume = 20 µl) was prepared using 10 µl of FAST SYBR Green Master Mix (Applied Biosystems), 1 µl of 10 µM primers (Forward and Reverse), 20 ng of cDNA, with the remaining volume made up with DNase/RNase free water. The mixture was gently inverted then centrifuged briefly for 20 sec. The 20 µl master mix was transferred to its corresponding well (MicroAmp Fast Optical 96-Well Reaction Plate) sealed firmly with an optical adhesive cover, and then centrifuged briefly at 20,000 x *g* for 1 minute to spin down contents and eliminate air bubbles. The thermal cycling conditions were set as follows: 20s hold at 95 ºC; 40 cycles of denaturation for 1 sec at 95 ºC; culminating with 30 secs annealing/polymerisation at 60 ºC. Standard curves were obtained

for each set of primers, allowing absolute quantification by plotting the threshold cycle against the logarithm of a known amount of copy numbers. The presence of target copies in the samples were then quantified by extrapolation from the linear regression of the standard curve. An RNA-only negative control lacking the reverse transcription step was also included. To avoid the presence of primer-dimers, a melting curve step was performed after the total amplification cycle (rapid heating up to 95 ºC for 15 secs for DNA denaturation, 1 min cooling to 60 ºC followed by increasing temperatures by 0.3 ºC/ sec up to 95 ºC for 15 secs).

2.11 Calculation of relative expression in qRTPCR

The approach was applied for qRTRCR analysis is delta-delta cycle threshold CT ($2^{-\Delta\Delta Ct}$) to identify the relative fold changes in gene expression (Livak and Schmittgen, 2001). In mathematics, the term delta (Δ) means the variation between to values. Thus, delta-delta Ct ($\Delta\Delta Ct$) means the difference in CT values between the control samples (aerobic conditions) and (microaerobic conditions) treated samples, and delta Ct (ΔCt) means the difference in CT value between housekeeping gene (*rpoB*) and interest gene (*prfA*). The Ct values of the samples were retrieved from the qrtPCR machine and calculated using Microsoft Excel software. The following delta-delta Ct formula was used to calculate fold gene expression:

Average of CT value for the PrfA (interest gene) and rpoB (housekeeping gene)

Calculate ΔCt = average Ct (PrfA) – average Ct (rpoB)

$\Delta\Delta Ct$ = ΔCt (Microaerobic condition) – ΔCt (Aerobic condition)

2^-($\Delta\Delta Ct$)

2.12. RNA-sequencing

Samples were sent to the Genomic Technology Core Facility to perform RNA-sequencing (RNAseq). This involved the Genomic Technology Core Facility carrying out the following steps. Ribosomal RNA was depleted from the samples with a ribosomal depletion kit (Illumina) as per kit instructions. Additional probes derived from *L. monocytogenes* were used to

efficiently deplete the rRNA as per Illumina's recommendations. The RNA was then fragmented and denatured using the Illumina Stranded Total RNA Prep kit. The first and second strands were synthesised, 3' ends were adenylated, followed by anchor ligation, fragment and library clean-up as well as amplification. qrtPCR (KAPA) was used to quantify the libraries added to an equimolar pool which was then denatured and loaded onto a lane on the SP NovaSeq 6000 flowcell.

2.13. Analysis of RNA-Seq results

Unmapped paired-end sequences obtained from the HiSeq 4000 sequencer (Illumina) were tested by FastQC. Quality control included removing sequence adapters and trimming reads using the Trimmomatic V0.39 (Bolger, Lohse and Usadel, 2014). The reads were mapped against the reference genome of *Listeria monocytogenes* EGDe Genome for further annotation. Counts per gene were calculated using feature Counts (subread_2.0.0; Liao, Smyth and Shi, 2014). Normalisation was carried out followed by Principal Component Analysis (PCA) and differential expression (DE) calculations with the DESeq2_1.36.0 (Love, Huber and Anders, 2014). Bioinformatic analysis of RNA-seq data was performed by Dr Leo Zeef from the Genomic Technologies Core Facility at the University of Manchester.

2.14. Generation of *L. monocytogenes* protein extracts.

L. monocytogenes were grown in MD10 defined medium shaking at 37 ºC to OD_{600} of ~ 1.1 either under aerobic conditions in a 50 ml flask or under micro-aerophilic conditions in a 6 well plate (Costar®). Ten ml of the cultures were then centrifuged at 30000 g and suspended in 100 μl of (167 mM Tris pH 6.8, 5.5 % w/v sodium dodecylsulfate (SDS), 28% v/v glycerol). The suspension was boiled at 100 ºC for 5 mins. The samples were stored at -20 ºC.

2.15. SDS-polyacrylamide gel electrophoresis and western blot

To resolve Listerial proteins tris-glycine SDS-polyacrylamide gel electrophoresis was performed (Laemmli 1970). A resolving gel of 12 % w/v acrylamide was made using the following mixture; 1.6 ml water, 2 ml 30 % acrylamide mix, 1.3 ml of 1.5 M Tris (pH 8.8), 50 μl 10 % w/v SDS, 50 μl 10% w/v ammonium pesulfate, 2 μl Temed. The stacking gel (upper gel) was made of 1.4 ml water, 330 μl 30 % w/v acrylamide mix, 250 μl 1 M Tris (pH 6.8), 20 μl 10 % w/v ammonium persulfate, 2 μl Temed. Following the preparation, the samples were boiled for 3-5 minutes at 100 ºC in SDS PAGE loading dye 2X (1.2 ml of 1 M Tris pH 6.8, 4 ml of 10 % w/v SDS, 2 ml glycerol, 20 mg bromophenol blue to the final volume of 9 ml and mixed with x μl of 2-meracptoethanol (1:100) dilution. The gels were electrophoresed at 150 V in SDS PAGE Polyacrylamide gelelectrophoresis running buffer 10X (Tris 250 mM, Glycine 1.92 M, SDS 1 % w/v and H_2O until a total volume of litre). Following the SDS PAGE, the proteins were transferred to PVDF membrane (Novex) using Trans-Blot Semi-Dry Transfer Cell (Bio-Rad). The transfer was performed in Tris-Glycine transfer buffer (192 mM glycine, 25 mM Tris, 20 % v/v methanol) with a constant voltage of 15 for 20 minutes. For PrfA and LLO proteins detection, the PVDF membrane was blocked overnight at 4 ºC in PBS with 4 % (w/v) BSA, 0.1 % (w/v) Tween 20. The membrane was then washed twice in PBS with 0.1 % (w/v) Tween 20 (w/v) and once in PBS for 10 minutes. This was followed by incubation for one hour at room temperature with anti-rabbit IgG HRP primary antibody diluted 1:10000 in PBS. The washed was the repeated and followed by one-hour incubation with *L. monocytogenes* anti-PrfA rabbit polyclonal antibody or anti-LLO (Edith Gouin *et al.*, 2010) polyclonal antibody diluted 1:5000 in PBS. For ActA protein and P60 (housekeeping proteins for loading control) detection, the membrane was blocked for 1 hour at 4 ºC with milk dissolved in PBS and it was then incubated overnight with anti-rabbit IgG HRP primary antibody (Sigma) diluted 1:10000 in milk dissolved in PBS. This was followed by incubation for two hours at room temperature with *L. monocytogenes* anti-ActA monoclonal antibody (Abnova) or anti-P60 monoclonal antibody (Abcam); both antibodies were diluted in milk dissolved in PBS 1:10000. After the incubation

completed, the membrane was washed twice in PBS with 0.1 % Tween 20 (w/v) and once in PBS for 10 minutes. All samples were treated with Plus Chemiluminescent substrate (Thermo-fisher) to visualise the bands for 5 minutes. ChemiDoc machine and Image Lab software were used to observe western blot gels and quantify protein bands. Image lab densitometry software was used to implement lane and band tools. Two steps are involved in this process: first identify the lane, and then identify the bands within that lane. After the bands had been detected, the quantity tools used to show the relative fold change for each band. The sample grown in aerobic glycerol was taken as 1 and all other conditions were compared against that value. The fold change for PrfA, LLO and ActA were normalized by dividing the fold change for each condition by the relative value of P60 normalised against the P60 value for the culture grown in under aerobic conditions with glycerol as a carbon source.

2.16 Graphs and statistical analyses

Numerical data was tabulated into Graphpad Prism 9 software and graphs were generated using this software. Statistical analysis was performed using GraphPad Prism 9 software. Multiple sample comparisons were analysed using ANOVA and t test. Where appropriate the data was analysed by a one/two way ANOVA using GraphPad Prism.

Chapter 3 The role of butyrate and serotonin on expression of the PrfA regulon

3.1. Introduction

To determine if the PrfA regulon, that encodes many of the virulence factors of *L. monocytogenes,* is switched on by signals first encountered within the intestinal lumen that could be important for subsequent interaction with the intestinal epithelia. Therefore, three signals were examined. Butyrate, a short chain fatty acid molecule synthesised by bacteria within the gut microbiota, microaerobic conditions (5 % v/v oxygen) and serotonin (5-HT), a key neurotransmitter that modulates brain behaviour. *L. monocytogenes* InlA strains with chromosomal *phly*::*gfp* or *pactA::gfp* transcriptional fusions were grown in both MD10 or TSB media with two different sources of carbon either aerobically or microaerobically with and without 5 mM butyrate or 100 µM 5-HT and Gfp expression monitored. These concentrations of butyrate and serotonin were chosen to mimic the known concentration in the small intestine (Peng *et al.,* 2007; Fung *et al.,* 2019). Two carbon sources were used for the following reasons. First, the choice of glucose was to mimic the carbon source most likely present in the intestine as well as being known to inhibit PrfA activation. Secondly, glycerol is the preferred intracellular carbon source used by *L. monocytogenes* and will allow any inhibitory effects of glucose to be identified (Gaballa *et al.,* 2019).

3.2. Generation of fluorescent *L. monocytogenes* strains

Two strains with transcriptional *gfp* fusions to either *phly*, an early PrfA regulated gene or *pactA* a late PrfA reguated gene were constructed by inserting the plasmids pCG8 (*phly::gfp*) and pAD3 (*pactA::gfp*) into *L. monocytogenes* InlA resulting in integration at the $tRNA^{Arg}$-*attBB* attachment site (See material and methods section 2.5). Therefore, the green fluorescent protein would be expressed from the chromosome under the control of the *hly* and *actA* promoters (Figure 3.1). The sequence of *phly/pctA* or *gfp* was PCR amplified from pCG8 or

pAD3 with F-phly/GFP R or NC16/PL95 primers (Table 2.3), generating 870 bp or 499 bp fragments respectively.

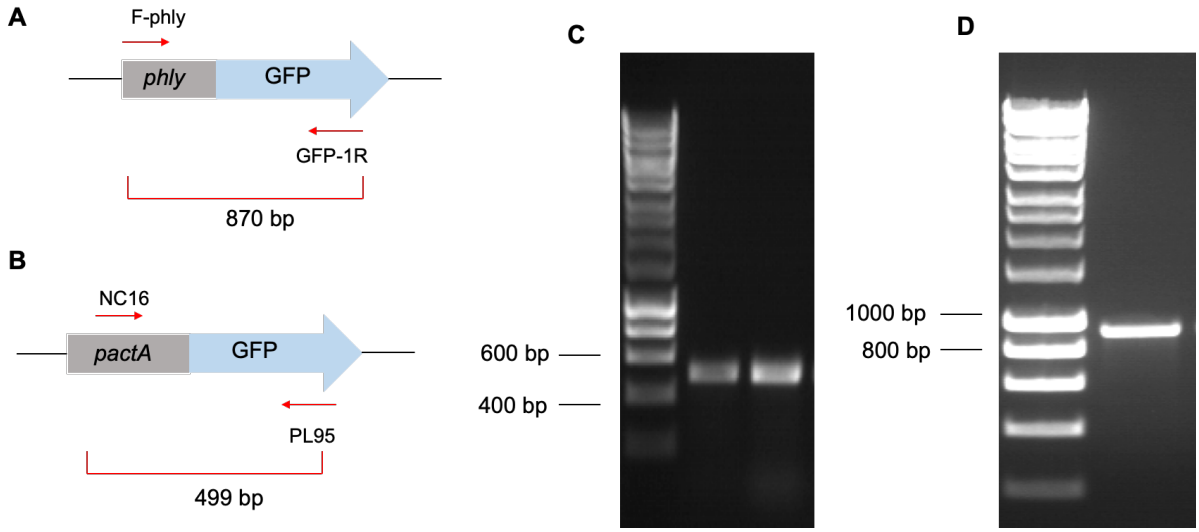

Figure 3.1 Construction of *phly::*gfp and *pactA::gfp* on the chromosome of *L. monocytogenes* InlA. Panel A shows the fragment size and primers used for *L. monocytogenes* InlA *phly::gfp*. Panel B shows shows the fragment size and primers used for *L. monocytogenes* InlA *pactA::gfp*. Panel C shows representative image for two strains of *L. monocytogenes* InlA *pactA::gfp*. Panel D shows representative image for strain *L. monocytogenes* InlA *phly::gfp*. Because neither primer GFP-1R nor PL95 bound to the *L. monocytogenes* InlA no PCR products were generated after PCR using the wild type strain (data not shown). This approach was used to introduce *phly::gfp* and *pactA::gfp* constructs onto the chromosome of *sigB* and *prfA* mutants.

3.3. The effect of butyrate on growth of *L. monocytogenes* InlA strains in TSB medium

To test what effect if any butyrate might have on the growth of *L. monocytogenes*, the growth was measured by following the OD_{600} under microaerobic and aerobic conditions in rich medium (TSB) supplemented with or without butyrate. The addition of butyrate has no detectable effect on the growth of *L. monocytogenes* strains under both aerobic and microaerobic conditions (Figure 3.2).

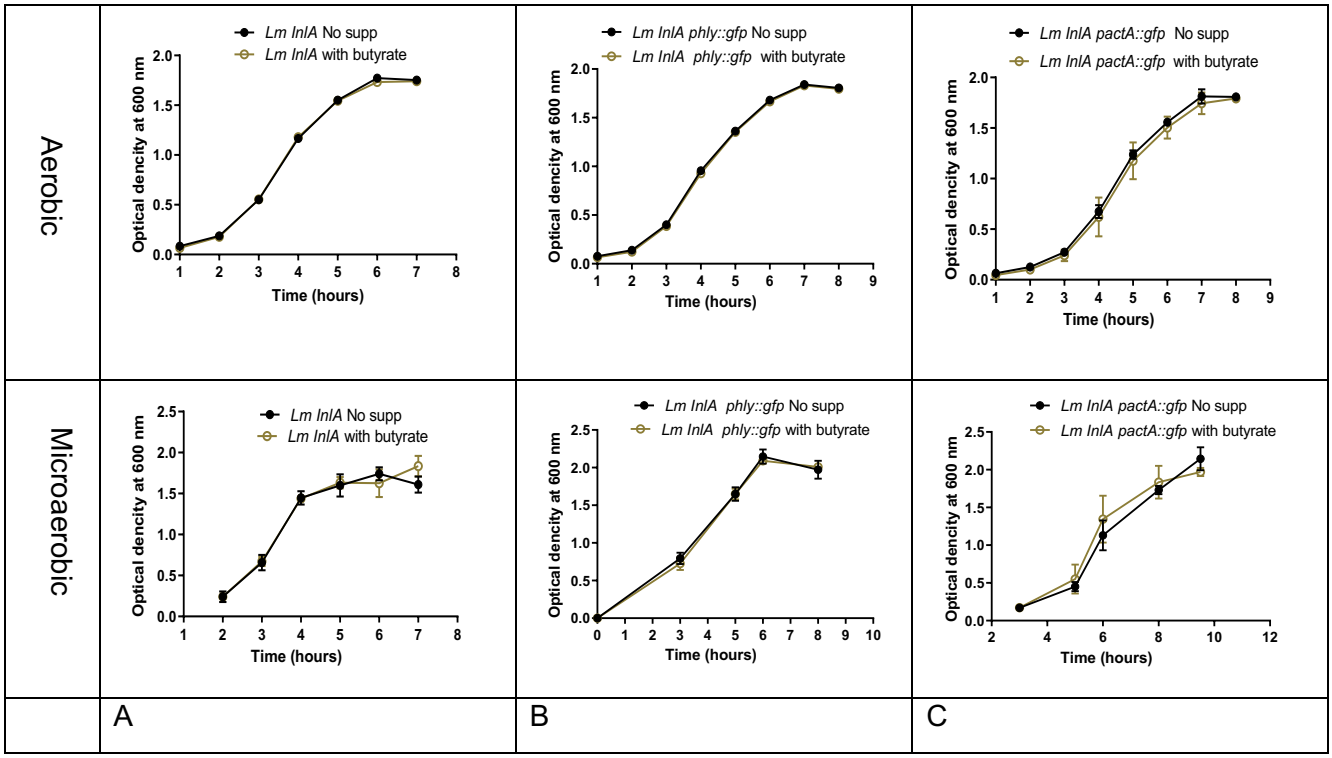

Figure 3.2 Growth curves of *L. monocytogenes* strains. They were grown at 37 ºC in TSB with and without 5 mM butyrate under aerobic and microaerobic conditions. The top row shows the growth under aerobic while the bottom row shows the growth under microaerobic conditions. Data in column A presents *L. monocytogenes* InlA while columns B and C show the growth of *L. monocytogenes* InlA *phly::gfp* and *L. monocytogenes* InlA *pactA::gfp* respectively. Means of triplicates were plotted with error bars representing standard deviation. The result is the mean of at least three independent experiments.

3.4. The level of Gfp expression from *phly* and *pactA* under different growth conditions in TSB

To investigate whether butyrate in the intestine was affecting expression of the PrfA regulon and what the effect of oxygen might be, the fluorescence assay was performed with strains *L. monocytogenes* InlA *phly::gfp* and *L. monocytogenes* InlA *pactA::gfp*grown overnight with and without 5 mM butyrate under aerobic or microaerobic conditions. The addition of 5 mM butyrate resulted in a significant decrease in the transcription from *phly* under both conditions (Figure 3.3). The expression of the *phly* was low (600-800 RFU/OD_{600}) following aerobic growth in TSB but increased to (1500-2500 RFU/OD_{600}) following microaerobic growth. Likewise, the addition of butyrate resulted in a significant reduction from *pactA* under

microaerobic conditions. The *gfp* expression from *pactA* was undetectable following aerobic growth in TSB but increased to 50 RFU/OD_{600} following microaerobic growth an increase that was not statistically significant (Figure 3.3).

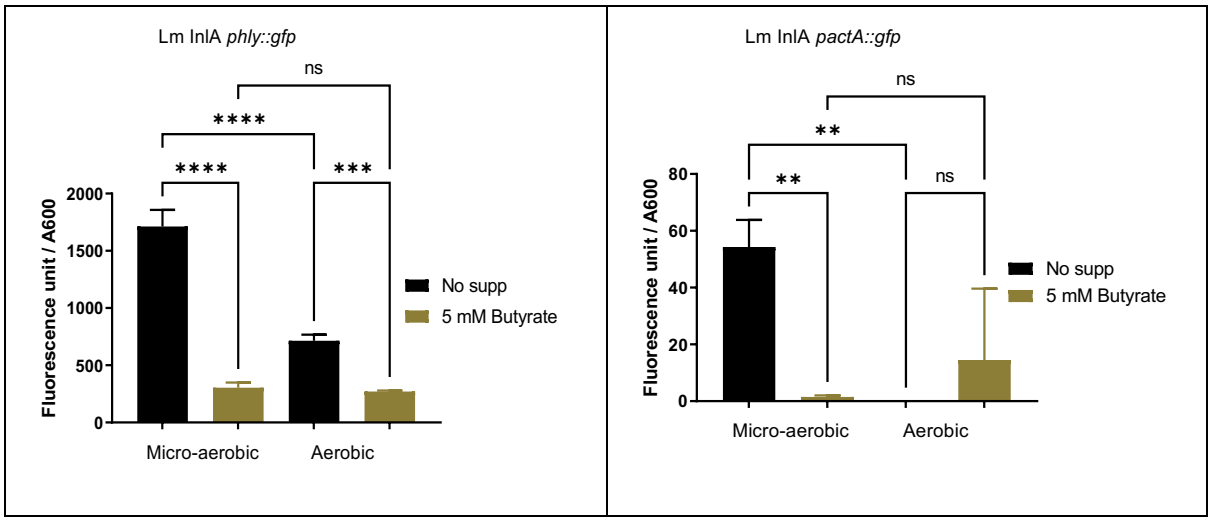

Figure 3.3 The induction of transcription from *phly* and *pactA* promoters under aerobic and microaerobic conditions with or without 5 mM butyrate. The strains were grown at 37 ºC in TSB medium under aerobic and microaerobic conditions and the Gfp expression was measured after O/N growth. The data are the mean of three independent experiments with error bars representing standard deviation. Significant differences (**p<0.001; ***p<0.0001; **** p < 0.0001) were calculated using two-way ANOVA.

3.5 The effect of butyrate on growth of *L. monocytogenes* InlA strains in MD10 medium using glucose and glycerol as carbon sources

To test the butyrate effect, the growth was measured for *L. monocytogenes* strains under microaerobic and aerobic conditions in defined medium MD10 using either glucose or glycerol as a carbon source. Regardless of carbon source, the strains grew significantly better under microaerobic conditions compared to aerobic conditions (Figure 3.4, 3.5). Also, butyrate has no effect on the growth of *L. monocytogenes* strains under all conditions used. In general, the strains showed better growth in TSB in aerobic conditions (Figure 3.2) compared to MD10 while under microaerobic conditions the strains grew slower in MD10 than TSB but reached a similar final OD_{600} (Figures 3.3, 3.4 and 3.5).

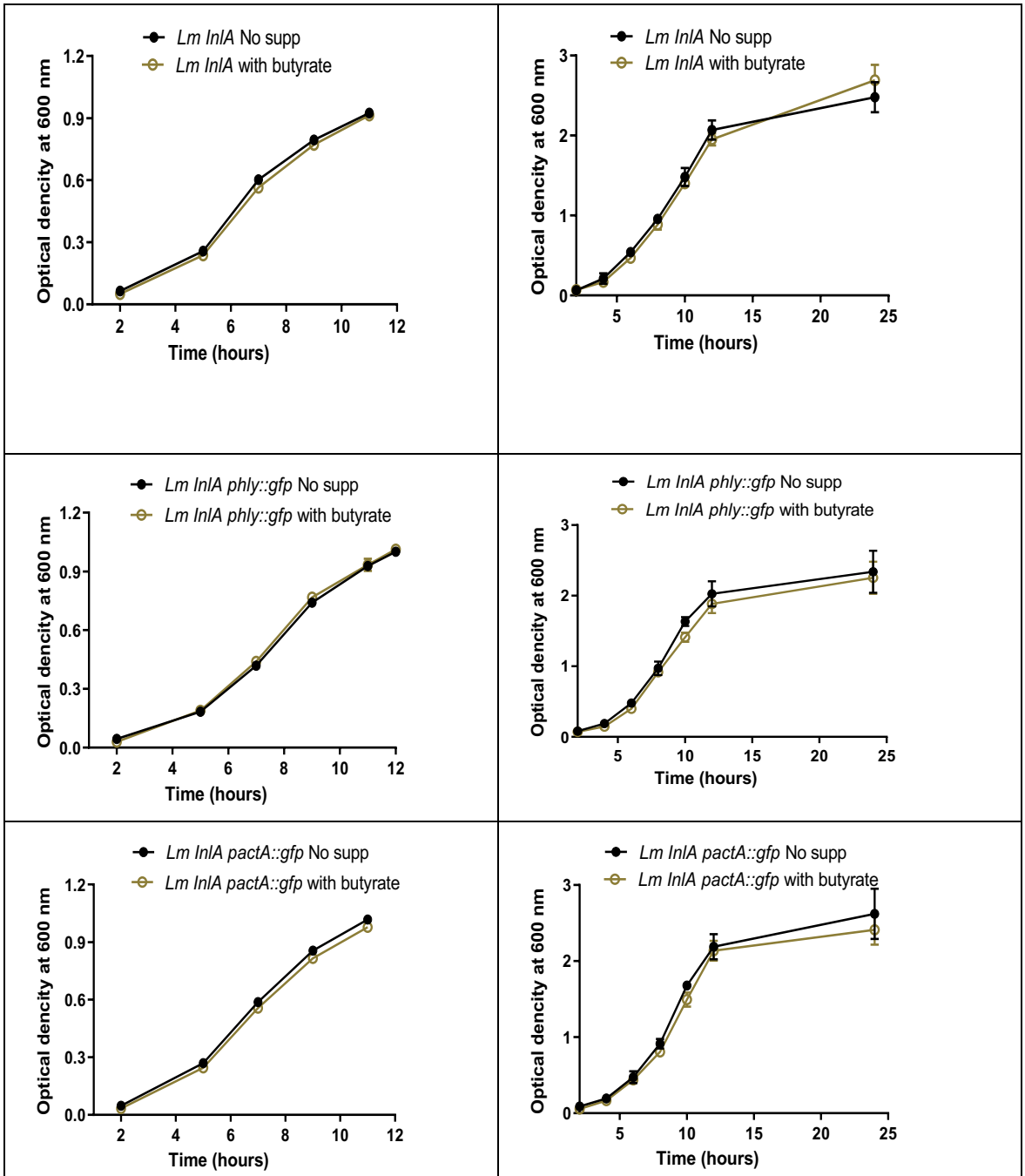

Figure 3.4 The growth curves of *L. monocytogenes* InlA strains grown aerobically or microaerobically in MD10 glucose medium with or without butyrate. The first column shows the growth under aerobic while the second column shows the growth under microaerobic conditions. The growth of *L. monocytogenes* InlA strain is shown in the top row while the middle and the bottom rows show the growth of *L. monocytogenes* InlA *phly*::*gfp* and *L. monocytogenes* InlA *pactA*.:*gfp* respectively. Means of triplicates were plotted with error bars representing standard deviation. The result is the mean of at least three independent experiments.

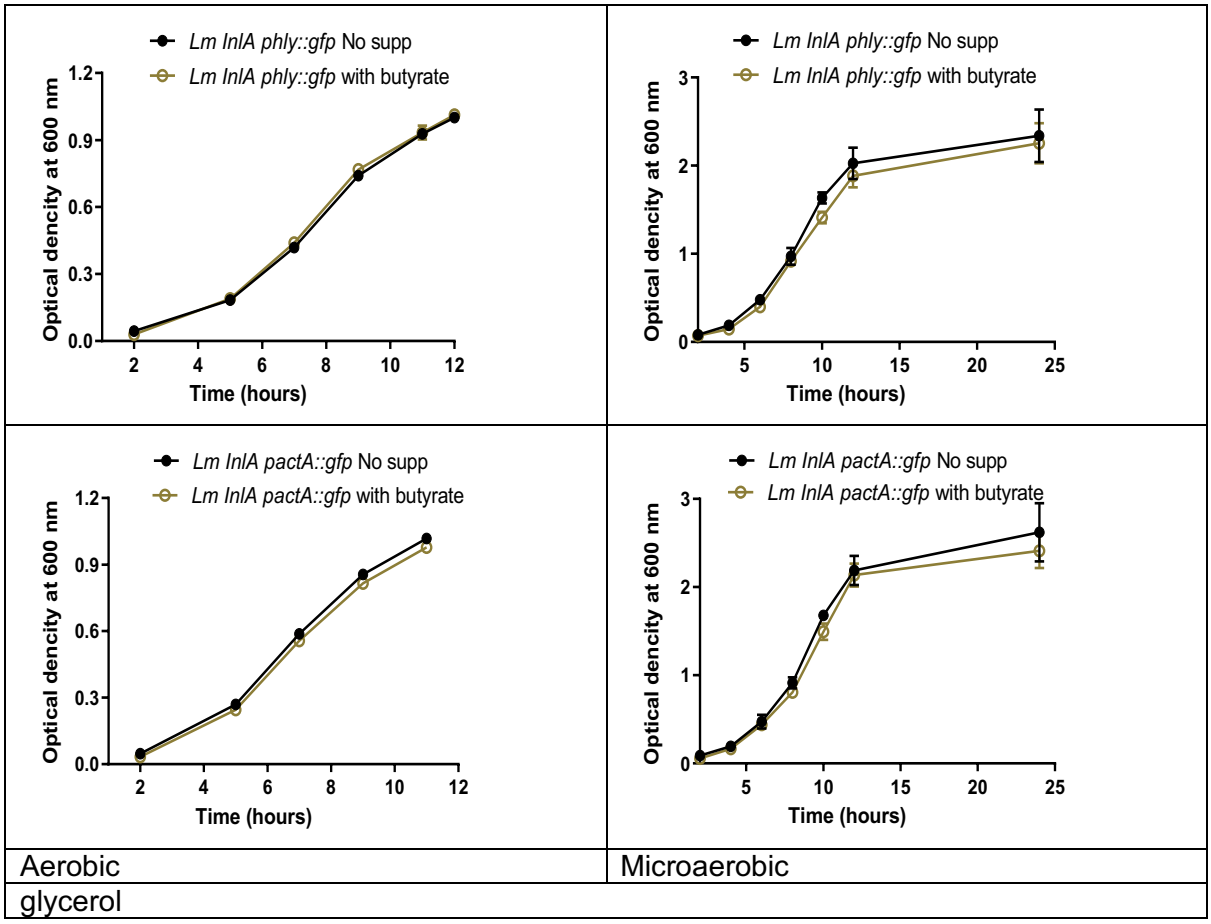

Figure 3.5 The growth curves of *L. monocytogenes* InlA strains grown aerobically or microaerobically in MD10 glycerol medium with or without 5 mM butyrate. The first column shows the growth under aerobic while the second column shows the growth under microaerobic conditions. The growth of *L. monocytogenes* InlA *phly*::*gfp* is shown in the top row and the bottom row shows the growth of *L. monocytogenes* InlA *pactA*::*gfp*. Means of triplicates were plotted with error bars representing standard deviation. The result is the mean of at least three independent experiments.

3.6. The effect of 5-HT on growth of *L. monocytogenes* InlA strains in MD10 using glucose as a carbon source

To establish effect if any of 5-HTon the growth of *L. monocytogenes*, the growth was measured for *L. monocytogenes* strains under microaerobic and aerobic conditions in minimal medium MD10 using glucose as a carbon source. The growth was measured for *L. monocytogenes* InlA, *L. monocytogenes* InlA *phly::gfp* and *L. monocytogenes* InlA *pactA::gfp* strains. The strains showed statistically signifiicant (*p* values 0.0003 to 0.00003) better growth in microaerobic conditions as the final OD_{600} reached to 2.3 compared to aerobic conditions

where is the final OD_{600} reached to 1.1 (Figure 3.6). The addition of 100 µM 5-HT has no significant effect on the growth of *L. monocytogenes* strains either aerobically (*p* values 0.08 to 0.27) or microaerobically (*p* values 0.04 to 0.08).

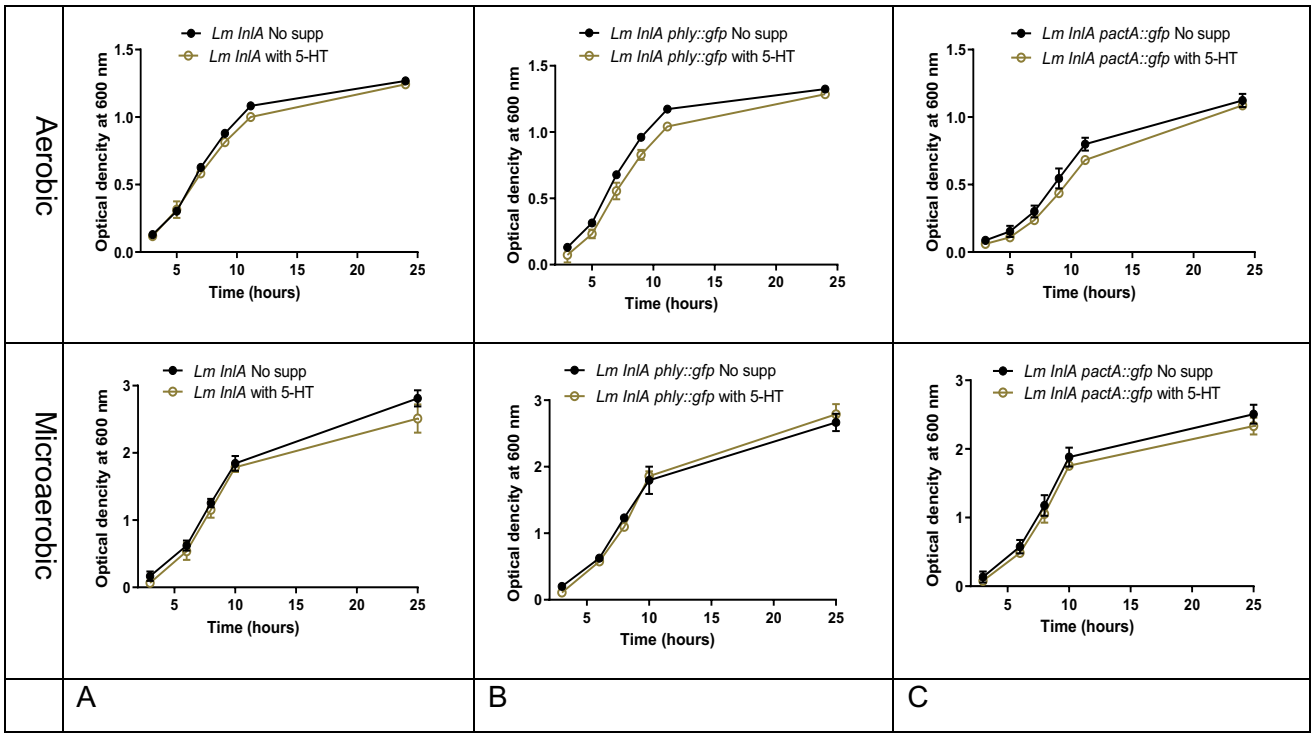

Figure 3.6 The growth curves of *L. monocytogenes* strains grown aerobically or microaerobically in MD10 glucose medium with or without 100 µM 5-HT. The data in column A represents *L. monocytogenes* InlA while panels B and C represent *L. monocytogenes* InlA *phly::gfp* and *L. monocytogenes* InlA *pactA*::*gfp* respectively. Means of triplicates were plotted with error bars representing standard deviation. The result is the mean of at least three independent experiments.

3.7. The effect of the combination of 5-HT and butyrate on growth of *L. monocytogenes* InlA strains in MD10 using glucose as a carbon source

To investigate whether butyrate and 5-HT might act together to affect the growth of *L. monocytogenes,* the growth of *L. monocytogenes* strains under microaerobic and aerobic conditions in defined medium MD10 using glucose as a carbon source was measured. The growth was measured for *L. monocytogenes* InlA, *L. monocytogenes* InlA *phly::gfp* and *L. monocytogenes* InlA *pactA::gfp* strains. (Figure 3.7) The results showed that the combination of 100 µM 5-HT with 5 mM butyrate inhibited the growth of the strains under microaerobic conditions whereas no changes were detected under aerobic conditions.

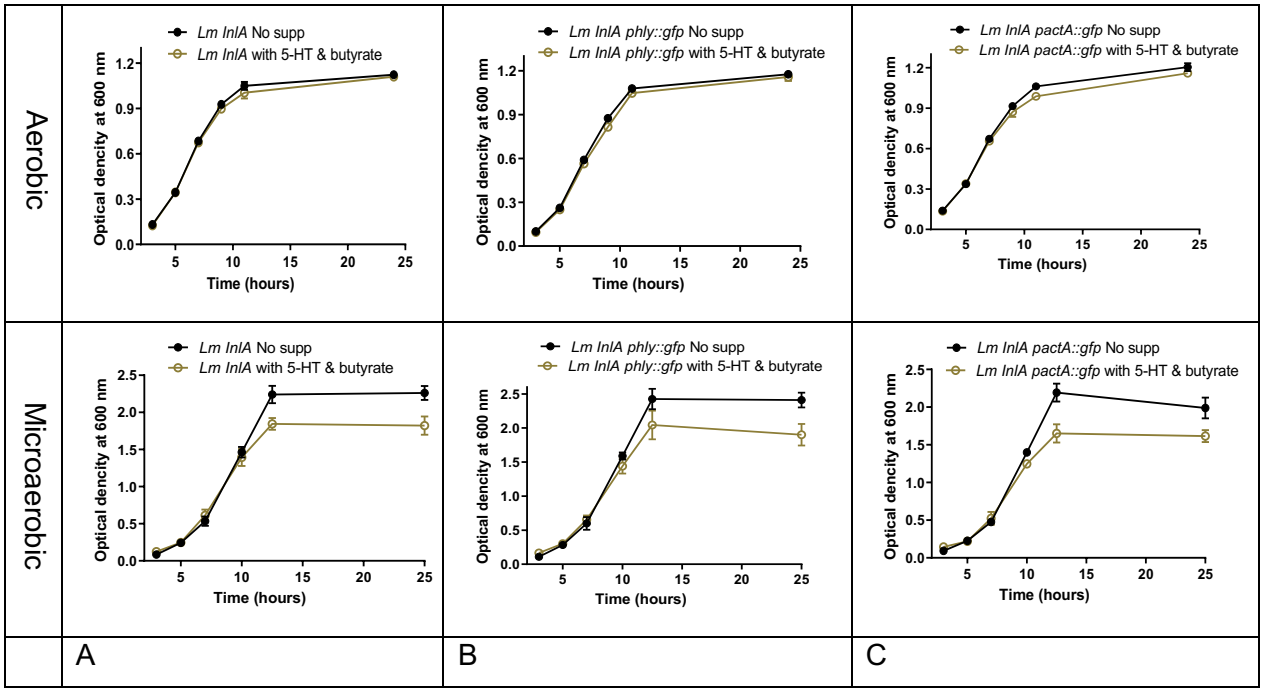

Figure 3.7 The growth curves of *L. monocytogenes* strains grown in MD10 glucose medium under aerobic and microaerobic conditions with or without butyrate or 5-HT. The strains were grown at 37 ºC with and without 100 µM 5-HT and 5 mM butyrate under aerobic (the top row) and microaerobic 5 % (v/v) oxygen (the bottom row) conditions. Data in column A presents *L. monocytogenes* InlA while columns B and C present *L. monocytogenes* InlA *phly*::*gfp* and *L. monocytogenes* InlA *pactA*::*gfp* respectively. Means of triplicates were plotted with error bars representing standard deviation. The result is the mean of at least three independent experiments.

3.8 The level of Gfp expression from *phly* and *pactA* using either glucose or glycerol as a carbon source, supplemented with either butyrate, 5-HT or both butyrate and 5-HT.

To test the variation of carbon source under different conditions of growth, the strains were grown in MD10 medium using glucose or glycerol as carbon source at 37 ºC under aerobic and microaerobic conditions. There was a significant increase (approximate ten-fold) from *phly* and *pactA* in MD10 under microaerobic conditions compared to aerobic conditions regardless of the carbon source (Figure 3.8). Expression of the *phly* was 5000 RFU/OD_{600} following aerobic growth in glucose but increased to 90,000 RFU/OD_{600} following microaerobic growth while in glycerol it reached 12,000 RFU/OD_{600} under aerobic conditions compared to 120,000 RFU/OD_{600} under microaerobic conditions. Expression of the *pactA* was low 700 RFU/OD_{600}following aerobic growth in glucose but increased to 8000 RFU/OD_{600} following

microaerobic growth whereas glycerol it reached 2500 RFU/OD_{600} under aerobic conditions compared to 20,000 RFU/OD_{600} under microaerobic conditions. From these data one can conclude the following. First, that as predicted expression from either *phly* or *pactA* was greater when glycerol was used as a carbon source compared to glucose regardless of the oxygen levels. Secondly, expression from both *phly* and *pactA* was increased following microaerobic growth. Thirdly, the expression from both *phly* and *pactA* was increased in microaerobic conditions when glucose was the carbon source. This indicates that the low oxygen conditions are able to relieve the catabolite repression of glucose.

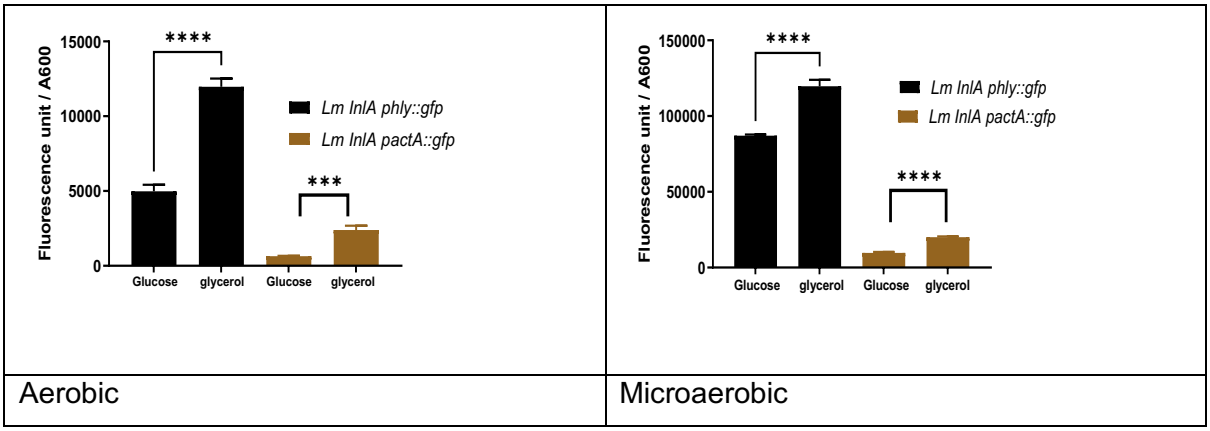

Aerobic	Microaerobic

Figure 3.8 The level of Gfp expression from *phly* and *pactA* under aerobic and microaerobic conditions using glucose or glycerol as a carbon source. The strains were grown at 37 ºC in MD10 medium using glucose or glycerol as a carbon source. The activity was measured after O/N growth. The data are the mean of three independent experiments. Significant differences (***p<0.0001; **** p < 0.00001) were calculated using one-way ANOVA.

3.9. The level of Gfp expression from *phly* and *pactA* under different growth conditions in MD10 using glucose as a carbon source

To assess potential transcriptional effects of the butyrate and 5-HT on the PrfA regulon and therefore likely pathogenesis of *L. monocytogenes*, we measured the levels of Gfp expression in cultures of *L. monocytogenes InlA phly::gfp* and *L. monocytogenes InlA pactA::gfp* under aerobic or microaerobic conditions with or without 100 µM 5-HT and 5 mM butyrate. There was higher induction from *phly* and *pactA* in MD10 using glucose as a carbon source under microaerobic conditions compared to aerobic conditions with and without butyrate (Figure 3.9).

Expression of the *pactA* was low (800-900 RFU/OD_{600}) following aerobic growth in MD10 but increased to (4,500 RFU/OD_{600}) following microaerobic growth. Similarly, expression of the *phly* was (6,400 RFU/OD_{600}) following aerobic growth in MD10 but increased to (40,000 RFU/OD_{600}) following microaerobic growth. Therefore, there was higher induction from *phly* and *pactA* in MD10 under microaerobic conditions compared to aerobic conditions with and without butyrate (Figure 3.9). The addition of 5 mM butyrate resulted in a significant decrease in the transcription from the *phly* and *pactA* in MD10 medium under aerobic and microaerobic conditions (Figure 3.9). However, there was no significant difference between expression from *phly* in MD10 with addition of 5-HT under aerobic and microaerobic conditions while addition of 5-HT resulted in a significant decrease in transcriptional from *pactA* only under microaerobic conditions (Figure 3.9). The addition of butyrate and 5-HTtogether resulted in a significant reduction in the expression through *phly* and *pactA* under microaerobic conditions whereas no significant reduction in expression was detected under aerobic conditions.

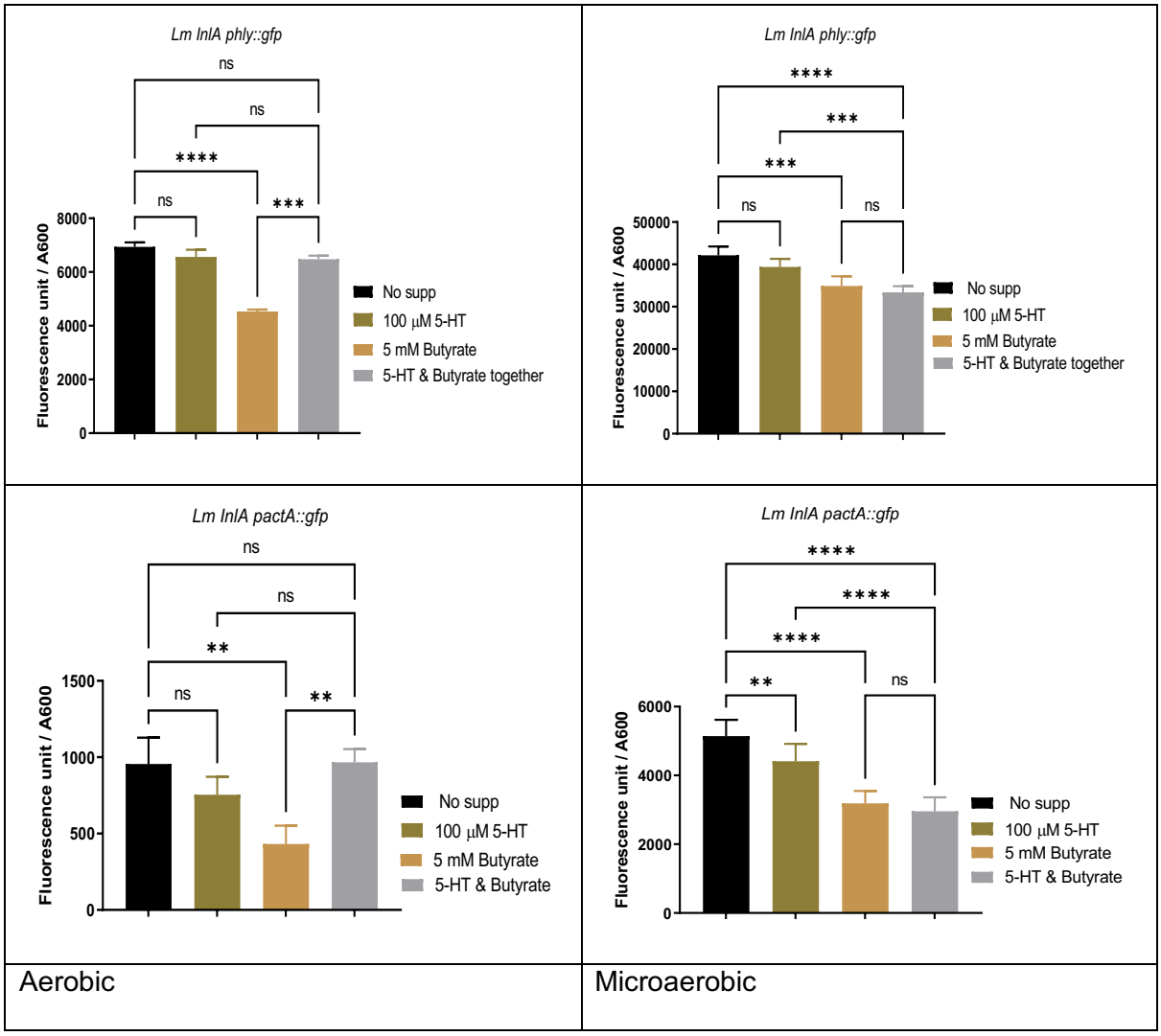

Figure 3.9 Transcription from *phly* and *pactA* promoters in *L. monocytogenes* strains grown aerobically or microaerobically in MD10 glucose medium with or without 5-HT, butyrate or both. The Gfp expression was measured after O/N growth. The data are the mean of five independent experiments. Significant differences (**p<0.05; ***p<0.0001; ****p< 0.00001) were calculated using two way ANOVA.

3.10. The effect of butyrate on level of Gfp expression from *phly* and *pactA* in MD10 using glycerol as a carbon source.

The effect of butyrate on *L. monocytogenes* was tested at the transcriptional level using *hly* and *actA* reporter strains. The reporter strains were cultured O/N in MD10 using glycerol as a carbon source with 5 mM butyrate under aerobic and microaerobic conditions (Figure 3.10). The addition of butyrate resulted in a significant decrease in the transcription from *phly* and *pactA* in MD10 medium under microaerobic conditions. In contrast, under aerobic conditions,

no effect on expression when supplemented with butyrate. There was higher induction from *phly* and *pactA* under microaerobic conditions compared to aerobic conditions with and without butyrate (Figure 3.10).

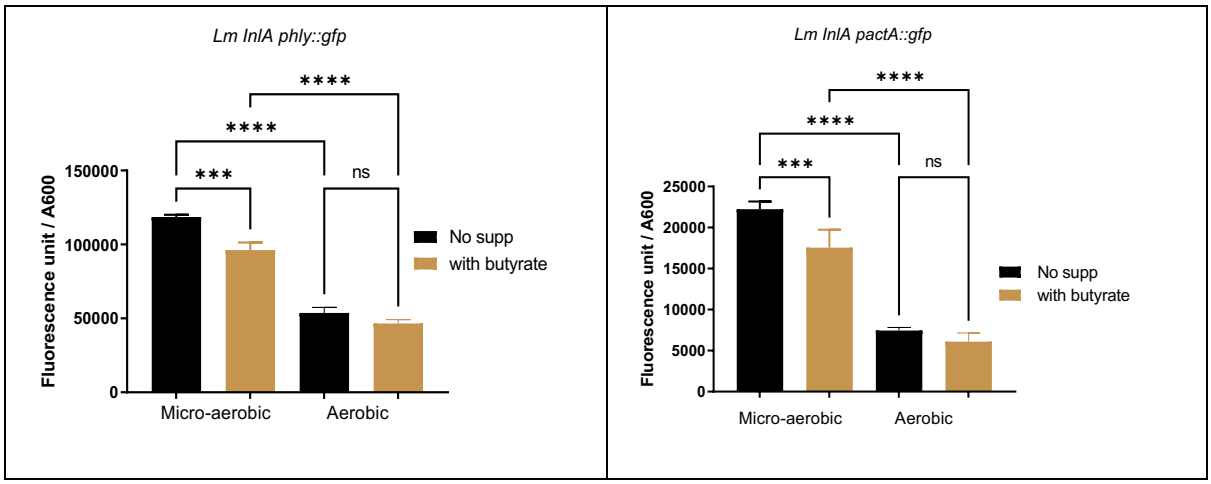

Figure 3.10 Transcription from *phly* and *pactA* promoters in *L. monocytogenes* strains grown aerobically or microaerobically in MD10 glycerol medium. The Gfp expression was measured after O/N growth. The data are the mean of five independent experiments. Significant difference (**p<0.05; ***p<0.0001; ****p< 0.00001) were calculated using two-way ANOVA.

3.11. Discussion

The intracellular life cycle of *L. monocytogenes* has been studied in immense detail and has provided many insights into the functioning of eukaryotic cells (Rolhion and Cossart, 2017). Although the mechanisms by which *L. monocytogenes* adapts to and resists the action of acid and bile salts has been studied (Gahan and Hill, 2005), much less is known about the adaptation to other stimuli encountered during transit in the intestine prior to invasion. Such stimuli that include microaerobic interaction, and competition with resident microbiota, exposure to host derived molecules such as 5-HT and secretions from mucosal surfaces. As well as SCFA which secreted by the host gut microbiota and play important roles in gut homeostasis and signalling between the gut microbiota and the host, exerting effects at sites distal to the gut (Spohn and Mawe, 2017). These signals will need to be integrated in adapting to the new environment. Therefore, the hypothesis of this study was that prior to adhesion and invasion *L. monocytogenes* adapts to the environment in the small intestine and switches on the PrfA regulon in response to signals like SCFA and 5-HT.

This study tested the effect of butyrate on PrfA regulon through transcription level of *phly* and *pactA*. Although the addition of 5 mM butyrate had no effect on the growth of *L. monocytogenes*, it resulted in a significant decrease in the transcription level from *phly* and *pactA* regardless of media or oxygen levels used in the experiment. Likewise, previous research reported that at high levels of butyrate (250 mM), the production of virulence factors was inhibited in *L. monocytogenes* (Sun *et al.,* 2012). The choice of 5 mM butyrate was based on the physiological concentration of butyrate in the intestine (Peng *et al.,* 2007) whereas 250 mM is 50 times greater than this and so any effects on gene expression in *L. monocytogenes* have to be treated with some caution. This inhibitory action of SCFA may represent some level of protection provided by the existing microbiota to *L. monocytogenes* infection.

In terms of the media, the defined medium was used to avoid the possibility that butyrate or 5-HT might be sequestered by proteins in TSB and to avoid any issues of contaminating

butyrate or 5-HT that might be in the TSB medium. In addition, the use of defined media allowed the effect of carbon source to be investigated. It is known that when *L. monocytogenes* are grown in culture medium containing phosphoenolpyruvate phosphotransferase system (PTS) sugars such as glucose, the expression of PrfA-regulated gene products is inhibited directly or indirectly (Hansen *et al*., 2020). The production of virulence factors can also be increased by carbon sources such as glucose-1-phosphate (Wallace, 2018). For that reason, glycerol was used in the medium as a control of the system and during intracellular growth glycerol and other 3 carbon sugars are the preferred sources of carbohydrate. In addition, the results showed a significant increase in the PrfA activity as measured by *phly* and *pactA* transcription when glycerol was used as carbon source and this expression was much higher under microaerobic condition compared to aerobic (Figure 3.10). This increased PrfA activity could reflect increased levels of the PrfA protein (see section 4.5). Thus, carbon sources play a significant role in virulence regulation in *L. monocytogenes*. Significantly, particularly in the context of growth in the small intestine under low oxygen conditions the effect of glucose on inhibiting PrfA activity, was overridden by microaerobic conditions. This suggests that even in the small intestine where levels of dietary glucose maybe high the effect of microaerobic condition still induces the PrfA regulon.

To date a little known about the interaction between 5-HT and *L. monocytogenes.* A previous study (Latorre *et al*., 2016) examined how *L. monocytogenes* inhibits expression of the 5-HT uptake transporter SERT in enterocytes. This inhibition of 5-HT uptake will locally increase the levels of 5-HT thereby affecting both *L. monocytogenes* and the physiology of epithelial cells at the site of invasion, potentially facilitating the invasion by *L. monocytogenes* (Latorre *et al*., 2016). In contrast, my data showed that no significant affect was detected on either the growth of *L. monocytogenes* or the *phly* or *pactA* expression with 5-HT supplementation except from *pactA* promoter under microaerobic conditions (Figure 3.9). However, the combination of 5-HT and butyrate resulted in inhibition of the growth under microaerobic conditions but not under aerobic conditions. Therefore, the results suggest that this combination might be toxic

for *L. monocytogenes* with low oxygen. On the whole, according to these results, oxygen concentrations play an important role in regulating the PrfA regulon in *L. monocytogenes.*

Chapter 4 The role of SigmaB and PrfA in regulating gene expression during microaerobic growth.

4.1. Introduction

SigmaB and PrfA are essential factors for *L. monocytogenes* to survive in different environments encountered within the host. As mentioned previously, PrfA is the master regulator of virulence gene expression in *L. monocytogenes* with a number of genes essential for virulence being part of the PrfA regulon including *hly* and *actA* which were investigated in this study. SigB is sigma factor activates the transcription of genes necessary to regulate the stress response in *L. monocytogenes* (Sibanda and Buys, 2022). The results from the previous chapter showed that an increase of the Gfp expression from *phly* and *pactA* in MD10 medium under microaerobic conditions. One of the next questions was whether this activity due to that PrfA or SigB regulations and how has the induction been mediated under the microaerobic conditions?

4.2. The effect of a SigmaB mutation on growth and level of *phly* and *pactA* expression in MD10 medium using glycerol as a carbon source

To establish if the *sigB* mutation affected the the growth of *L. monocytogenes* strains in the defined MD10 medium with glycerol as a carbon source, the growth was measured by following OD_{600} under aerobic (Figure 4.1 panel B) and microaerobic (Figure 4.2 panel B). Under aerobic conditions, the *sigB* mutation resulted in an increase in the lag phase with an OD_{600} of 0.28 after 10.5 h in strain *ΔsigB phly*, although once growth was initiated the growth rate appeared similar to that of the wild type strain with both strains reaching a similar OD_{600} of 1.5 after 25 h (Figure 4.1 panel B). Similarly, under microaerobic conditions, the *sigB* mutation resulted in a pronounced lag phase but both strains reached to the same OD_{600} of 2.5 in stationary phase after 30 h. Because *sigB* mutations are known to affect the survival of the bacteria in stationary phase (Sibanda and Buys, 2022), the prounounced lag phase with

the *sigB* mutant could reflect that there are less viable cells in the inoculum from the overnight culture. To further investigate the role of *sigB* on the expression from *phly* and *pactA,* gfp expression was measured in *L. monocytogenes strains* carrying a *sigB* mutation (Figure 4.1, Figure 4.2 panel A). As a result, transcription from *phly* with *sigB* mutation increased significantly under microaerobic and aerobic conditions at all point of growth process. In contrast, transcription from *pactA* showed a trend of increased activity in a *sigB* mutation but this increase was only significant in mid-log phase during aerobic growth.

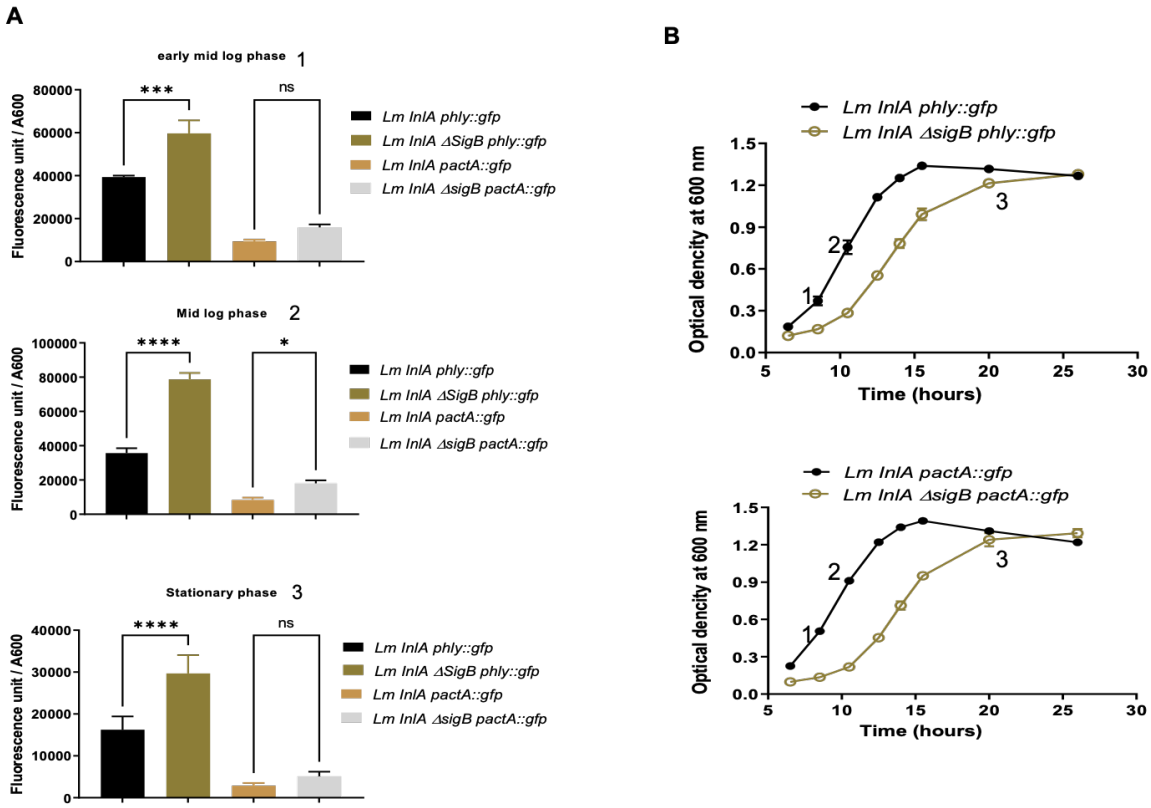

Figure 4.1 The growth curves and level of Gfp expression of *L. monocytogenes sigB* mutant in MD10 medium with glycerol as a carbon source under aerobic conditions. Panel A shows Gfp expression level. Panel B shows the growth of *L. monocytogenes InlA* Δ*sigB phly::gfp* and *L. monocytogenes* InlA Δ*sigB pactA*::*gfp*. The number in the curves 1,2 and 3 represent the time points at which Gfp was measured. Means of triplicates were plotted with error bars representing standard deviation. The result is the mean of at least three independent experiments. Significant difference (*p<0.05; ***p<0.0001; ****p<0.00001) were calculated using one-way ANOVA.

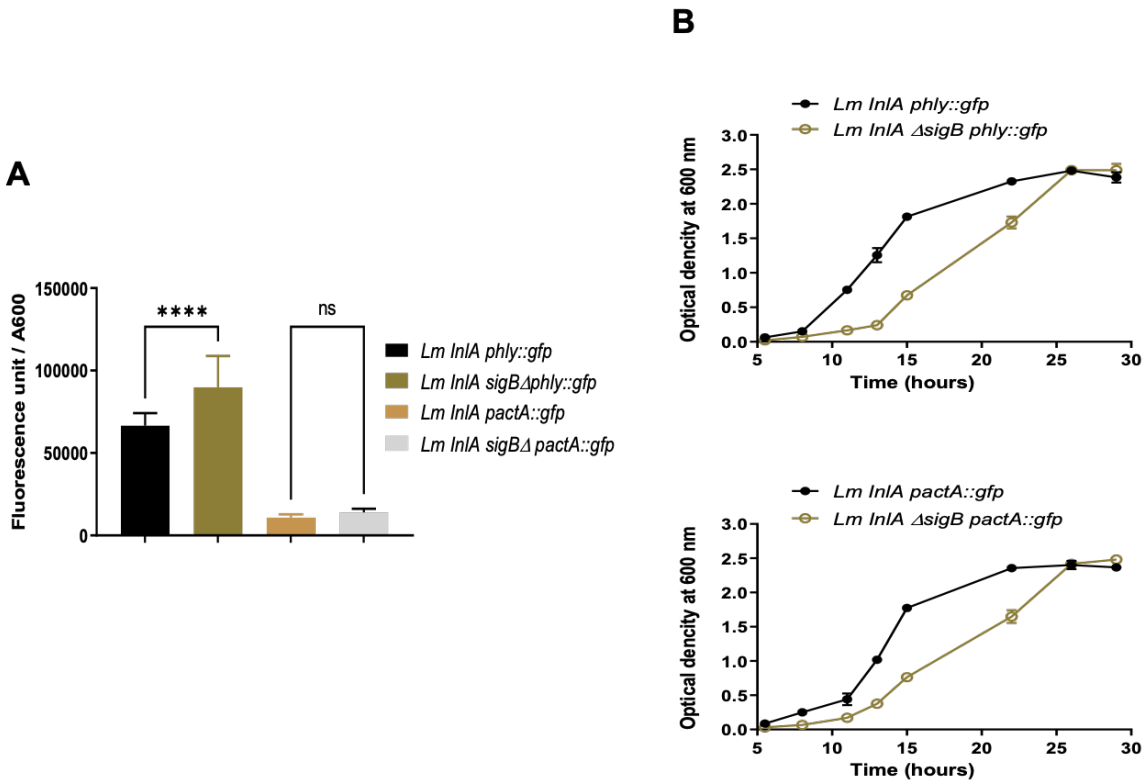

Figure 4.2 The growth curves and level of Gfp expression of *L. monocytogenes sigB* mutant grown under microaerobic conditions in MD10 medium with glycerol as a carbon source. Panel A shows gfp expression level. Panel B shows the growth of *L. monocytogenes InlA* Δ*sigB phly::gfp* and *L. monocytogenes* InlA Δ*sigB pactA*::*gfp*. The data are the mean of three independent experiments. Significant difference (0.00001< ****, p < 0.0001) were calculated using one-way ANOVA.

4.3. The effect of a *sigB* mutation on growth and level of *phly* and *pactA* expression in MD10 medium using glucose as a carbon source

To determine the consequences of a *sigB* mutation on the growth of *L. monocytogenes* strains using glucose as a carbon source, the growth was measured by following OD_{600} under aerobic and microaerobic conditions (Figure 4.3) in MD10 using glucose as a carbon source. Under aerobic conditions, the *sigB* mutation in the strains resulted in a reduction in the growth rate compared to isogenic strains with *sigB* (*L. monocytogenes InlA phly::gfp* or *pactA::gfp*) but reached to the same final OD_{600} of 1.9 in stationary phase after 25 h. Similarly, under microaerobic conditions, the *sigB* mutation resulted in a slight reduction in the growth rate compared to *sigB* wildtype strains but reached to the same final OD_{600} of 3.3 in stationary

phase after 25 h. To find out the role of SigB on the expression of *phly* and *pactA* the level of Gfp expression was measured following growth (Figure 4.4). The results showed no significant difference in the transcription from *phly* or *pactA* in a *sigB* mutant under aerobic growth conditions around 467 RFU/OD_{600} or 389 RFU/OD_{600} respectively. In contrast in microaerobic growth conditions the *sigB* mutation resulted in a significant increase in transcription from *phly* that reached 25272 RFU/OD_{600} compared to wildtype 22887 RFU/OD_{600}. The *sigB* mutation had no significant effect on transcription from *pactA* with both the mutant and wildtype reaching under microaerobic around 3360 RFU/OD_{600} (Figure 4.4)

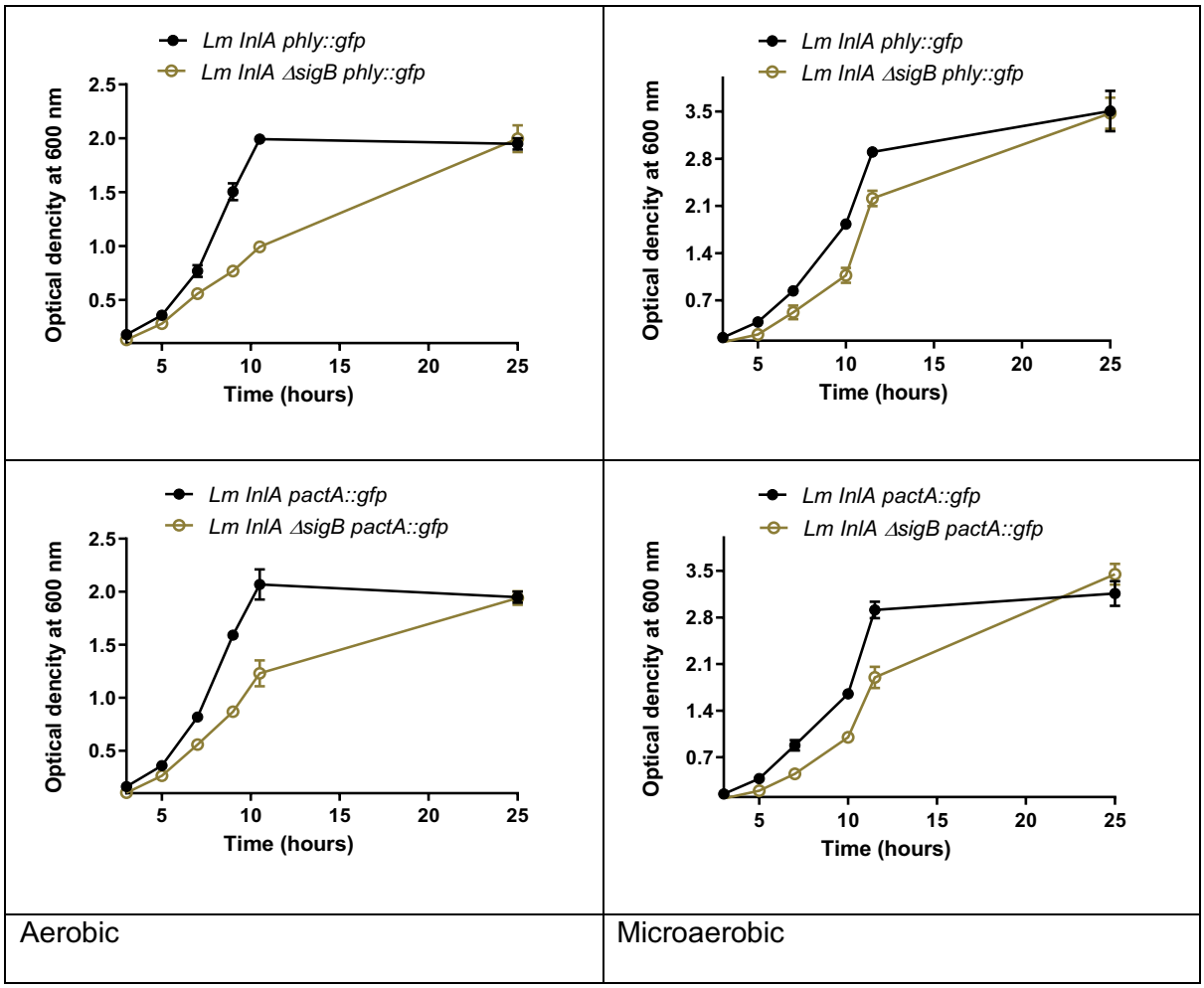

Figure 4.3 The effect of a *sigB* mutation on the growth of *L. monocytogenes* in MD10 medium using glucose as carbon source under aerobic and microaerobic conditions. The top row presents *L. monocytogenes* InlA Δ*sigB phly::gfp* while the middle row presents *L. monocytogenes* InlA Δ*sigB pactA::gfp*. Means of triplicates were plotted with error bars representing standard deviation. The result is the mean of at least three independent experiments.

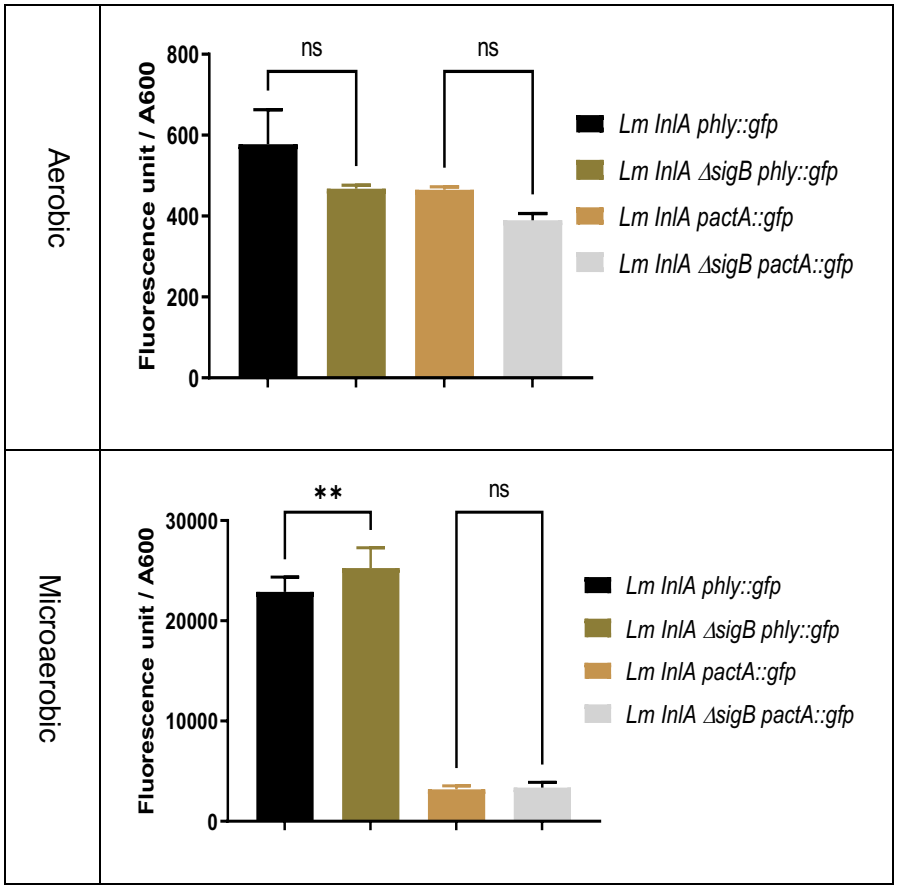

Figure 4.4 The effect of a sigB mutation on expression from *phly* or *pactA* following growth of *L. monocytogenes* in MD10 medium using glucose as a carbon source under aerobic and microaerobic conditions, The Gfp expression was measured after O/N growth. The data are the mean of three independent experiments. Significant differences (**p<0.001) were calculated using one-way ANOVA.

4.4. The effect of a *prfA* mutation on the growth and level of *phly* or *pactA* transcription in MD10 medium.

To test the effect of a *prfA* mutation on the growth of *L. monocytogenes*, the growth was measured of *prfA* mutant strains with either *phly::gfp* and *pactA::gfp* fusions and compared to an isogenic wild type strain harbouring the same fusions by following OD_{600} under aerobic (Figure 4.5) and microaerobic (Figure 4.6) conditions in MD10 medium using glucose or glycerol as a carbon source. The presence of a *prfA* mutation had no effect on the growth of *L. monocytogenes* strains under aerobic conditions, regardless of the carbon source used with the exception of the strain with a *phly::gfp* fusion where the *prfA* mutation had a significant

effect following growth with glycerol as a carbon source (*p* value 0.003) (Figure 4.5). The presence of a *prfA* mutation led to a reduction in the final OD_{600} of 1.2 after 11 h when glucose was used as a carbon source for the *L. monocytogenes InlA phly::gfp* strain compared with OD_{600} of 1.9 for the wildtype strain under microaerobic conditions. Similarly, the effect of *prfA* mutation on the same strain resulted in reducing the OD_{600} of 1.1 after 15 h growth. This was compared to an OD_{600} of 2 of the wildtype strain when glycerol was provided as a carbon source. Furthermore, the presence of *prfA* mutation in the *L. monocytogenes InlA pactA::gfp* when glucose was used as a carbon source resulted in reducing the OD_{600} of 0.1 in lag phase after 6 h and the growth continuous to reach OD_{600} 0.8 after 10 h in log phase and then to OD_{600} of 1.2 after 13.5 h compared to the wildtype strain which was the OD_{600} 0.5 in lag phase after 6 h and the growth continuous to reach OD_{600} 1.5 after 10 h in log phase and then to OD_{600} of 1.9 after 13.5 h. Overall, the mutation of *prfA* affected negatively the growth of *L. monocytogenes* under microaerobic conditions.

The prediction was that the observed changes in *phly* and *pactA* activity were due to the PrfA protein, to confirm this, the fluorescence assay was carried out in a *L. monocytogenes prfA* mutant (Figure 4.7). The results revealed that *prfA* mutants abolished detectable transcription from *phly* and *pactA* in MD10 when glucose or glycerol was used as the carbon source under aerobic or microaerobic conditions.

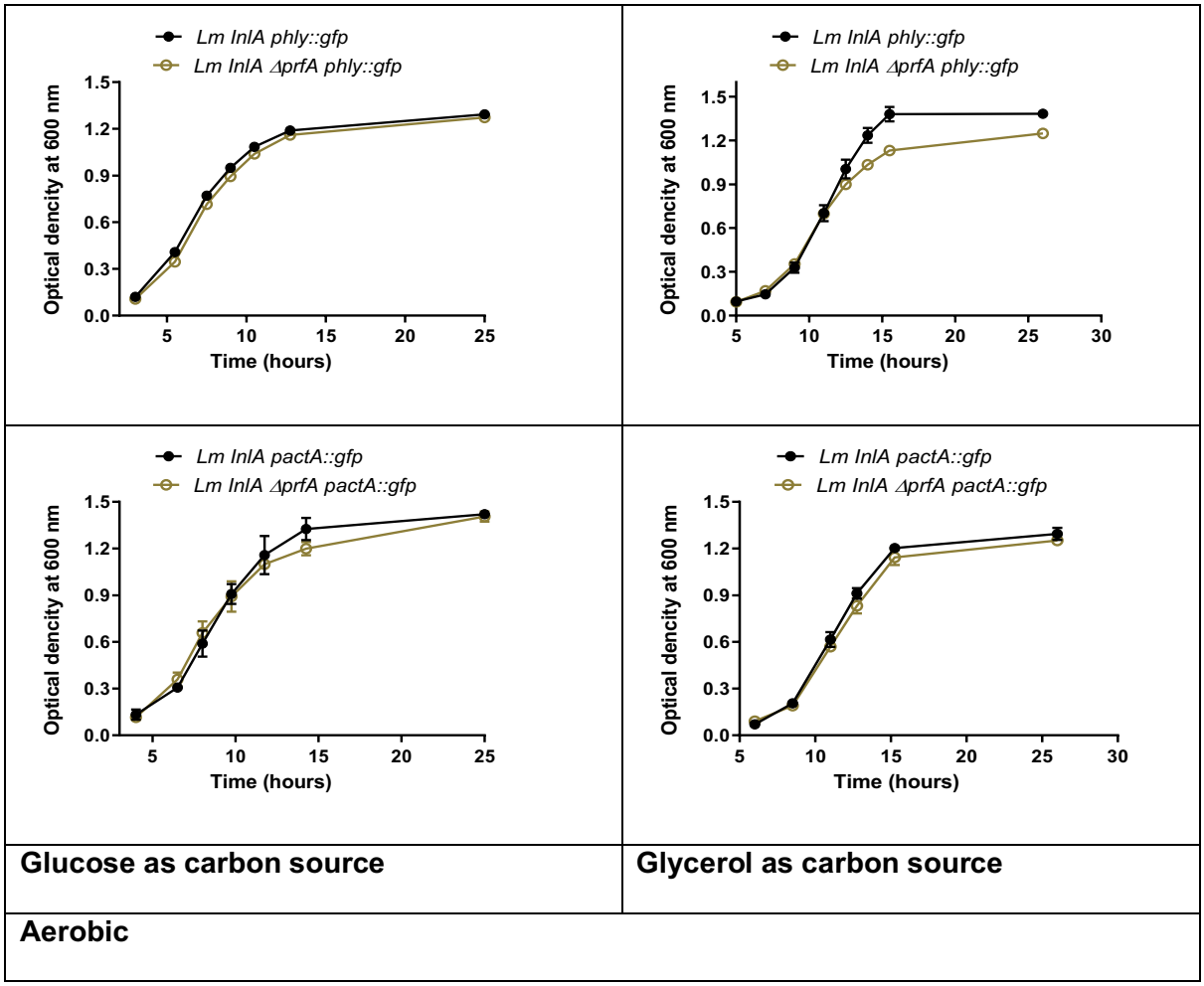

Figure 4.5 The effect of a *prfA* mutation on growth of *L. monocytogenes* in MD10 under aerobic growth conditions. The top row presents *L. monocytogenes InlA ΔprfA phly::gfp* while the middle row presents *L. monocytogenes InlA ΔprfA pactA::gfp*. Means of triplicates were plotted with error bars representing standard deviation. The result is the mean of at least three independent experiments.

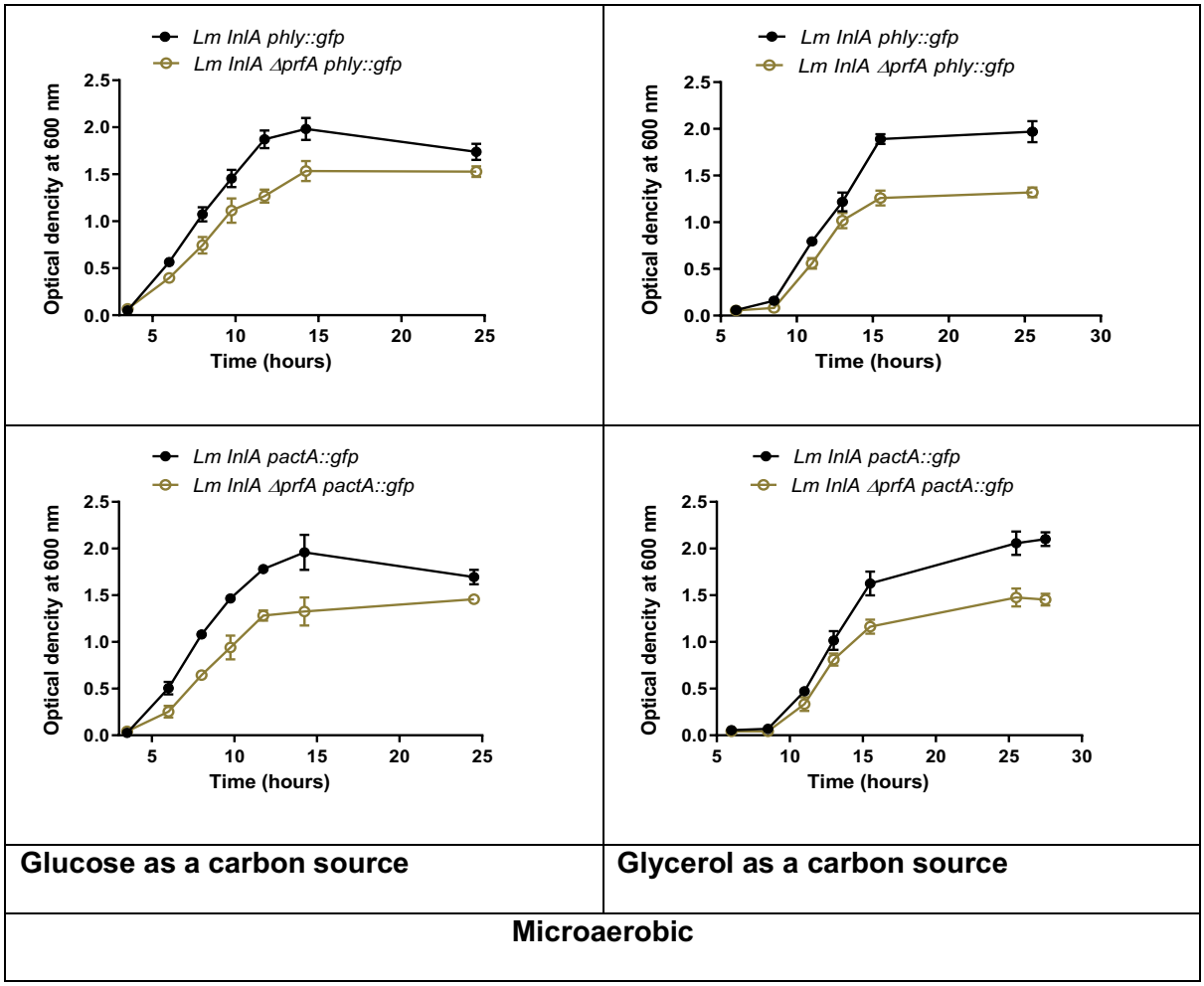

Figure 4.6 The effect of a *prfA* mutation on growth of *L. monocytogenes* in MD10 under microaerobic growth conditions. The top row presents *L. monocytogenes InlA ΔprfA phly::gfp* while the middle row presents *L. monocytogenes InlA ΔprfA pactA::gfp*. Means of triplicates were plotted with error bars representing standard deviation. The result is the mean of at least thr ee independent experiments. The effect of the *prfA* mutation on growth was significant in all cases. For the strain *L. monocytogenes InlA ΔprfA phly::gfp* the *p* values were 0.023 and 0.0008 respectively for growth with glucose or glycerol as a carbon source. For the strain *L. monocytogenes InlA ΔprfA pactA::gfp* the *p* values were 0.007 and 0.008 respectively for growth with glucose or glycerol as a carbon source. The *p* values were calculated using a Multiple T test.

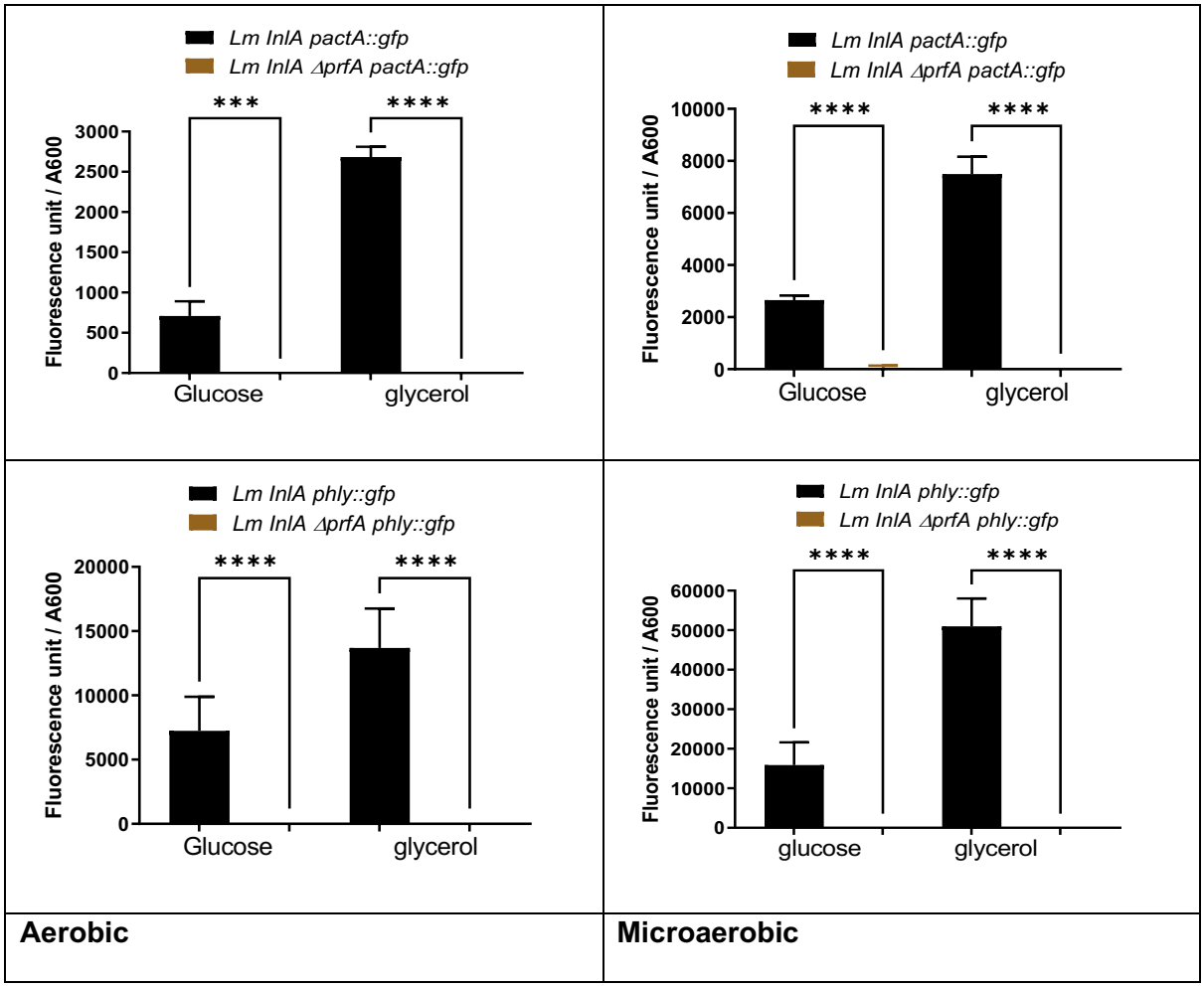

Figure 4.7 The effect of a *prfA* mutation on level of expression from *phly* and *pactA* during growth in MD10 with either glucose or glycerol as a carbon source under aerobic and microaerobic conditions. The gfp expression was measured after O/N growth. The data are the mean of three independent experiments. Significant differences (***p<0.0001; ****p<0.00001) were calculated using one-way ANOVA.

4.5. The effect of microaerobic conditions on the level of the PrfA, LLO and ActA proteins.

The results to date have measured the level of both the *phly* and *pactA* promoters, but it is important to establish if these increases in transcription also result in increased levels of the LLO and ActA proteins. Likewise, it is important to establish if the increased activity of the *phly* and *pactA* promoters was due to increased levels of the PrfA protein under these conditions. To examine the effect of microaerobic conditions on levels of PrfA, LLO and ActA proteins western blotting using specific antisera was performed. Image lab densitometry software was

used to determine the fold change in protein levels. The sample grown in glycerol containing medium aerobically was taken as 1 and all other conditions were compared against that value. The fold changes for PrfA, LLO and ActA were normalized by dividing the fold change for each condition by the relative value of P60 normalised against the P60 value for the culture grown in glycerol containing medium aerobically (Figure 4.8). The results showed that under aerobic conditions there was greater PrfA protein levels when glucose was a carbon source rather than glycerol. Microaerobic conditions induce expression of PrfA regardless of the carbon source, but the levels of PrfA protein are greatest when glucose is the carbon source. The levels of the LLO and ActA proteins are increased under microaerobic conditions with the highest levels being when glycerol is the carbon source (Figure 4.8).

Specifically, the LLO protein showed a 3.72-fold increase under microaerobic conditions utilizing glycerol as a carbon source in comparison to aerobic conditions with the same carbon source. No LLO was detectable following growth in aerobic conditions with glucose as a carbon source. However, following growth in microaerobic conditions with glucose as a carbon source there was detectable LLO expression at a level of 0.2 fold compared to that following aerobic growth with glycerol as the carbon source (Figure 4.8). Therefore microaerobic condtions are switching on expression of LLO when either glucose or glycerol was used as the carbon source. The ActA protein was detectable following growth in aerobic conditions with glycerol as the carbon source but showed a 15.43-fold increase under microaerobic conditions. No ActA expression was detected following aerobic growth with glucose as the carbon source, but following microaerobic growth there was a 1.15-fold increase. As a whole, these results indicate that the increased *phly* and *pactA* promoter activity induced by microaerobic conditions do result in increased levels of LLO and ActA and was in part due to increase PrfA expression.

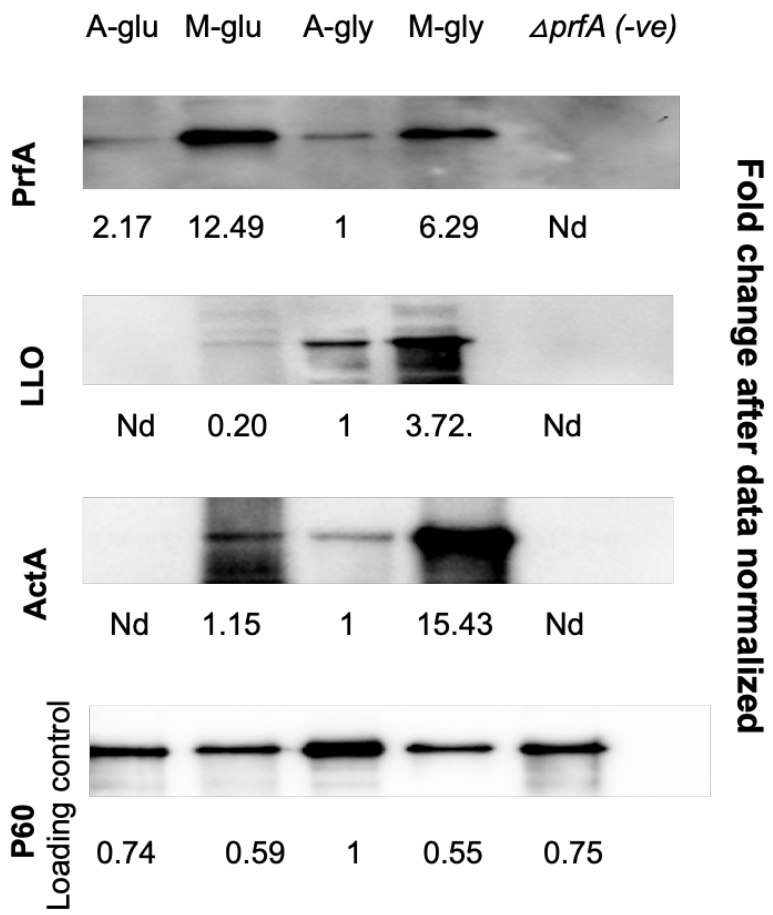

Figure 4.8 Representative expression of PrfA-regulated proteins under different growth condition. The protein was extracted from *L. monocytogenes InlA* wt grown in MD10 medium to an OD_{600} of 1.1 and analysed by Western blotting with anti-PrfA, anti-LLO, anti-ActA and anti-P60 antibodies (see material and method 2.15, 2.16). A-glu and A-gly mean (under aerobic condition using glucose or glycerol as a carbon source respectively), M-glu and M-gly mean (under microaerobic condition using glucose or glycerol as a carbon source respectively) and Nd (no detected band). Δ*prfA* was used as a negative control and P60 levels were used as a loading control. The loading of P60 in A-gly was taken as 1 and all other data normalized against that value. The numbers below the Western bolt reflect the normalized fold change. Additional Western blot data are presented in Appendix A.

4.6. Discussion

The general stress response in *L. monocytogenes* is controlled by the alternative sigma factor, SigB, which regulates gene expression, facilitating survival and protection from harsh environments (Guerreiro *et al*., 2020). It has been determined that SigB plays several roles in *L. monocytogenes* with the general stress response involving over 200 genes which include environmental stress survival, metabolism, and virulence (Sibanda and Buys, 2022). This ability to respond to a plethora of stress stimuli allows the smooth transition from the saprophytic environment to the pathogenic environment inside the host (Sibanda and Buys, 2022). Specifically, SigB is vital for *L. monocytogenes* to reach and survive in the gastrointestinal tract, regulating resistance to acid, osmotic stress and bile salts (Cotter *et al*., 2001; Sleator *et al*., 2001; Begley *et al*., 2005; Guariglia-Oropeza *et al*., 2018). In addition, there is overlap between the *sigB* and the *prfA* regulons showing the interdependence on adaptation to stress and virulence. For example, the *bsh* and *bilE* genes responsible for bile resistance are co-regated by both PrfA and SigB (O'Byrne and Karatzas) and likewise the *inlA* and *inlB* genes encoding essential adhesins for crossing the intestinal barrier are also co-regulated by both PrfA and SigB (Ollinger *et al.,* 2008). The observation that a *sigB* mutant showed increase *phly* activity in both aerobic and microaerobic conditions but had no significant effect on *pactA* activity is curious because SigB is not believed to be involved in the regulation of *phly* (Sibanda and Buys 2022). This might suggest that SigB is acting indirectly to activate *phly* something that merits further investigation.

The observation that a *sigB* mutant showed an increased lag phase in both aerobic and microaerobic conditions when glycerol and glucose were used as carbon source (Figures 4.1, 4.2 and 4.3) probably reflects the state of the inoculum. It is known that *sigB* mutants adapt less well to the stationary phase (Sibanda and Buys, 2022) such that the inoculum from an overnight culture of a *sigB* mutant may contain less viable bacteria. It had been shown previously that a *sigB* mutant of *L. monocytogenes* strain *10403S* displays an extended lag

phase of around 5 h when grown in defined medium utilizing glycerol as carbon sources (Abram *et al.,* 2008). In future experiments it would appropriate to enumerate the number of viable bacteria in the inocula used to avoid this problem.

The observation that a *prfA* mutant lacked any transcriptional activity from *phly* and *pactA* is not surprising based on the known function of PrfA (Gaballa *et al.,* 2019). What is interesting is that the increased transcription observed in microaerobic conditions is also PrfA dependent confirming that the microaerobic stimulus for increased *phly* and *pactA* activity is acting via PrfA and not some other microaerobic specific regulator. Of course, this raises the question of how this PrfA-mediated increase in expression of the PrfA regulon in microaerobic conditions is achieved. It is possible that there is more PrfA made under microaerobic conditions and/or that there is greater activation of the existing PrfA under microaerobic conditions via glutathione. The western blot shows that there is more PrfA protein in microaerobic conditions regardless of the carbon source (Figure 4.8). The finding that the levels of PrfA were greater in microaerobic conditions would indicate that more protein been made either in transcriptional level or post-transcriptional level (see Chapter 5.1).

The absence of *prfA* resulted in lower growth rates compared to the wildtype strains under microaerobic conditions. This suggests that some of the PrfA regulated genes are important but not essential for growth under microaerobic conditions. That could be due to the fact that the metabolism of the *prfA* mutant strain is altered in microaerobic conditions such that toxic by-products accumulate more rapidly or all of the available nutrients cannot be utilised. It is currently unknown if a *prfA* mutant is affected for anaerobic growth.

Overall, these results demonstrate that microaerobic conditions induce greater levels of the PrfA protein which in turn results in increased expression of key virulence factors *hly* and *actA.* As such, exposure to such conditions in the intestine of the host may indeed activate the PrfA regulon. One should appreciate that the microaerobic conditions used were generated in a VAIN incubator, which means that in addition to low oxygen there was also high levels of CO_2

(10%v/v). However, since the levels of CO_2 in the intestine range from 5-29% (Scaldaferri *et al.,* 2013) the level of CO_2 generated in the VAIN incubator would be in the range likely to be encountered by *L. monocytogenes.* The next question is to understand how this increased PrfA protein is achieved.

Chapter 5 The influence of microaerobic conditions on global gene expression

5.1. The effect of microaerobic conditions on *L. monocytogenes* transcript levels

5.1.1. Measuring the transcript levels of *prfA* by qRTPCR

To determine if the increase of the LLO, PrfA and ActA proteins under microaerobic conditions was due to increase of *prfA* transcription, qRTPCR was used to quantify the relative transcript under microaerobic conditions, using glucose or glycerol as a carbon source, by amplification of the target regions of *prfA* using the primer sets shown in Figure 5.1. Additionally, F-rpoB and R-rpoB primers were used to amplify 120 bp from housekeeping gene *rpoB* which served as an internal control. Before quantifying the relative transcript levels under microaerobic conditions, the standard curve for each gene was established by amplifying the targeted DNA using colony PCR of *L. monocytogenes* InlA strain with the corresponding primers' sets shown in Figure 5.1. The amplified DNA fragments were purified and the DNA concentration was defined using Qubit® 2.0 Fluorometer. The DNA stock concentration was prepared according to the required concentration to start with then serially diluted 1:10. The following delta-delta Ct formula was used to calculate fold gene expression (See section 2.12):

Average of CT value for the PrfA (interest gene) and rpoB (housekeeping gene)

Calculate ΔCt = average Ct (PrfA) – average Ct (rpoB)

$\Delta\Delta$Ct = ΔCt (Microaerobic condition) – ΔCt (Aerobic condition)

2^-($\Delta\Delta$Ct)

The relative standard curve for each gene is shown in Figure 5.2 and no primer dimer was detected in any of them.

The RNA was extracted from strains *L. monocytogenes* InlA after growing at 37 °C in MD10 using glucose or glycerol as a carbon source under aerobic and microaerobic conditions until

an OD_{600} of 0.5. From the extracted total RNA, 500 ng was used for reverse transcription into cDNA and 20 ng of cDNA was used per 20 µl reaction to perform qrtPCR assay.

As seen in Figure 5.3, the fold expression of *prfA* under microaerobic conditions compared with aerobic conditions using glucose as a carbon source reached 29-fold while it reached 10-fold when glycerol was used as a carbon source (*p* value 0.025). This increased level of transcription of the *prfA* gene under microaerobic conditions could explain the increased levels of PrfA protein observed following microaerobic growth.

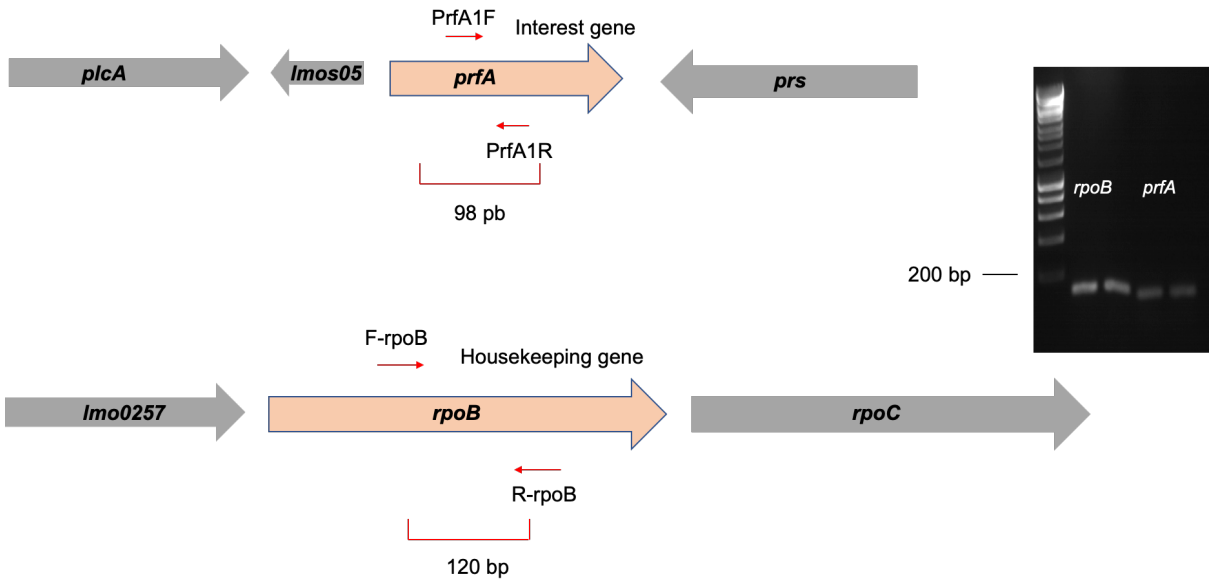

Figure 5.1 Illustration of the primers used in qrtPCR and their corresponding amplification. The figure shows the *prfA* and *rpoB* genes and the location of the primers used to amplify products for the qrtPCR. The agarose gel show the specific PCR products amplified.

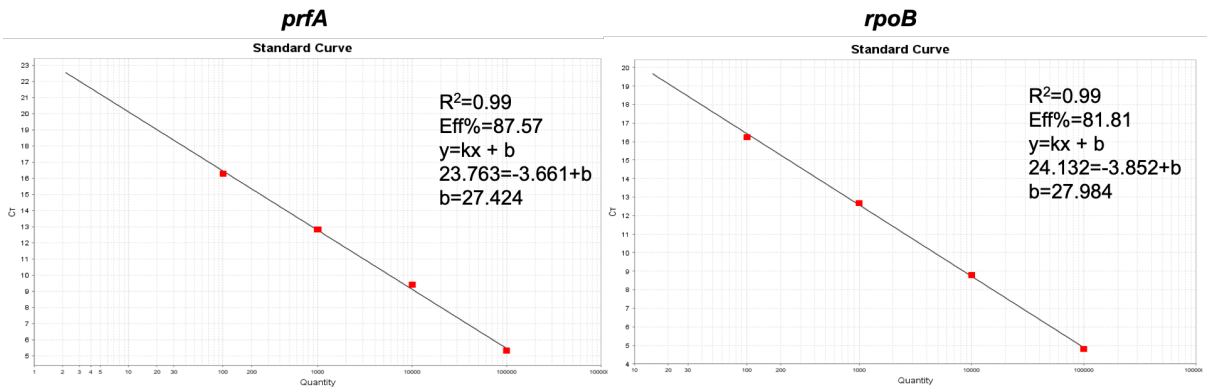

Figure 5.2 Standard curves for *prfA* and *rpoB* amplicons performed in qrtPCR assay. The graphs were generated by plotting the CT values against the logarithm of the initial copy numbers using StepOneTM software v2.3. X-axis unit is copies/µl. The R2 is the regression coefficient calculated from the regression line. The R^2 value indicates the closeness of fit between the standard curve regression line and the individual CT data points from the standard reactions. A value of 1 indicates that the regression line is perfectly fitted to the data points. The Eff% represents the efficiency of amplification. The linear regression equation is shown on each standard curve as y=kx+b. An y-intercept indicates the predicted CT value for a sample (x) with a quantity equal to 1, and K is the slope of the curve. From the given values, the b was calculated for each amplicon using the linear regression equation.

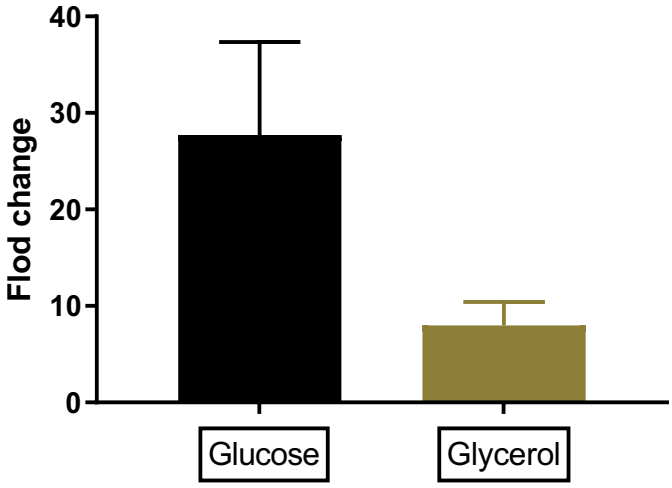

Figure 5.3 Fold changes in expression of *prfA* under microaerobic conditions using either glucose or glycerol as a carbon source. RNA was extracted at OD_{600} =0.5 for *L. monocytogenes InlA* strain grown in MD10 using glucose or glycerol as a carbon source. qrtPCR was performed using the primer sets mentioned in Figure 5.1. Values are the mean of three independent experiments normalised against *rpoB* transcripts and aerobic conditions. Error bars represent the standard error of the mean. (p value 0.025) using t test.

5.1.2. The level of Gfp expression from *p/prfA* and *p/plcA* under aerobic and microaerobic conditions using glucose or glycerol as a carbon source.

To confirm that transcript levels were higher under microaerobic conditions compared to aerobic conditions, a fluorescence assay was performed in *L. monocytogenes InlA* using the *prfA* and *plcA* promoters fused to *gfp* in the plasmids (Table 2.2) to determine PrfA activity. As seen in Figure 5.4, transcription from *p/prfA* showed a significant decrease during growth under microaerobic conditions using glycerol as a carbon source. On the other hand, transcription from *p/plcA* increased significantly under microaerobic conditions regardless of carbon sources. In addition, the levels of PrfA activity from *p/prfA* was low (1500 RFU/OD_{600}) following aerobic glucose growth but increased to (15000 RFU/OD_{600}) from *p/plcA.*

For example, expression from the *p/prfA* was 900 RFU/OD_{600} following growth under microaerobic conditions using glucose as a carbon source compared to 39000 RFU/OD_{600} from *p/plcA* following growth under the same conditions. As a whole, these data indicate that the *prfA* transcriptionfrom *p/plcA* was higher than the transcription from *p/prfA*. These results

confirm that the regulation of *prfA* transcription is controlled by a positive regulatory feedback loop mediated by *p/plcA* (Gaballa *et al.,* 2019).

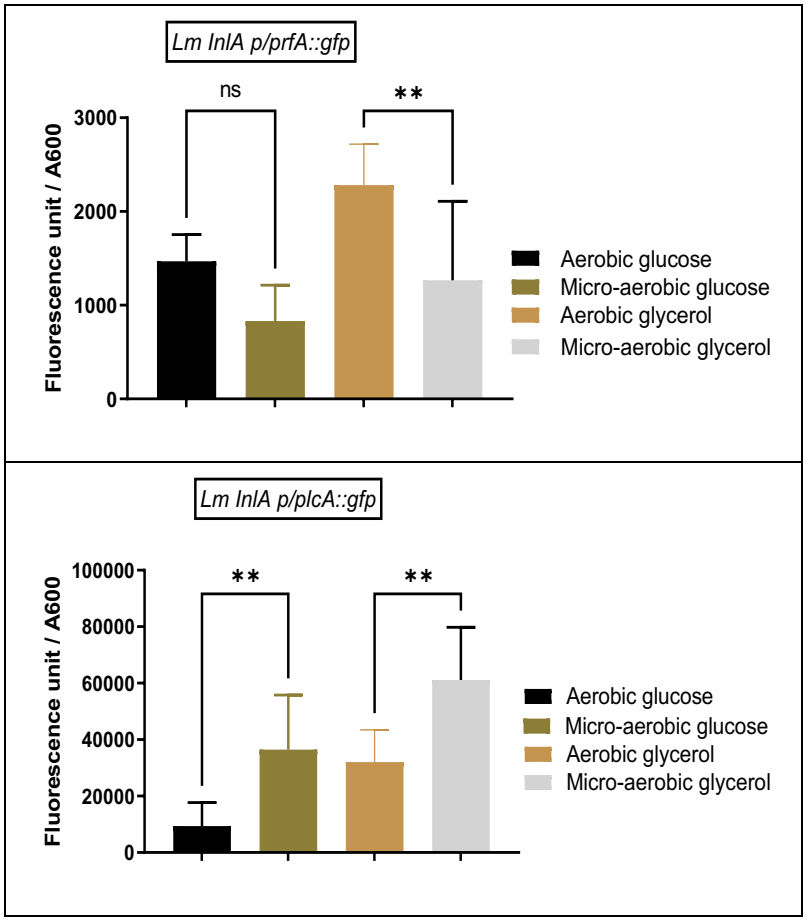

Figure 5.4 The level of Gfp expression from the *p/prfA* and *p/*plcA promoters of *L. monocytogenes* during growth in MD10 glycerol or glucose medium under aerobic and microaerobic conditions. The strains were grown at 37 ºC and the Gfp expression was measured after O/N growth. The data are the mean of three independent experiments. Significant differences (**,0.001<p<0.01) were calculated using t test.

5.2. Transcriptomic analysis of *L. monocytogenes* under microaerobic or aerobic conditions using glucose or glycerol as a carbon source

To investigate the changes in the global gene expression, RNA-seq was performed on *L. monocytogenes* InlA following growth at 37 ºC under microaerobic and aerobic conditions using either glucose or glycerol as a carbon source. The RNA-seq analysis represents two biological replicates in each condition. In the principal component analysis (PCA) for media and oxygen, there was robust separation among the different conditions. Specifically, the first

principal component (PC1) accounted for 57 % of the variance, and the second principal component (PC2) accounted for 22 % (Figure 5.5). All conditions showed robust separation and oxygen type (microaerobic or aerobic) caused a larger effect on gene expression than media glucose and glycerol (GLU, GLY). The statistical analysis on duplicate data sets was performed to determine p values and padjusted (padj) values, which in part used information from all datasets (section 2.14). Bioinformatic analysis of RNA-seq data was performed by Dr Leo Zeef from the Genomic Technologies Core Facility at the University of Manchester.

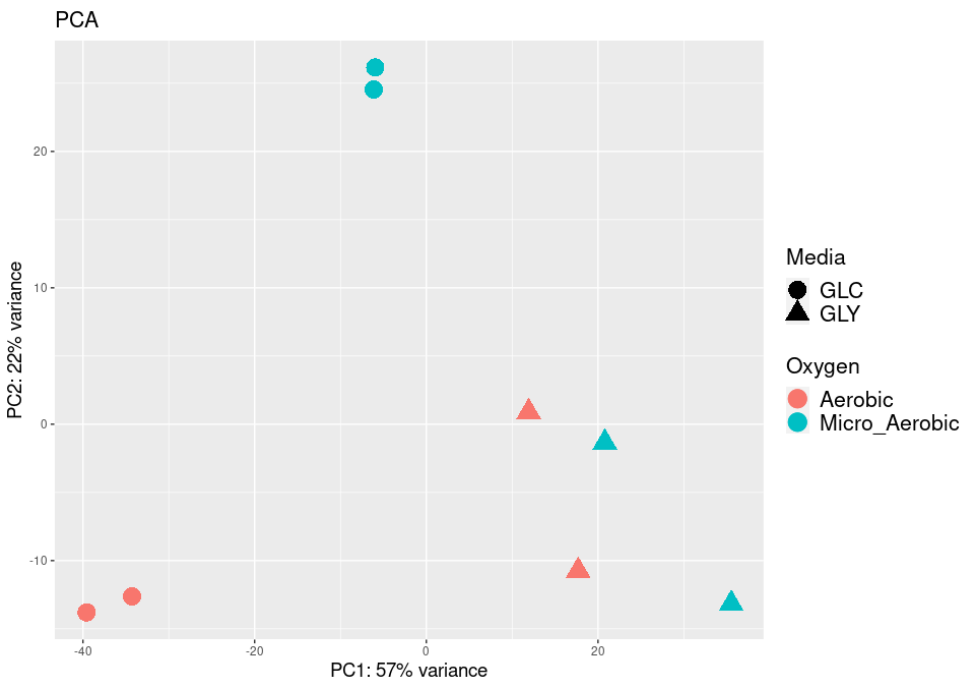

Figure 5.5 Principal component analysis of gene expression for *L. monocytogenes inlA* in microaerobic and aerobic conditions using glycerol or glucose as a carbon source. All four conditions were replicated twice. Each data point represents one replicate. Aerobic conditions are represented in red and microaerobic are represented in green. When glycerol was used as a carbon source, this is represented by triangles and when glucose was used as a carbon source, this is shown by circles. Variance explained by PC1 and PC2 are shown on the x-axis and y-axis respectively. This figure was generated by Dr Leo Zeef.

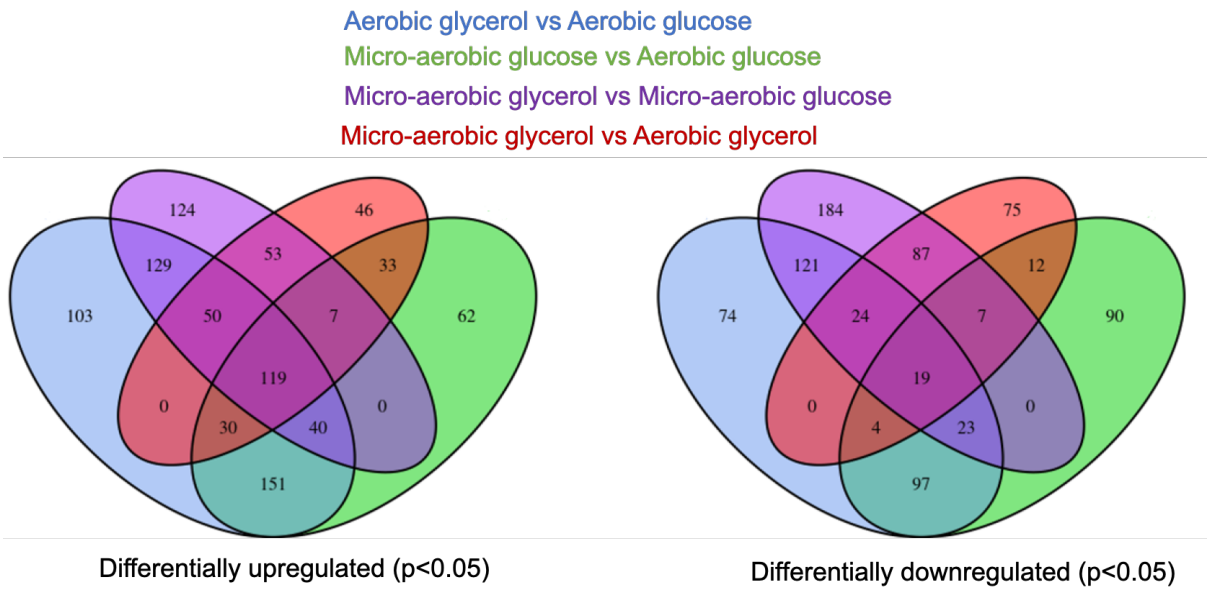

Figure 5.6 Venn diagram showing overlapping gene sets between the analysed conditions. The Venn diagram on the left shows genes differentially upregulated, while the Venn diagram on the right shows genes differentially downregulated. Blue group represents genes differentially expressed in aerobic condition using glycerol as a carbon source compared aerobic condition using glucose as a carbon source. Green represents genes differentially expressed microaerobic condition using glucose as a carbon source compared to aerobic condition using glucose as a carbon source. Purple represents genes differentially expressed in microaerobic using glycerol as a carbon source compared to microaerobic condition using glucose as a carbon source. Red represents genes differentially expressed in microaerobic condition using glycerol as a carbon source compared to aerobic condition using glycerol as a carbon source. The numbers indicate the number of genes and the overlaps highlight the number of gene sets that are shared between conditions. This figure was generated by Dr Leo Zeef.

A Venn diagram of overlapping gene sets assigned to pairwise comparisons is presented in Figure 5.6. The p-value for all genes was <0.05, which indicates statistical significance. Under microaerobic conditions with glucose as a carbon source, there were 62 genes specifically upregulated and 90 were downregulated (Figure 5.6, shown in green). In contrast, there were 170 genes specifically upregulated and 259 were downregulated under microaerobic with glycerol as a carbon source (Figure 5.6, shown in red and purple separately). These genes

are those exclusively regulated by microaerobic conditions. In addition, there were 612 upregulated genes which were shared with glucose or glycerol as a carbon source while 394 were downregulated in response to microaerobic conditions (Figure 5.6, shown in the green-purple-red overlap). Interestingly, this set of shared genes also includes genes from the PrfA regulon which were upregulated in microaerobic conditions regardless of the carbon source was used. It should be noted that regardless of the growth conditions the change of carbon source induced significant transcriptional changes. For instance, 103 genes were significantly upregulated under aerobic conditions when glycerol was used as a carbon source compared to glucose (Figure 5.6). However, what is clear is that microaerobic conditions induce significant transcriptional change in *L. monocytogenes* compared to aerobic growth.

Gene	Description	Mean Log2 fold change	
		Glucose	Glycerol
Downregulated			
hbp2	hemoglobin-binding protein Hbp2	-2.19669	-4.06704
isdC	heme uptake protein IsdC	-1.72912	-4.59968
isdE	heme ABC transporter substrate-binding protein IsdE	-2.89462	-2.27652
eno	phosphopyruvate hydratase	-0.51256	-0.51948
srtB	class B sortase	-2.1045	-1.74502
atpF	F0F1 ATP synthase subunit B	-0.38219	-0.39642
dusB	tRNA dihydrouridine synthase DusB	-0.63584	-0.86337
gpmI	2,3-bisphosphoglycerate-independent phosphoglycerate mutase	-0.78561	-0.56991
Upregulated			
betL	BCCT family glycine betaine transporter BetL	0.863202	0.646697
dhaL	dihydroxyacetone kinase subunit L	1.939652	1.234477
chiA	chitinase ChiA	1.514774	0.872986

nagA	N-acetylglucosamine-6-phosphate deacetylase	1.283911	1.047034
mogR	motility genes transcriptional repressor MogR	1.35957	0.624905
dinB	DNA polymerase IV	0.970003	-0.79653
nagB	glucosamine-6-phosphate deaminase	1.139103	1.043328
lapB	surface-anchored adhesin LapB	1.267968	1.103791
dhaK	dihydroxyacetone kinase subunit DhaK	2.071572	2.071572

Table 5.1 Annotated genes that showed significant up or down regulation in microaerobic conditions regardless of whether glycerol or glucose was used as a carbon source (padj<0.05).

There were 17 annotated genes the expression of which changed either being up or down regulated in microaerobic conditions compared to aerobic conditions regardless of whether glycerol or glucose was used as a carbon source (Table 5.1). Eight of these genes were upregulated with both glycerol and glucose with the exception of the *dhak* gene the log2 fold change being higher when grown using glucose as a carbon source. In contrast, eight genes were downregulated when either glycerol or glucose was used as a carbon source. Curiously, only the *dinB* gene was upregulated with glucose as a carbon source (0.97 log2 fold change) but downregulated with glycerol as a carbon source (-0.79 log2 fold change).

5.3. Differentially expressed genes in microaerobic conditions specific with glucose as a carbon source

RNA-seq analysis identified a total of 694 significantly differential expressed genes above log2 fold change in microaerobic conditions compared to aerobic conditions when glucose was used as a carbon source (Figure 5.7A). 442 genes were downregulated and 252 genes were upregulated, of which 151 had known functions. The Log2 fold changes and names of the most highly up/downregulated characterised genes are shown on a heat map (Figure 5.7B). Although more genes were downregulated than genes upregulated, the log2 fold change was much larger in upregulated genes (Figure 5.7A).

The heat map shows Log2 fold-change values for 16 characterised genes that had a mean of Log2 fold change >1 or <-1. Most of these genes were upregulated for example, *ssb* which encodes for single-stranded DNA-binding protein had mean log2 fold change of 3.36, *bsh* which encodes for choloylglycine hydrolase had mean log2 fold change of 3.31, *phoU* which encodes for phosphate signaling complex protein PhoU had mean log2 fold change of 2.81. However, 5 of these genes were downregulated which include *isdE*, *hbp2*, *ilvD*, *pflB* and *fabH* that had -2.89, -2.20, -2.1, -2.0 and -1.20 mean log2 fold changes respectively.

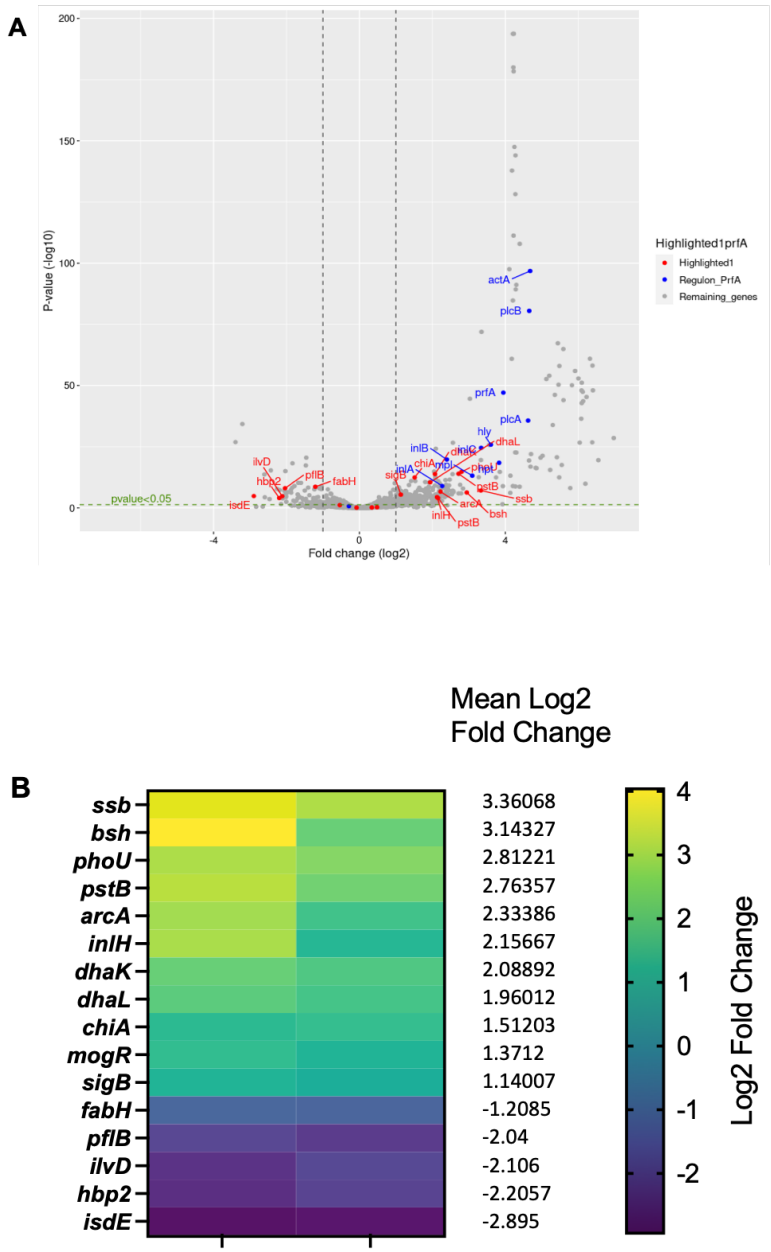

Figure 5.7 Genes showing significant transcriptomic changes under microaerobic conditions specific with glucose as a carbon source. A) The volcano plot shows differential gene expression in two biological replicates under microaerobic versus aerobic conditions. An individual gene is represented by circles while Filtering differentially expressed genes is represented by dotted lines. Circles in red show genes that are differentially upregulated, while circles in blue show genes that are differentially downregulated. This figure was generated by Dr Leo Zeef. **B)** Heat map showing log2 fold-change of annotated genes of known function with significant padj<0.05 for two replicates. On the right, gene values are ordered from highest to lowest fold change, from top to bottom. The key indicates the log2 fold change values for each colour.

The analysis was then conducted to determine whether microaerobic conditions affected the expression of PrfA-regulated virulence genes when glucose was used as a carbon source (Figure 5.8). All of the PrfA regulon genes were upregulated as expected. The Log2 fold change of *actA* and *plcB/A* were the highest, with a mean Log2 fold change of 4.6 across the replicates. *There was a mean log2 fold change of 3.9, 3.7, 3.6, 3.3, and 3.0 respectively for the PrfA itself, hpt, hly, inlC, and mpl.* However, the mean Log2 fold change of *inlB* was 2.3 and 2.2 for *inlA* which both showed the lowest values. These genes are regulated by SigB as well which had a mean log2 fold change of 1.14 (Figure 5.7B). Overall, all the values showed statistically significant (padj < 0.05) Log2 fold increase.

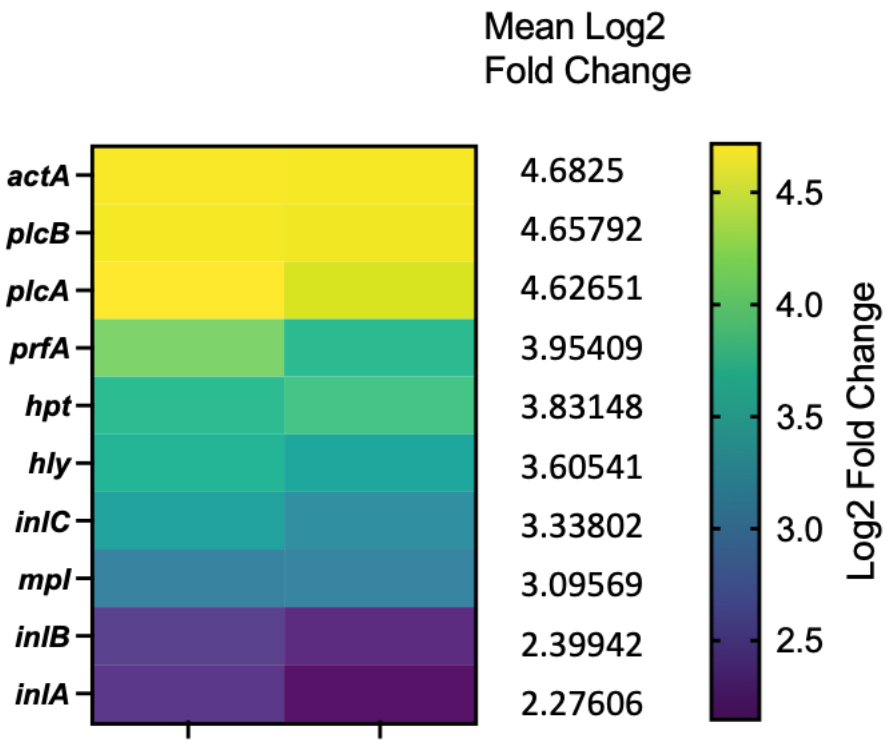

Figure 5.8 PrfA regulon transcriptomic changes under microaerobic conditions when glucose was used as a carbon source. Heat map showing log2 fold-change for PrfA regulon with padj<0.05 for two replicates. On the right, gene values are ordered from highest to lowest fold change, from top to bottom. The key indicates the log2 fold change values for each colour.

5.4. Differentially expressed genes in microaerobic conditions specific with glycerol as a carbon source

RNA-seq analysis identified a total of 566 significantly differential expressed genes above log2 fold change in microaerobic conditions compared to aerobic conditions when glycerol was used as a carbon source (Figure 5.9A). 338 genes were downregulated and 228 genes were upregulated, of which 89 had known functions. The Log2 fold changes and names of the most highly up/downregulated characterised genes are shown on a heat map (Figure 5.9B).

The heat map shows Log2 fold-change values for 15 characterised genes that had a mean of Log2 fold change >1 or <-1. Most of these genes were downregulated for example, *isdC, isdG* which encode for heme oxygenase and *isdC* was the highest mean log2 fold change of -4.4 while *isdG* was -2.35. *hbp2* which encodes for hemoglobin-binding protein Hbp2 and was the second highest mean log2 fold change of -3.92. *tatC* and *tatA* are genes in Twin-arginine translocation pathway and had log2 fold change of -1.97, -2.35 respectively. *purF*, *purL* and *purQ* which encode for phosphoribosyl formyl glycin amidine synthase group showed log2 fold change of -1.2, -1.0 and -1.0 respectively. However, only 4 genes were upregulated which including *pduA* with log2 fold change of 1.53, and *rpiB*, *rpe* and *tkt* which all had an average of 2.7 log2 fold change.

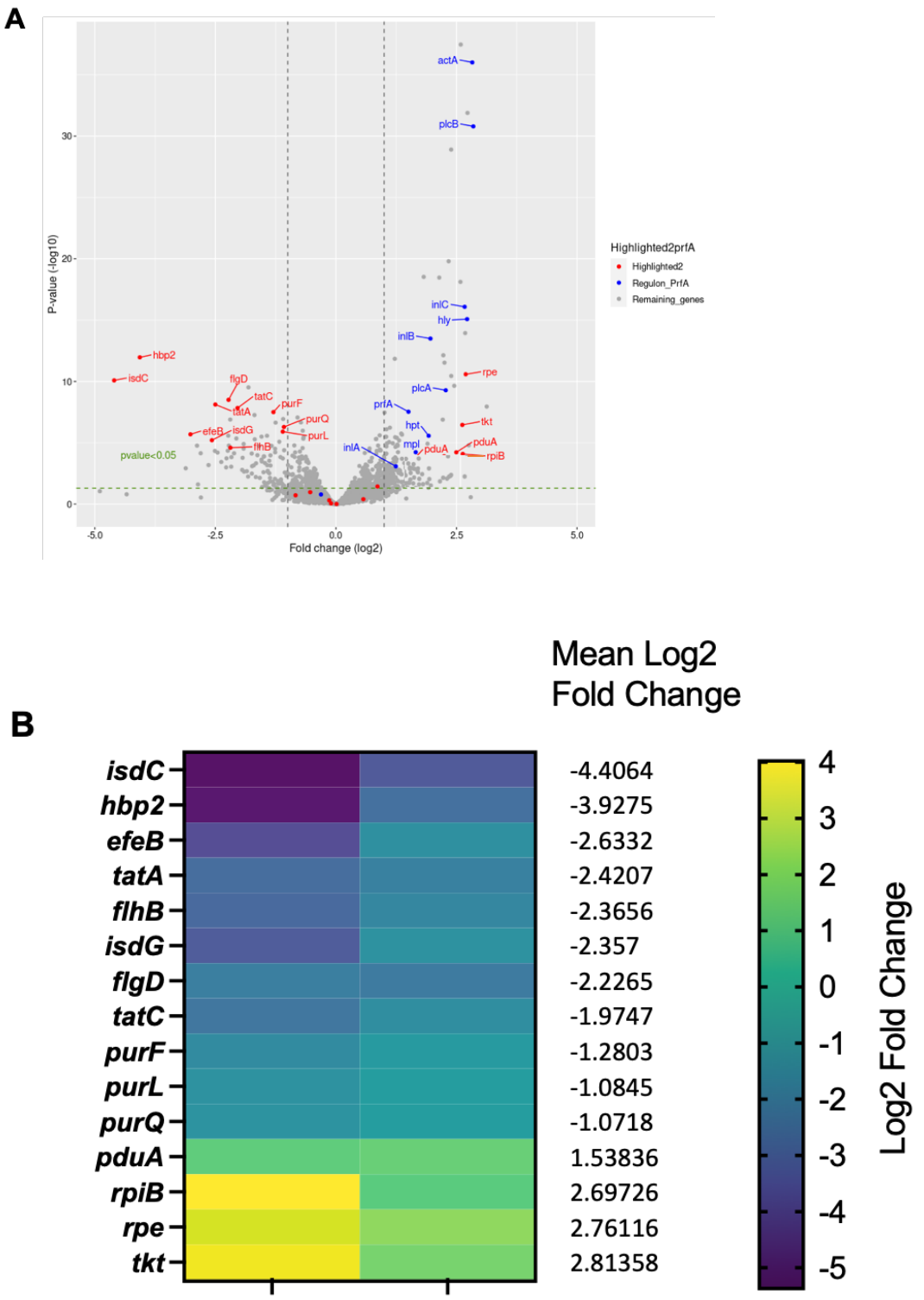

Figure 5.9 Genes showing significant transcriptomic changes under microaerobic conditions specific with glycerol as a carbon source. A) The volcano plot shows differential gene expression in two biological replicates under microaerobic versus aerobic conditions. An individual gene is represented by circles while Filtering differentially expressed genes is represented by dotted lines. Circles in red show genes that are differentially

upregulated, while circles in blue show genes that are differentially downregulated. This figure was generated by Dr Leo Zeef. **B)** Heat map showing log2 fold-change for some of the genes that characterised and significant with padj<0.05 for two replicates. On the right, gene values are ordered from lowest to highest fold change, from top to bottom. The key indicates the log2 fold change values for each colour.

The analysis was then conducted to determine whether microaerobic conditions affected the expression of PrfA-regulated virulence genes when glycerol was used as a carbon source (Figure 5.10). Similar to the PrfA regulon when glucose was used as a carbon source, all of the PrfA regulon genes were upregulated. The Log2 fold change of *actA* and *plcB* were the highest, with a mean Log2 fold change of 2.8 across the replicates. There was a mean log2 fold change of 2.7, 2.6, 2.2, 1.9, 1.8, 1.5 and 1.4 respectively for the *hly, inlC, plcA, inlB, hpt, mpl and prfA.* However, the mean Log2 fold change of *inlA* was 1.2 which showed the lowest value. Overall, all the values showed statistically significant (padj < 0.05) Log2 fold increase.

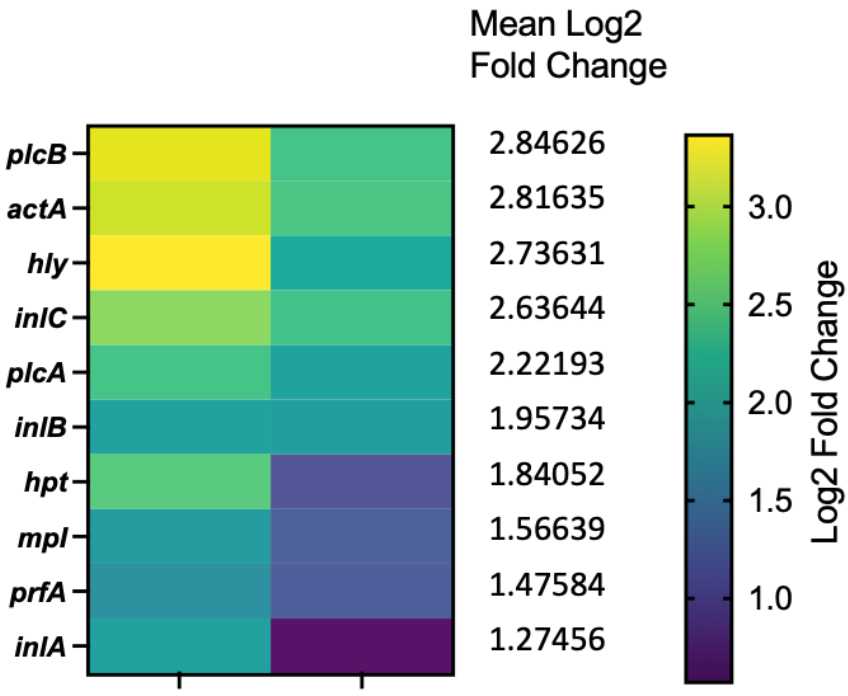

Figure 5.10 PrfA regulon transcriptomic changes under microaerobic conditions when glycerol was used as a carbon source. Heat map showing log2 fold-change for PrfA regulon with padj<0.05 for two replicates. On the right, gene values are ordered from highest to lowest fold change, from top to bottom. The key indicates the log2 fold change values for each colour.

5.5. Discussion

L. monocytogenes is one of the most virulent foodborne pathogens, with a mortality rate higher than most of other bacteria such as Salmonella (Coats, 2019). *As with other enteric pathogens,* it is necessary for *L. monocytogenes* to be capable of responding to the different environments within the host which include microaerobic deep within the intestines in order to cause infections through the gastrointestinal tract (Coats, 2019). *L. monocytogenes* undergoes vast variations in oxygen concentration in the gastrointestinal tract, ranging from anaerobic and microaerobic conditions within the intestines to high levels of oxygen in the stomach (Albenberg *et al.,* 2014). It is possible for bacteria to detect the concentration of oxygen in their environment and adjust expression of their virulence factors to promote colonisation and subsequent infection (Green *et al.,* 2014). However, it is poorly understood how this occurs in *L. monocytogenes. This chapter investigated the changes that occurred in L. monocytogenes when it was exposed to a microaerobic environment.* In particular, studying for the effect of microaerobic conditions on PrfA regulon virulence genes.

The qRTPCR experiment showed an increase in the level of *prfA* transcript under microaerobic conditions using glucose or glycerol as a carbon source. This was confirmed by the fluorescence reporter assay, which showed under microaerobic conditions increased expression of PrfA from the *p/plcA* promoter (Figure 5.4). In contrast transcription from the *p/prfA* promoter decreased under the same conditions (Figure 5.4). Transcriptional regulation of the *prfA* gene is complex. There are three known promoters, *prfAP1* and *prfAP2* proximal to *prfA* and present on plasmid pLL1 (Table 2.2) and the distal *p/*plcA promoter which generates the bicistronic *plcA-prfA* message (Gaballa *et al.,* 2019). It is known that the positive autofeedback loop by which PrfA increases its expression is mediated via the *p/plcA* promoter to rapidly increase the levels of PrfA upon infection (Camilli *et al.* 1993). As such the data here, that indicates an increase in activity of the *p/plcA* promoter in microaerobic conditions would be in keeping with regulatory model where in response to microaerobic conditions there

is an upegulation of the *p/plcA* promoter. It should be noted that although expression with glycerol as a carbon source was higher than glucose, the fold change with glucose as a carbon source was higher than glycerol. Both experiments suggest that the increase of the levels of PrfA reflect an increase in transcription of the *prfA* gene, however at this stage post-transcriptional regulation cannot be ruled out.

A study has linked anaerobiosis with virulence, suggesting that anaerobiosis may act as an environmental trigger for *L. monocytogenes* virulence gene expression (Müller-Herbst *et al.,* 2014). For example, induction of InlB and InlA expression by anaerobic conditions, which contributes to adherence and invasion of the intestinal wall (Müller-Herbst *et al.,* 2014). In addition, the transcriptional activator PrfA regulates *bsh* and increases its level of transcription in low oxygen (Dussurget *et al*., 2002). In this study, RNA-seq analysis revealed an increase in virulence gene expression throughout the PrfA regulon including *inlA, inlB* and *bsh,* in response to microaerobic conditions regardless of the carbon source was used.

ResD is required for aerobic respiration in *L. monocytogenes* (Corbett *et al.,* 2017). The expression of several virulence genes, including *inlA*, has been altered as a result of ResD regulating *prfA* activity in *L. monocytogenes* (Larsen *et al.,* 2006). A Therefore, ResD may play a critical role in regulating virulence factors and stress reactions in microaerobic environments (Davis *et al,* 2019). The two terminal oxidases CydAB, a *bd* type oxidase and qQoxB an aa_3 menaquinone oxidase are critical for *L. monocytogenes* infection as they allow *L. monocytogenes* to adapt to different conditions during infections by switching between different terminal electron acceptors under varying oxygen concentrations 1 % or 2 % (Corbett *et al*., 2017). However, the RNA-seq analysis did not show significant upregulation by microaerobic conditions for *cydB* (padj = 0.44, 0.12 when glucose or glycerol was used as a carbon source respectively) and *qoxB* (padj = 0.84, 0.13 when glucose or glycerol was used as a carbon source respectively) (data not shown). The difference between these data and previous research might be due to the different oxygen levels used. In these experiments the

microaerobic conditions contained 5.5% (v/v) oxygen whereas studies on the role of the CydAB and QoxB oxidases used oxygen levels of 1% (v/v) or lower (Corbett *et al.* 2017). Of course, it is also possible that switching between oxidases at low oxygen levels is not regulated transcriptionally.

The RNA-seq result showed 27 annotated genes were specifically regulated by microaerobic conditions either up or down including the PrfA regulon virulence factors. These genes were expressed differently in response to the specific conditions used in the experiment. One of these genes important for virulence is *mogR* which showed log2 fold change 1.35 with glucose and 0.624 with glycerol at 37 ºC. Previous studies reported that MogR is the master regulator of flagellar motility where *L. monocytogenes* is motile below 30 ºC but none motile at temperatures above this (Gründling *et al*., 2004; Cho *et al*., 2022). Curiously *mogR* mutants are attenuated (Grundling *et al.,* 2004). The role and regulation of *mogR* under microaerobic conditions is discussed in next Chapter section 6.3. On the whole, it seems clear that microaerobic conditions induce gene expression in *L. monocytogenes* and allow it to adapt to the environment better.

Chapter 6 General discussion and future works

L. monocytogenes is a food-borne pathogen which causes listeriosis. There have been extensive studies of the intracellular life cycle of *L. monocytogenes*, yielding many insights into the workings of eukaryotic cells (Rolhion and Cossart, 2017). Despite the fact that acid and bile salts are known to cause *L. monocytogenes* to adapt and resist their action (Gahan and Hill, 2005), little is known about other stimuli encountered during transit in the intestine before invasion. There are a number of stimuli that can trigger this process, such as microaerobic conditions, competition with resident microbiota, exposure to SCFA which are secreted by the host gut microbiota and play critical roles in gut homeostasis and signalling between the gut microbiota and the host, (Spohn and Mawe, 2017) and exposure to molecules derived from the host such as 5-HT. It will be necessary to integrate these signals in order to adapt to a new environment. Therefore, this study aimed to investigate the adaptation of *L. monocytogenes* to signals encountered in the environment of the lumen of the small intestine before invasion. This aim was achieved by investigating the specific roles of 5-HT, butyrate and oxygen levels on expression of the PrfA regulon.

6.1. The role of butyrate and 5-HT on expression of the PrfA regulon

To test the effect of butyrate on the PrfA regulon the level of transcription from the *phly* and *pactA* promoters was assayed. This showed that butyrate at 5 mM resulted in a significant decrease in transcription from both the *phly* and *pactA* promoters under aerobic and microaerobic conditions in defined media using glucose or glycerol as a carbon source. Likewise, previous research reported that at level of 250 mM of butyrate, the production of virulence factors was inhibited in *L. monocytogenes* under aerobic conditions in brain heart infusion medium (Sun *et al.,* 2012). However, it should be noted that the concentration of 5 mM butyrate used in these studies is more physiologically relevant, being comparable tro the levels present in the small intestine (Peng *et al.,* 2007). In contrast, another study reported that at 5 mM butyrate increased transcription from the *phly* promoter under anaerobic

conditions in brain heart infusion medium (Rinehart *et al*., 2020). The difference in these results may reflect the difference in oxygen levels between microaerobic and anaerobic conditions as well as differences in the media used. Therefore, the data in this thesis support the hypothesis that *L. monocytogenes* is responding to physiological levels of butyrate that would be encountered in the small intestine by switching on the PrfA regulon.

The data showed that addition of 5-HT had no significant affect on the growth of *L. monocytogenes* under either aerobic or microaerobic conditions. However, in combination with butyrate there was an inhibition of growth under microaerobic conditions but not under aerobic conditions. This inhibitory action of butyrate in combination with 5-HT in microaerobic conditions may represent some level of protection provided by the production of SCFA by existing microbiota to *L. monocytogenes* infection.

In terms of expression of the PrfA regulon the effect of 5-HT was to decrease transcription from both the *phly* and *pactA* promoters under microaerobic conditions but this effect was only significant in the case of the *pactA* promoter (Figure 3.9). Therefore, the data in this thesis indicate that 5-HT is reducing transcription of the PrfA regulon under microaerobic conditions but in a less pronounced way than the addition of butyrate. The observation that a combination of 5-HT and butyrate affected the growth of *L. monocytogenes* specifically under microaerobic conditions was unexpected and should be investgated further to understand the mechanism of this inhibitory effect. For instance, is it specific to butyrate or is it common to other SCFAs in the presnce of 5-HT.

6.2. The role of sigmaB and PrfA in regulating gene expression under microaerobic affect

Previously it had been shown that the absence of SigB resulted in very slow growth of *L. monocytogenes 10403S* strain with a lag phase of around 5 h when grown in defined medium utilizing glycerol as a carbon source (Abram *et al.,* 2008). Likewise, my study showed that a *sigB* mutation resulted in slow growth of *L. monocytogenes InlA* strain in MD10 defined medium supplemented with glycerol or glucose as a carbon source under aerobic and

microaerobic conditions. This similarity in both studies suggest that SigB plays an important role in adapting to growth in defined media whether glucose or glycerol is the carbon source. The observation that, no difference was observed in the presence of a *sigB* mutation in *L. monocytogenes EGDe* strains grown in nutrient broth supplemented with 0.4 % (w/v) glucose or glycerol as a carbon source would support the notion that the effect of the *sigB* mutation is dependent on the use of defined medium (Tapia *et al.,* 2020). The use of defined media is preferred to complex rich media since it minimises the effects of carbohydrates and other nutrient sources that may be in the rich media. This allows greater confidence when assigning possible affects to the added carbohydrate in question.

The *sigB* mutation led to a significant increase in transcription from the *phly* promoter regardless of the oxygen concentration or carbon source used in the experiment. The same trend was observed with the *pactA* promoter but was only significant in mid-log phase under aerobic conditions. This might suggest that SigB is somehow repressing expression of the PrfA regulon under the conditions used here. To test this, it would be worth investigating the expression of other PrfA regulated promoters in a *sigB* mutant background. How such a SigB mediated input might operate mechanistically is unclear, but these data in this thesis confirm that there is an overlap in the SigB and PrfA regulons (Sibanda and Buys, 2022).

The absence of PrfA resulted in lower final OD_{600} compared to the wildtype strains under microaerobic conditions (Figure 4.6). This suggests that some of the PrfA regulated genes are important but not essential for growth under microaerobic conditions. That could be due to the fact that the metabolism of the *prfA* mutant strain is altered in microaerobic conditions such that toxic by-products accumulate more rapidly or all of the available nutrients cannot be utilised. It would be interesting to perform some metabolomic studies on microaerobically grown wild type and a *prfA* mutant to identify what, if any, metabolic differences there are between these two strains. Likewise, one could perform metabolomic experiemnts on a *prfA**

strain to determine what effect over expression of PrfA was having on the metabolism of *L. monocytogenes* under microaerobic conditions.

The observation that a *prfA* mutant lacked any transcriptional activity from *phly* and *pactA* is not surprising based in the known function of PrfA (Gaballa *et al.,* 2019). My results revealed that *prfA* mutants abolished detectable transcription from *phly* and *pactA* in MD10 when glucose or glycerol was used as the carbon source under aerobic or microaerobic conditions (Figure 4.7). Interestingly, the increased transcription observed in microaerobic conditions is also PrfA dependent. My result also showed an increase of LLO, ActA and PrfA proteins under microaerobic conditions. The increase in PrfA under these conditions reflects increased transcription of the *prfA* gene (see below)

6.3. The role of microaerobic condition on the global gene expression

It is important to note that *L. monocytogenes* faces variations in oxygen concentration in the gastrointestinal tract. Anaerobic and microaerobic conditions can be found within the intestines and high oxygen concentrations can be found within the stomach of the organism (Albenberg *et al.,* 2014). The virulence factors of bacteria can be adjusted based on the oxygen concentration in their environment such as *Mycobacterium tuberculosis* and *Staphylococcus aureus* (Green *et al*., 2014). This study investigated the changes that occurred in *L. monocytogenes* when it was exposed to a microaerobic environment.

The qrtPCR results showed an increase in the level of *prfA* transcription under microaerobic conditions using glucose or glycerol as a carbon source. This was also confirmed by the fluorescence assay, which showed an increased expression of PrfA through the *p/plcA* promoter under microaerobic conditions. Although expression when glycerol was used as a carbon source, was higher compared to glucose, the fold change when glucose was used as a carbon source, was higher compared to glycerol. Both experiments suggest that the increase of PrfA, LLO and ActA proteins under microaerobic conditions was due to the

increase of *prfA* at the transcriptional level. Therefore, this suggests that in addition to the known regulators of *prfA* transcription, low oxygen levels are also somehow regulating *prfA* transcription. To date it is unknown how this regulation might be achieved. One way to investigate this would be to screen a transposon mutant library for mutants that fail to show increased *prfA* transcription under microaerobic conditions. One would perform the transposon mutagenesis in a strain with a *prfA-gfp* transcription fusion such that mutations that affected *prfA* transcription in microaerobic conditions could be readily identified. The RNA-seq analysis confirmed the qrtPCR results for the *prfA* gene with a 3.95 Log2 fold change in microaerobic conditions with glucose as a carbon source and 1.47 Log2 fold change when glycerol was the carbon source. This would indicate that the increased PrfA protein levels detected following microaerobic growth were primarily due to increased transcription of the *prfA* gene. The observation that the expression of the *gshF* gene that encodes the glutathione synthase responsible for the production of intracellular glutathione for post-translational activation of PrfA (Reniere *et al.,* 2016) was unaltered during microaerobic growth would indicate that increased PrfA activity is not driven by increased glutathione production during microaerobic growth. In keeping with the increased *prfA* transcription under microaerobic conditions the RNA-seq demonstrated an increase in virulence gene expression throughout the PrfA regulon in response to microaerobic conditions regardless of the carbon source was used. This matches with previous study showed that the transcriptional activator PrfA regulates *bsh* and increases its level of transcription in low oxygen (Dussurget *et al*., 2002).

Furthermore, the RNA-seq data showed that in addition to the PrfA regulon 17 annotated genes showed significant changes (*p* value 0.05) in transcription either up or down following microaerobic growth. One of these genes is *mogR*, the transcriptional repressor of flagellar expression at 37 ºC that showed upregulation at 37 ºC in microaerobic conditions (the log2 fold change =1.35 with glucose and 0.62 with glycerol). This is of interest since flagellar are not expressed at 37 ºC (Lebreton and Cossart, 2017). Expression of flagella genes is regulated by a complex network of transcriptional regulators which are the MogR, motility gene

repressor, and GmaR, motility anti-repressor, antagonize to allow flagella production at 30 ºC and repress it at 37 ºC (Lebreton and Cossart, 2017). MogR acts as a master repressor for the transcription of both flagella genes and *gmaR* (Lebreton and Cossart, 2017). MogR has a DNA-binding domain at its N-terminus and an oligomerization domain at its C-terminus (Shen *et al.,* 2009). MogR blocks flagellar transcription by binding to both major groove interaction sites and minor groove interaction sites at DNA binding domain (Cho *et al*., 2022). GmaR is an anti-repressor that can suppress flagellar transcription mediated by MogR (Shen et al., 2006). During low temperature, GmaR interacts with MogR and inhibits its binding to DNA (Dorey *et al*., 2019). At higher temperature, the thermosensitive interaction between MogR and GmaR, cause MogR and GmaR to dissociate thereby allowing MogR to bind to target DNA and repress the flagellar regulon (Dorey *et al.*, 2019).

A deletion of *mogR* resulted in a significant increase of *flaA*, encoding flagellin, at 37 ºC and at room temperature (Gründling *et al.,* 2004). Also, the deletion of *mogR* led to deregulate in a similar manner of transcription of two flagellar motility genes *lmo0675* and *cheY* (Gründling *et al.,* 2004). Furthermore, the deletion of *mogR* resulted in attenuation of the virulence by 250-fold in mouse model with *mogR* mutants displaying reduced cell to cell spread in *in vitro* tissue culture models of infection (Gründling *et al.,* 2004). This reduced virulence appeared to be through the overexpression of flagellar at 37 ºC which caused pleiotropic effects on cell division with long chains of bacteria being formed (Shen *et al*., 2006).

It is unclear why lower levels of oxygen should induce increased expression of MogR, perhaps it is vital that there is no leaky flagellar expression during the intestinal phase of the life cycle of *L. monocytogenes* where any flagellar expression might be deleterious to infection. It would be interesting to look at the growth of a *mogR* mutant in microaerobic conditions to explore further the role of MogR during microaerobic growth.

In addition, the RNA-seq data showed a significant downregulation of *hbp2*, *isdC/E* and *srtB* specific under microaerobic conditions which encode the HbP2, heme uptake protein IsdC/E and class B sortase (Table 5.1). A previous study showed that at low concentrations (below 50 nM) of heme *L monocytogenes*, acquires heme via the Hbp2 heme-binding proteins 2

which requires Sortase B to anchor to cell wall (Dos Santos *et al*., 2018). It has been demonstrated that Hbp2 scavenges for heme and hemoglobin and facilitates the transport through the cell wall (Dos Santos *et al*., 2018). HupDGC ABC transporters allow heme to cross the membrane (Dos Santos *et al*., 2018). Heme molecules should diffuse through peptidoglycan pores at higher heme concentrations (Dos Santos *et al*., 2018). As a result, they are bound by the cytoplasmic membrane and transported into the cell by HupD. In the cell, heme can be a cofactor enzyme that transports and stores oxygen (Chiabrando *et al*., 2014). It is also possible to liberate free iron from heme by breaking it down with heme oxygenases, such as Isd-LmHde and/or Lmo0484, which are both Isd-type heme-degradation enzymes (Dos Santos *et al*., 2018). The linkage between heme metabolism and microaerobic conditions is interesting suggesting that in low oxygen there is a reduction in the uptake of heme groups. The next stage would be to confirm the RNAseq data with qrtPCR of the *hbp2* and *isdC/E* genes and subsequently to study the growth of strains with mutations in these gene under conditions of low oxygen.

In conclusion, the data in this study confirmed the hypothesis that *L. monocytogenes* responds to microaerobic conditions likely to be encountered in the small intestine by switching on the PrfA regulon and that this appears to be driven by increased *prfA* transcription under these conditions. This response may function to “pump prime” the pathogen thereby increasing the possibility of adhesion and invasion of the host. How this regulation by low oxyge levels is achieved is as yet unknown and offers a future avenue for research.

References

Abram, F., Su, W.L., Wiedmann, M., Boor, K.J., Coote, P., Botting, C., Karatzas, K.A.G. and O'Byrne, C.P., 2008. Proteomic analyses of a *Listeria monocytogenes* mutant lacking σB identify new components of the σB regulon and highlight a role for σB in the utilization of glycerol. *Applied and Environmental Microbiology*, *74*(3), pp.594-604.

Albenberg, L., Esipova, T.V., Judge, C.P., Bittinger, K., Chen, J., Laughlin, A., Grunberg, S., Baldassano, R.N., Lewis, J.D., Li, H. and Thom, S.R., 2014. Correlation between intraluminal oxygen gradient and radial partitioning of intestinal microbiota. *Gastroenterology*, *147*(5), pp.1055-1063.

Andersen, J.B., Roldgaard, B.B., Christensen, B.B. and Licht, T.R., 2007. Oxygen restriction increases the infective potential of *Listeria monocytogenes* in vitro in Caco-2 cells and in vivo in guinea pigs. *BMC Microbiology*, *7*(1), p.55.

Armstrong, R.W. and Fung, P.C., 1993. Brainstem encephalitis (rhombencephalitis) due to *Listeria monocytogenes*: case report and review. *Clinical Infectious Diseases*, *16*(5), pp.689-702.

Axe, D.D. and Bailey, J.E., 1995. Transport of lactate and acetate through the energized cytoplasmic membrane of *Escherichia coli*. *Biotechnology and Bioengineering*, *47*(1), pp.8-19.

Balestrino, D., Hamon, M.A., Dortet, L., Nahori, M.A., Pizarro-Cerda, J., Alignani, D., Dussurget, O., Cossart, P. and Toledo-Arana, A., 2010. Single-cell techniques using chromosomally tagged fluorescent bacteria to study *Listeria monocytogenes* infection processes. *Applied and Environmental Microbiology*, *76*(11), pp.3625-3636.

Bavdek, A., Kostanjšek, R., Antonini, V., Lakey, J.H., Dalla Serra, M., Gilbert, R.J. and Anderluh, G., 2012. pH dependence of listeriolysin O aggregation and pore-forming ability. *The FEBS Journal*, *279*(1), pp.126-141.

Begley, M., Sleator, R.D., Gahan, C.G. and Hill, C., 2005. Contribution of three bile-associated loci, bsh, pva, and btlB, to gastrointestinal persistence and bile tolerance of Listeria monocytogenes. *Infection and Immunity*, *73*(2), pp.894-904

Berndt, B.E., Zhang, M., Owyang, S.Y., Cole, T.S., Wang, T.W., Luther, J., Veniaminova, N.A., Merchant, J.L., Chen, C.C., Huffnagle, G.B. and Kao, J.Y., 2012. Butyrate increases IL-23 production by stimulated dendritic cells. *American Journal of Physiology-Gastrointestinal and Liver Physiology*, *303*(12), pp.G1384-G1392.

Bielecki, J., Youngman, P., Connelly, P. and Portnoy, D.A., 1990. Bacillus subtilis expressing a haemolysin gene from *Listeria monocytogenes* can grow in mammalian cells. *Nature*, *345*(6271), pp.175-176.

Bierne, H. and Cossart, P., 2007. *Listeria monocytogenes* surface proteins: from genome predictions to function. *Microbiology and molecular biology reviews*, *71*(2), pp.377-397.
Bierne, H., Sabet, C., Personnic, N. and Cossart, P., 2007. Internalins: a complex family of leucine-rich repeat-containing proteins in *Listeria monocytogenes*. *Microbes and Infection*, *9*(10), pp.1156-1166.

Bischoff, S.C., Mailer, R., Pabst, O., Weier, G., Sedlik, W., Li, Z., Chen, J.J., Murphy, D.L. and Gershon, M.D., 2009. Role of serotonin in intestinal inflammation: knockout of serotonin

reuptake transporter exacerbates 2, 4, 6-trinitrobenzene sulfonic acid colitis in mice. *American Journal of Physiology-Gastrointestinal and Liver Physiology*, *296*(3), pp.G685-G695.

Bolger, A.M., Lohse, M. and Usadel, B., 2014. Trimmomatic: a flexible trimmer for Illumina sequence data. *Bioinformatics*, *30*(15), pp.2114-2120.

Booth, I.R., 1985. Regulation of cytoplasmic pH in bacteria. *Microbiological Reviews*, *49*(4), p.359.

Borcan, A.M., Huhulescu, S., Munteanu, A. and Rafila, A., 2014. *Listeria Monocytogenes*–characterization of strains isolated from clinical severe cases. *Journal of Medicine and Life*, *7*(Spec Iss 2), p.42

Bruno Jr, J.C. and Freitag, N.E., 2010. Constitutive activation of PrfA tilts the balance of *Listeria monocytogenes* fitness towards life within the host versus environmental survival. *PLoS One*, *5*(12), p.e15138.

Buchanan, R.L. and Golden, M.H., 1995. Model for the non-thermal inactivation of *Listeria monocytogenes* in a reduced oxygen environment. *Food Microbiology*, *12*, pp.203-212.

Bucur, F.I., Grigore-Gurgu, L., Crauwels, P., Riedel, C.U. and Nicolau, A.I., 2018. Resistance of *Listeria monocytogenes* to stress conditions encountered in food and food processing environments. *Frontiers in Microbiology*, *9*, p.2700.

Burkholder, K.M., Kim, K.P., Mishra, K.K., Medina, S., Hahm, B.K., Kim, H. and Bhunia, A.K., 2009. Expression of LAP, a SecA2-dependent secretory protein, is induced under anaerobic environment. *Microbes and Infection*, *11*(10-11), pp.859-867.

Camejo, A., Carvalho, F., Reis, O., Leitão, E., Sousa, S. and Cabanes, D., 2011. The arsenal of virulence factors deployed by *Listeria monocytogenes* to promote its cell infection cycle. *Virulence*, *2*(5), pp.379-394.

Camilli, A., Tilney, L.G. and Portnoy, D.A., 1993. Dual roles of plcA in *Listeria monocytogenes* pathogenesis. *Molecular Microbiology*, *8*(1), pp.143-157.

Chen, C., Nguyen, B.N., Mitchell, G., Margolis, S.R., Ma, D. and Portnoy, D.A., 2018. The listeriolysin O PEST-like sequence co-opts AP-2-mediated endocytosis to prevent plasma membrane damage during *Listeria* infection. *Cell Host and Microbe*, *23*(6), pp.786-795.

Chen, S.Y., Lu, F.L., Lee, P.I., Lu, C.Y., Chen, C.Y., Chou, H.C., Tsao, P.N. and Hsieh, W.S., 2007. Neonatal listeriosis. *Journal of the Formosan Medical Association*, *106*(2), pp.161-164.

Cherrington, C.A., Hinton, M. and Chopra, I., 1990. Effect of short-chain organic acids on macromolecular synthesis in *Escherichia coli*. *Journal of Applied Bacteriology*, *68*(1), pp.69-74.

Chiabrando, D., Vinchi, F., Fiorito, V., Mercurio, S. and Tolosano, E., 2014. Heme in pathophysiology: a matter of scavenging, metabolism and trafficking across cell membranes. *Frontiers in Pharmacology*, *5*, p.61.

Chico-Calero, I., Suárez, M., González-Zorn, B., Scortti, M., Slaghuis, J., Goebel, W. and Vázquez-Boland, J.A., 2002. Hpt, a bacterial homolog of the microsomal glucose-6-

phosphate translocase, mediates rapid intracellular proliferation in *Listeria*. *Proceedings of the National Academy of Sciences*, *99*(1), pp.431-436.

Cho, S.Y., Na, H.W., Oh, H.B., Kwak, Y.M., Song, W.S., Park, S.C., Jeon, W.J., Cho, H., Oh, B.C., Park, J. and Kang, S.G., 2022. Structural basis of flagellar motility regulation by the MogR repressor and the GmaR antirepressor in *Listeria monocytogenes*. *Nucleic Acids Research*, *50*(19), pp.11315-11330.

Coats, A.N., 2019. The Impact of Oxygen on the Intracellular Survival of *Listeria monocytogenes* University of Southern Mississippi. (United States of America)

Conlan, J.W. and North, R.J., 1992. Early pathogenesis of infection in the liver with the facultative intracellular bacteria *Listeria monocytogenes*, Francisella tularensis, and Salmonella typhimurium involves lysis of infected hepatocytes by leukocytes. *Infection and Immunity*, *60*(12), pp.5164-5171.

Conlan, J.W., 1996. Early pathogenesis of *Listeria monocytogenes* infection in the mouse spleen. *Journal of Medical Microbiology*, *44*(4), pp.295-302.

Corbett, D., Goldrick, M., Fernandes, V.E., Davidge, K., Poole, R.K., Andrew, P.W., Cavet, J. and Roberts, I.S., 2017. *Listeria monocytogenes* has both cytochrome bd-type and cytochrome aa 3-type terminal oxidases, which allow growth at different oxygen levels, and both are important in infection. *Infection and Immunity*, *85*(11), pp.e00354-17.

Corbett, D., Schuler, S., Glenn, S., Andrew, P.W., Cavet, J.S. and Roberts, I.S., 2011. The combined actions of the copper-responsive repressor CsoR and copper-metallochaperone CopZ modulate CopA-mediated copper efflux in the intracellular pathogen *Listeria monocytogenes*. *Molecular Microbiology*, *81*(2), pp.457-472.

Cossart, P. and Bierne, H., 2001. The use of host cell machinery in the pathogenesis of *Listeria monocytogenes*. *Current Opinion in Immunology*, *13*(1), pp.96-103.

Cossart, P. and Lecuit, M., 1998. Interactions of *Listeria monocytogenes* with mammalian cells during entry and actin-based movement: bacterial factors, cellular ligands and signaling. *The EMBO Journal*, *17*(14), pp.3797-3806.

Cossart, P., Pizarro-Cerdá, J. and Lecuit, M., 2003. Invasion of mammalian cells by *Listeria monocytogenes*: functional mimicry to subvert cellular functions. *Trends in Cell Biology*, *13*(1), pp.23-31.

Cotter, P.D., O'reilly, K. and Hill, C., 2001. Role of the glutamate decarboxylase acid resistance system in the survival of Listeria monocytogenes LO28 in low pH foods. *Journal of Food Protection*, *64*(9), pp.1362-1368.

Crum, N.F., 2002. Update on *Listeria monocytogenes* infection. *Current Gastroenterology Reports*, *4*(4), pp.287-296.

Cummings, J., Pomare, E.W., Branch, W.J., Naylor, C.P. and Macfarlane, G.T., 1987. Short chain fatty acids in human large intestine, portal, hepatic and venous blood. *Gut*, *28*(10), pp.1221-1227.

Davis, M.L., Ricke, S.C. and Donaldson, J.R., 2019. Establishment of *Listeria monocytogenes* in the gastrointestinal tract. *Microorganisms*, *7*(3), p.75.

de las Heras, A., Cain, R.J., Bielecka, M.K. and Vazquez-Boland, J.A., 2011. Regulation of *Listeria* virulence: PrfA master and commander. *Current Opinion in Microbiology*, *14*(2), pp.118-127.

Dhama, K., Karthik, K., Tiwari, R., Shabbir, M.Z., Barbuddhe, S., Malik, S.V.S. and Singh, R.K., 2015. Listeriosis in animals, its public health significance (food-borne zoonosis) and advances in diagnosis and control: a comprehensive review. *Veterinary Quarterly*, *35*(4), pp.211-235.

Diez-Gonzalez, F. and Russell, J.B., 1997. The ability of *Escherichia coli* O157: H7 to decrease its intracellular pH and resist the toxicity of acetic acid. *Microbiology*, *143*(4), pp.1175-1180.

Doganay, M., 2003. Listeriosis: clinical presentation. *FEMS Immunology and Medical Microbiology*, *35*(3), pp.173-175.

Donohoe, D.R., Holley, D., Collins, L.B., Montgomery, S.A., Whitmore, A.C., Hillhouse, A., Curry, K.P., Renner, S.W., Greenwalt, A., Ryan, E.P. and Godfrey, V., 2014. A gnotobiotic mouse model demonstrates that dietary fiber protects against colorectal tumorigenesis in a microbiota-and butyrate-dependent manner. *Cancer Discovery*, *4*(12), pp.1387-1397.

Dorey, A., Marinho, C., Piveteau, P. and O'byrne, C., 2019. Role and regulation of the stress activated sigma factor sigma B (σB) in the saprophytic and host-associated life stages of *Listeria monocytogenes*. *Advances in Applied Microbiology*, *106*, pp.1-48.

Dortet, L., Mostowy, S. and Cossart, P., 2012. *Listeria* and autophagy escape: involvement of InlK, an internalin-like protein. *Autophagy*, *8*(1), pp.132-134.

Dos Santos, P.T., Menendez-Gil, P., Sabharwal, D., Christensen, J.H., Brunhede, M.Z., Lillebæk, E.M. and Kallipolitis, B.H., 2018. The small regulatory RNAs LhrC1–5 contribute to the response of *Listeria monocytogenes* to heme toxicity. *Frontiers in Microbiology*, *9*, p.599.

Dramsi, S., Dehoux, P., Lebrun, M., Goossens, P.L. and Cossart, P., 1997. Identification of four new members of the internalin multigene family of *Listeria monocytogenes EGD*. *Infection and Immunity*, *65*(5), pp.1615-1625.

Drolia, R. and Bhunia, A.K., 2019. Crossing the intestinal barrier via *Listeria* adhesion protein and internalin A. *Trends in Microbiology*, *27*(5), pp.408-425.

Dussurget, O., Cabanes, D., Dehoux, P., Lecuit, M., European Listeria Genome Consortium, Buchrieser, C., Glaser, P. and Cossart, P., 2002. Listeria monocytogenes bile salt hydrolase is a PrfA-regulated virulence factor involved in the intestinal and hepatic phases of listeriosis. *Molecular Microbiology*, *45*(4), pp.1095-1106.

Fiorica-Howells, E., Maroteaux, L. and Gershon, M.D., 2000. Serotonin and the 5-HT2B receptor in the development of enteric neurons. *Journal of Neuroscience*, *20*(1), pp.294-305.

Fischbach, M.A. and Sonnenburg, J.L., 2011. Eating for two: how metabolism establishes interspecies interactions in the gut. *Cell Host and Microbe*, *10*(4), pp.336-347.

Freese, E., Sheu, C.W. and Galliers, E., 1973. Function of lipophilic acids as antimicrobial food additives. *Nature*, *241*(5388), pp.321-325.

Freitag, N.E. and Portnoy, D.A., 1994. Dual promoters of the *Listeria monocytogenes* prfA transcriptional activator appear essential in vitro but are redundant in vivo. *Molecular Microbiology*, *12*(5), pp.845-853.

Freitag, N.E., Port, G.C. and Miner, M.D., 2009. *Listeria monocytogenes*—from saprophyte to intracellular pathogen. *Nature Reviews Microbiology*, *7*(9), pp.623-628.

Fuchs, T.M., Eisenreich, W., Kern, T. and Dandekar, T., 2012. Toward a systemic understanding of *listeria monocytogenes* metabolism during infection. *Frontiers in Microbiology*, *3*, p.23.

Fukuda, S., Toh, H., Hase, K., Oshima, K., Nakanishi, Y., Yoshimura, K., Tobe, T., Clarke, J.M., Topping, D.L., Suzuki, T. and Taylor, T.D., 2011. *Bifidobacteria* can protect from enteropathogenic infection through production of acetate. *Nature*, *469*(7331), pp.543-547.

Fung, T.C., Vuong, H.E., Luna, C.D., Pronovost, G.N., Aleksandrova, A.A., Riley, N.G., Vavilina, A., McGinn, J., Rendon, T., Forrest, L.R. and Hsiao, E.Y., 2019. Intestinal serotonin and fluoxetine exposure modulate bacterial colonization in the gut. *Nature Microbiology*, *4*(12), pp.2064-2073.

Gaballa, A., Guariglia-Oropeza, V., Wiedmann, M. and Boor, K.J., 2019. Cross talk between SigB and PrfA *in Listeria monocytogenes* facilitates transitions between extra-and intracellular environments. *Microbiology and Molecular Biology Reviews*, *83*(4), pp.e00034-19.

Gahan, C.G.M. and Hill, C., 2005. Gastrointestinal phase of *Listeria monocytogenes* infection. *Journal of Applied Microbiology*, *98*(6), pp.1345-1353.

Gallo, R.L. and Hooper, L.V., 2012. Epithelial antimicrobial defence of the skin and intestine. *Nature Reviews Immunology*, *12*(7), pp.503-516.

Gedde, M.M., Higgins, D.E., Tilney, L.G. and Portnoy, D.A., 2000. Role of listeriolysin O in cell-to-cell spread of Listeria monocytogenes. *Infection and Immunity*, *68*(2), pp.999-1003.

Gekara, N.O., Zietara, N., Geffers, R. and Weiss, S., 2010. *Listeria monocytogenes* induces T cell receptor unresponsiveness through pore-forming toxin listeriolysin O. *The Journal of Infectious Diseases*, *202*(11), pp.1698-1707.

Geoffroy, C., Raveneau, J., Beretti, J.L., Lecroisey, A., Vazquez-Boland, J.A., Alouf, J.E. and Berche, P., 1991. Purification and characterization of an extracellular 29-kilodalton phospholipase C from *Listeria monocytogenes*. *Infection and Immunity*, *59*(7), pp.2382-2388.

Gershon, M.D. and Liu, M.T., 2007. Serotonin and neuroprotection in functional bowel disorders. *Neurogastroenterology and Motility*, *19*, pp.19-24.

Gershon, M.D., 2012. Serotonin is a sword and a shield of the bowel: serotonin plays offense and defense. *Transactions of the American Clinical and Climatological Association*, *123*, p.268.

Ghia, J.E., Li, N., Wang, H., Collins, M., Deng, Y., El–Sharkawy, R.T., Côté, F., Mallet, J. and Khan, W.I., 2009. Serotonin has a key role in pathogenesis of experimental colitis. *Gastroenterology*, *137*(5), pp.1649-1660.

Goldfine, H. and Knob, C., 1992. Purification and characterization of *Listeria monocytogenes* phosphatidylinositol-specific phospholipase C. *Infection and Immunity*, *60*(10), pp.4059-4067.

Goldfine, H., Johnston, N.C. and Knob, C., 1993. Nonspecific phospholipase C of *Listeria monocytogenes*: activity on phospholipids in Triton X-100-mixed micelles and in biological membranes. *Journal of Bacteriology*, *175*(14), pp.4298-4306.

Gouin, E., Mengaud, J. and Cossart, P., 1994. The virulence gene cluster of Listeria monocytogenes is also present in *Listeria ivanovii*, an animal pathogen, and *Listeria seeligeri,* a nonpathogenic species. *Infection and Immunity*, *62*(8), pp.3550-3553.

Green, J., Rolfe, M.D. and Smith, L.J., 2014. Transcriptional regulation of bacterial virulence gene expression by molecular oxygen and nitric oxide. *Virulence*, *5*(8), pp.794-809.

Gross, E.R., Gershon, M.D., Margolis, K.G., Gertsberg, Z.V. and Cowles, R.A., 2012. Neuronal serotonin regulates growth of the intestinal mucosa in mice. *Gastroenterology*, *143*(2), pp.408-417.

Gründling, A., Burrack, L.S., Bouwer, H.A. and Higgins, D.E., 2004. *Listeria monocytogenes* regulates flagellar motility gene expression through MogR, a transcriptional repressor required for virulence. *Proceedings of the National Academy of Sciences*, *101*(33), pp.12318-12323.

Guariglia-Oropeza, V., Orsi, R.H., Guldimann, C., Wiedmann, M. and Boor, K.J., 2018. The Listeria monocytogenes bile stimulon under acidic conditions is characterized by strain-specific patterns and the upregulation of motility, cell wall modification functions, and the PrfA regulon. *Frontiers in Microbiology*, *9*, p.120.

Guerreiro, D.N., Arcari, T. and O'Byrne, C.P., 2020. The σB-Mediated general stress response of *Listeria monocytogenes*: life and death decision making in a pathogen. *Frontiers in Microbiology*, *11*, p.1505.

Guldimann, C., Guariglia-Oropeza, V., Harrand, S., Kent, D., Boor, K.J. and Wiedmann, M., 2017. Stochastic and differential activation of σB and PrfA in *Listeria monocytogenes* at the single cell level under different environmental stress conditions. *Frontiers in Microbiology*, *8*, p.348.

Hall, M., Grundström, C., Begum, A., Lindberg, M.J., Sauer, U.H., Almqvist, F., Johansson, J. and Sauer-Eriksson, A.E., 2016. Structural basis for glutathione-mediated activation of the virulence regulatory protein PrfA in *Listeria*. *Proceedings of the National Academy of Sciences*, *113*(51), pp.14733-14738.

Hamon, M.A., Ribet, D., Stavru, F. and Cossart, P., 2012. Listeriolysin O: the Swiss army knife of *Listeria*. *Trends in Microbiology*, *20*(8), pp.360-368.

Hanahan, D., 1983. Studies on transformation of *Escherichia coli* with plasmids. *Journal of Molecular Biology*, *166*(4), pp.557-580.

Hansen, S., Hall, M., Grundström, C., Brännström, K., Sauer-Eriksson, A.E. and Johansson, J., 2020. A novel growth-based selection strategy identifies new constitutively active variants of the major virulence regulator PrfA in *Listeria monocytogenes*. *Journal of Bacteriology*, *202*(11).

Hartwig, J.H., Bokoch, G.M., Carpenter, C.L., Janmey, P.A., Taylor, L.A., Toker, A. and Stossel, T.P., 1995. Thrombin receptor ligation and activated Rac uncap actin filament barbed ends through phosphoinositide synthesis in permeabilized human platelets. *Cell*, *82*(4), pp.643-653.

Hashino, M., Tachibana, M., Nishida, T., Hara, H., Tsuchiya, K., Mitsuyama, M., Watanabe, K., Shimizu, T. and Watarai, M., 2015. Inactivation of the MAPK signaling pathway by *Listeria monocytogenes* infection promotes trophoblast giant cell death. *Frontiers in Microbiology*, *6*, p.1145.

Henry, R., Shaughnessy, L., Loessner, M.J., Alberti-Segui, C., Higgins, D.E. and Swanson, J.A., 2006. Cytolysin-dependent delay of vacuole maturation in macrophages infected with *Listeria monocytogenes*. *Cellular Microbiology*, *8*(1), pp.107-119.

Ireton, K., 2007. Entry of the bacterial pathogen *Listeria monocytogenes* into mammalian cells. *Cellular Microbiology*, *9*(6), pp.1365-1375.

Johansson, J. and Freitag, N.E., 2019. Regulation of *Listeria monocytogenes* virulence. *Microbiology Spectrum*, *7*(4), pp.7-4.

Johansson, J., Mandin, P., Renzoni, A., Chiaruttini, C., Springer, M. and Cossart, P., 2002. An RNA thermosensor controls expression of virulence genes in *Listeria monocytogenes*. *Cell*, *110*(5), pp.551-561.

Jones, G.S. and D'Orazio, S.E., 2017. Monocytes are the predominant cell type associated with *Listeria monocytogenes* in the gut, but they do not serve as an intracellular growth niche. *The Journal of Immunology*, *198*(7), pp.2796-2804

Joseph, B., Przybilla, K., Stühler, C., Schauer, K., Slaghuis, J., Fuchs, T.M. and Goebel, W., 2006. Identification of *Listeria monocytogenes* genes contributing to intracellular replication by expression profiling and mutant screening. *Journal of Bacteriology*, *188*(2), pp.556-568.

Jung, C., Matzke, A., Niemann, H.H., Schwerk, C., Tenenbaum, T. and Orian-Rousseau, V., 2009. Involvement of CD44v6 in InlB-dependent *Listeria* invasion. *Molecular Microbiology*, *72*(5), pp.1196-1207.

Jung, T.H., Park, J.H., Jeon, W.M. and Han, K.S., 2015. Butyrate modulates bacterial adherence on LS174T human colorectal cells by stimulating mucin secretion and MAPK signaling pathway. *Nutrition Research and Practice*, *9*(4), pp.343-349.

Junttila, J.R., Niemelä, S.I. and Hirn, J., 1988. Minimum growth temperatures of *Listeria monocytogenes* and non-haemolytic *listeria*. *Journal of Applied Bacteriology*, *65*(4), pp.321-327.

Kaneda, T., 1991. Iso-and anteiso-fatty acids in bacteria: biosynthesis, function, and taxonomic significance. *Microbiology and Molecular Biology Reviews*, *55*(2), pp.288-302.

Katsui, R., Kojima, Y., Kuniyasu, H., Shimizu, J., Koyama, F., Fujii, H., Nakajima, Y. and Takaki, M., 2008. A new possibility for repairing the anal dysfunction by promoting regeneration of the reflex pathways in the enteric nervous system. *American Journal of Physiology-Gastrointestinal and Liver Physiology*, *294*(4), pp.G1084-G1093.

Kazmierczak, M.J., Wiedmann, M. and Boor, K.J., 2005. Alternative sigma factors and their roles in bacterial virulence. *Microbiology and Molecular Biology Reviews*, *69*(4), pp.527-543.

Kessler, S.L. and Dajani, A.S., 1990. *Listeria* meningitis in infants and children. *The Pediatric infectious disease journal*, *9*(1), pp.61-62.

Khelef, N., Lecuit, M., Bierne, H. and Cossart, P., 2006. Species specificity of the *Listeria monocytogenes* InlB protein. *Cellular Microbiology*, *8*(3), pp.457-470.

Kim, J.J., Bridle, B.W., Ghia, J.E., Wang, H., Syed, S.N., Manocha, M.M., Rengasamy, P., Shajib, M.S., Wan, Y., Hedlund, P.B. and Khan, W.I., 2013. Targeted inhibition of serotonin type 7 (5-HT7) receptor function modulates immune responses and reduces the severity of intestinal inflammation. *The Journal of Immunology*, *190*(9), pp.4795-4804.

Kim, J.J., Wang, H., Terc, J.D., Zambrowicz, B., Yang, Q.M. and Khan, W.I., 2015. Blocking peripheral serotonin synthesis by telotristat etiprate (LX1032/LX1606) reduces severity of both chemical-and infection-induced intestinal inflammation. *American Journal of Physiology-Gastrointestinal and Liver Physiology*, *309*(6), pp.G455-G465.

Kirchner, M. and Higgins, D.E., 2008. Inhibition of ROCK activity allows InlF-mediated invasion and increased virulence of *Listeria monocytogenes*. *Molecular Microbiology*, *68*(3), pp.749-767.

Kirkpatrick, C., Maurer, L.M., Oyelakin, N.E., Yoncheva, Y.N., Maurer, R. and Slonczewski, J.L., 2001. Acetate and formate stress: opposite responses in the proteome of *Escherichia coli*. *Journal of Bacteriology*, *183*(21), pp.6466-6477.

Korsak, D., Borek, A., Daniluk, S., Grabowska, A. and Pappelbaum, K., 2012. Antimicrobial susceptibilities of *Listeria monocytogenes* strains isolated from food and food processing environment in Poland. *International Journal of Food Microbiology*, *158*(3), pp.203-208.

Kumar, A., Russell, R.M., Pifer, R., Menezes-Garcia, Z., Cuesta, S., Narayanan, S., MacMillan, J.B. and Sperandio, V., 2020. The serotonin neurotransmitter modulates virulence of enteric pathogens. *Cell Host and Microbe*, *28*(1), pp.41-53.

Laemmli, U.K., 1970. Cleavage of structural proteins during assembly of the head of bacteriophage T4. *Nature, 227 pp.680-685.*

La Pietra, L., Hudel, M., Pillich, H., Abu Mraheil, M., Berisha, B., Aden, S., Hodnik, V., Lochnit, G., Rafiq, A., Perniss, A. and Anderluh, G., 2020. Phosphocholine antagonizes listeriolysin o-induced host cell responses of *Listeria monocytogenes*. *The Journal of Infectious Diseases*.

Lam, G.Y., Fattouh, R., Muise, A.M., Grinstein, S., Higgins, D.E. and Brumell, J.H., 2011. Listeriolysin O suppresses phospholipase C-mediated activation of the microbicidal NADPH oxidase to promote *Listeria monocytogenes* infection. *Cell Host and Microbe*, *10*(6), pp.627-634.

Lambrechts, A., Gevaert, K., Cossart, P., Vandekerckhove, J. and Van Troys, M., 2008. *Listeria* comet tails: the actin-based motility machinery at work. *Trends in Cell Biology*, *18*(5), pp.220-227.

Larsen, M.H., Kallipolitis, B.H., Christiansen, J.K., Olsen, J.E. and Ingmer, H., 2006. The response regulator ResD modulates virulence gene expression in response to carbohydrates in *Listeria monocytogenes*. *Molecular Microbiology*, *61*(6), pp.1622-1635.

Latorre, E., Pradilla, A., Chueca, B., Pagán, R., Layunta, E., Alcalde, A.I. and Mesonero, J.E., 2016. *Listeria monocytogenes* inhibits serotonin transporter in human intestinal Caco-2 cells. *Microbial Ecology*, *72*(3), pp.730-739.

Lauer, P., Chow, M.Y.N., Loessner, M.J., Portnoy, D.A. and Calendar, R., 2002. Construction, characterization, and use of two *Listeria monocytogenes* site-specific phage integration vectors. *Journal of Bacteriology*, *184*(15), pp.4177-4186.

Lawhon, S.D., Maurer, R., Suyemoto, M. and Altier, C., 2002. Intestinal short-chain fatty acids alter *Salmonella typhimurium* invasion gene expression and virulence through BarA/SirA. *Molecular Microbiology*, *46*(5), pp.1451-1464.

Lebreton, A. and Cossart, P., 2017. RNA-and protein-mediated control of *Listeria monocytogenes* virulence gene expression. *RNA Biology*, *14*(5), pp.460-470.

Lecuit, M., 2007. Human listeriosis and animal models. *Microbes and Infection*, *9*(10), pp.1216-1225.

Lecuit, M., Dramsi, S., Gottardi, C., Fedor-Chaiken, M., Gumbiner, B. and Cossart, P., 1999. A single amino acid in E-cadherin responsible for host specificity towards the human pathogen *Listeria monocytogenes*. *The EMBO Journal*, *18*(14), pp.3956-3963.

Li, L., Bennett, S.A. and Wang, L., 2012. Role of E-cadherin and other cell adhesion molecules in survival and differentiation of human pluripotent stem cells. *Cell Adhesion and Migration*, *6*(1), pp.59-73.

Li, N., Ghia, J.E., Wang, H., McClemens, J., Cote, F., Suehiro, Y., Mallet, J. and Khan, W.I., 2011. Serotonin activates dendritic cell function in the context of gut inflammation. *The American Journal of Pathology*, *178*(2), pp.662-671.

Li, Z., Chalazonitis, A., Huang, Y.Y., Mann, J.J., Margolis, K.G., Yang, Q.M., Kim, D.O., Côté, F., Mallet, J. and Gershon, M.D., 2011. Essential roles of enteric neuronal serotonin in gastrointestinal motility and the development/survival of enteric dopaminergic neurons. *Journal of Neuroscience*, *31*(24), pp.8998-9009.

Liao, Y., Smyth, G.K. and Shi, W., 2014. featureCounts: an efficient general purpose program for assigning sequence reads to genomic features. *Bioinformatics*, *30*(7), pp.923-930.

Liu, M.T., Kuan, Y.H., Wang, J., Hen, R. and Gershon, M.D., 2009. 5-HT4 receptor-mediated neuroprotection and neurogenesis in the enteric nervous system of adult mice. *Journal of Neuroscience*, *29*(31), pp.9683-9699.

Liu, Y., Orsi, R.H., Boor, K.J., Wiedmann, M. and Guariglia-Oropeza, V., 2017. Home alone: elimination of all but one alternative sigma factor in *Listeria monocytogenes* allows prediction of new roles for σB. *Frontiers in Microbiology*, *8*, p.1910.

Lobel, L., Sigal, N., Borovok, I., Ruppin, E. and Herskovits, A.A., 2012. Integrative genomic analysis identifies isoleucine and CodY as regulators of *Listeria monocytogenes* virulence.

Loh, E., Dussurget, O., Gripenland, J., Vaitkevicius, K., Tiensuu, T., Mandin, P., Repoila, F., Buchrieser, C., Cossart, P. and Johansson, J., 2009. A trans-acting riboswitch controls expression of the virulence regulator PrfA in *Listeria monocytogenes*. *Cell*, *139*(4), pp.770-779.

Lomonaco, S., Nucera, D. and Filipello, V., 2015. The evolution and epidemiology of *Listeria monocytogenes* in Europe and the United States. *Infection, Genetics and Evolution*, *35*, pp.172-183.

Love, M.I., Huber, W. and Anders, S., 2014. Moderated estimation of fold change and dispersion for RNA-seq data with DESeq2. *Genome Biology*, *15*(12), pp.1-21.

Low, J.C. and Donachie, W., 1997. A review of *Listeria monocytogenes* and listeriosis. *The Veterinary Journal*, *153*(1), pp.9-29.

Lungu, B., Ricke, S.C. and Johnson, M.G., 2009. Growth, survival, proliferation and pathogenesis of *Listeria monocytogenes* under low oxygen or anaerobic conditions: a review. *Anaerobe*, *15*(1-2), pp.7-17.

Lyte, J.M., Shrestha, S., Wagle, B.R., Liyanage, R., Martinez, D.A., Donoghue, A.M., Daniels, K.M. and Lyte, M., 2021. Serotonin modulates Campylobacter jejuni physiology and in vitro interaction with the gut epithelium. *Poultry Science*, *100*(3), p.100944.

Macfarlane, G.T. and Macfarlane, S., 2012. Bacteria, colonic fermentation, and gastrointestinal health. *Journal of AOAC International*, *95*(1), pp.50-60.

Malet, J.K., Cossart, P. and Ribet, D., 2017. Alteration of epithelial cell lysosomal integrity induced by bacterial cholesterol-dependent cytolysins. *Cellular Microbiology*, *19*(4), p.e12682.

Mansell, A., Khelef, N., Cossart, P. and O'Neill, L.A., 2001. Internalin B activates nuclear factor-κB via Ras, phosphoinositide 3-kinase, and Akt. *Journal of Biological Chemistry*, *276*(47), pp.43597-43603.

Margolis, K.G., Stevanovic, K., Li, Z., Yang, Q.M., Oravecz, T., Zambrowicz, B., Jhaver, K.G., Diacou, A. and Gershon, M.D., 2014. Pharmacological reduction of mucosal but not neuronal serotonin opposes inflammation in mouse intestine. *Gut*, *63*(6), pp.928-937.

Marteyn, B., West, N.P., Browning, D.F., Cole, J.A., Shaw, J.G., Palm, F., Mounier, J., Prévost, M.C., Sansonetti, P. and Tang, C.M., 2010. Modulation of Shigella virulence in response to available oxygen in vivo. *Nature*, *465*(7296), pp.355-358.

Matsuyoshi, H., Kuniyasu, H., Okumura, M., Misawa, H., Katsui, R., Zhang, G.X., Obata, K. and Takaki, M., 2010. A 5-HT4-receptor activation-induced neural plasticity enhances in vivo reconstructs of enteric nerve circuit insult. *Neurogastroenterology and Motility*, *22*(7), pp.806-e226.

Mawe, G.M. and Hoffman, J.M., 2013. Serotonin signalling in the gut—functions, dysfunctions and therapeutic targets. *Nature reviews Gastroenterology and Hepatology*, *10*(8), p.473.

McGuckin, M.A., Lindén, S.K., Sutton, P. and Florin, T.H., 2011. Mucin dynamics and enteric pathogens. *Nature Reviews Microbiology*, *9*(4), pp.265-278.

McNeil, N.I., 1984. The contribution of the large intestine to energy supplies in man. *The American journal of Clinical Nutrition*, *39*(2), pp.338-342.

Melton-Witt, J.A., Rafelski, S.M., Portnoy, D.A. and Bakardjiev, A.I., 2012. Oral infection with signature-tagged *Listeria monocytogenes* reveals organ-specific growth and dissemination routes in guinea pigs. *Infection and Immunity*, *80*(2), pp.720-732.

Milohanic, E., Glaser, P., Coppée, J.Y., Frangeul, L., Vega, Y., Vázquez-Boland, J.A., Kunst, F., Cossart, P. and Buchrieser, C., 2003. Transcriptome analysis of *Listeria monocytogenes* identifies three groups of genes differently regulated by PrfA. *Molecular Microbiology*, *47*(6), pp.1613-1625.

Mohammad-Zadeh, L.F., Moses, L. and Gwaltney-Brant, S.M., 2008. Serotonin: a review. *Journal of Veterinary Pharmacology and Therapeutics*, *31*(3), pp.187-199.

Monack, D.M. and Theriot, J.A., 2001. Actin-based motility is sufficient for bacterial membrane protrusion formation and host cell uptake. *Cellular Microbiology*, *3*(9), pp.633-647.

Moran, J., Feltham, L., Bagnall, J., Goldrick, M., Lord, E., Nettleton, C., Spiller, D.G., Roberts, I. and Paszek, P., 2022. Single-cell imaging reveals non-cooperative and cooperative infection strategies of *Listeria monocytogenes* in macrophages. *bioRxiv*, pp.2022-06.

Motomura, Y., Ghia, J.E., Wang, H., Akiho, H., El-Sharkawy, R.T., Collins, M., Wan, Y., McLaughlin, J.T. and Khan, W.I., 2008. Enterochromaffin cell and 5-hydroxytryptamine responses to the same infectious agent differ in Th1 and Th2 dominant environments. *Gut*, *57*(4), pp.475-481.

Müller-Herbst, S., Wüstner, S., Mühlig, A., Eder, D., M. Fuchs, T., Held, C., Ehrenreich, A. and Scherer, S., 2014. Identification of genes essential for anaerobic growth of *Listeria monocytogenes*. *Microbiology*, *160*(4), pp.752-765.

Neanover, S., 2020. Effects of Oxygen Levels and Short Chain Fatty Acid Exposure on Antibiotic Susceptibility in *Listeria monocytogenes.*

Neish, A.S., 2009. Microbes in gastrointestinal health and disease. *Gastroenterology*, *136*(1), pp.65-80.

Nguyen, B.N., Peterson, B.N. and Portnoy, D.A., 2019. Listeriolysin O: A phagosome-specific cytolysin revisited. *Cellular Microbiology*, *21*(3), p.e12988.

NicAogáin, K. and O'Byrne, C.P., 2016. The role of stress and stress adaptations in determining the fate of the bacterial pathogen *Listeria monocytogenes* in the food chain. *Frontiers in Microbiology*, *7*, p.1865.

Nwaiwu, O., 2020. What are the recognized species of the genus Listeria?. *Access Microbiology*, *2*(9).

O'Riordan, M. and Portnoy, D.A., 2002. The host cytosol: front-line or home front?. *Trends in Microbiology*, *10*(8), pp.361-364.

O'Byrne, C.P. and Karatzas, K.A., 2008. The role of sigma B (sB) in the stress adaptations of *Listeria monocytogenes*: overlaps between stress adaptation and virulence. *Adv. Appl. Microbiol*, *65*(11).

Obaidat, M.M., Bani Salman, A.E., Lafi, S.Q. and Al-Abboodi, A.R., 2015. Characterization of *Listeria monocytogenes* from three countries and antibiotic resistance differences among countries and *Listeria monocytogenes* serogroups. *Letters in Applied Microbiology*, *60*(6), pp.609-614.

Ooi, A., Hussain, S., Seyedarabi, A. and Pickersgill, R.W., 2006. Structure of internalin C from *Listeria monocytogenes*. *Acta Crystallographica Section D: Biological Crystallography*, *62*(11), pp.1287-1293

Ortega, F.E., Rengarajan, M., Chavez, N., Radhakrishnan, P., Gloerich, M., Bianchini, J., Siemers, K., Luckett, W.S., Lauer, P., Nelson, W.J. and Theriot, J.A., 2017. Adhesion to the host cell surface is sufficient to mediate *Listeria monocytogenes* entry into epithelial cells. *Molecular Biology of the Cell*, *28*(22), pp.2945-2957.

Page, I.H., Rapport, M.M. and Green, A.A., 1948. The crystallization of serotonin. *The Journal of Laboratory and Clinical Medicine*, *33*(12), p.1606.

Park, S.F. and Stewart, G.S., 1990. High-efficiency transformation of *Listeria monocytogenes* by electroporation of penicillin-treated cells. *Gene*, *94*(1), pp.129-132.

Peng, L., He, Z., Chen, W., Holzman, I.R. and Lin, J., 2007. Effects of butyrate on intestinal barrier function in a Caco-2 cell monolayer model of intestinal barrier. *Pediatric Research*, *61*(1), pp.37-41.

Peng, L., Li, Z.R., Green, R.S., Holzman, I.R. and Lin, J., 2009. Butyrate enhances the intestinal barrier by facilitating tight junction assembly via activation of AMP-activated protein kinase in Caco-2 cell monolayers. *The Journal of Nutrition*, *139*(9), pp.1619-1625.

Pentecost, M., Kumaran, J., Ghosh, P. and Amieva, M.R., 2010. *Listeria monocytogenes* internalin B activates junctional endocytosis to accelerate intestinal invasion. *PLoS Pathogens*, *6*(5), p.e1000900

Peterson, B.N., Portman, J.L., Feng, Y., Wang, J. and Portnoy, D.A., 2020. Secondary structure of the mRNA encoding listeriolysin O is essential to establish the replicative niche of *Listeria monocytogenes*. *Proceedings of the National Academy of Sciences*, *117*(38), pp.23774-23781.

Phalipon, A. and Sansonetti, P.J., 2007. Shigella's ways of manipulating the host intestinal innate and adaptive immune system: a tool box for survival?. *Immunology and Cell biology*, *85*(2), pp.119-129.

Pillich, H., Loose, M., Zimmer, K.P. and Chakraborty, T., 2012. Activation of the unfolded protein response by *Listeria monocytogenes*. *Cellular Microbiology*, *14*(6), pp.949-964.

Pizarro-Cerdá, J. and Cossart, P., 2006. Bacterial adhesion and entry into host cells. *Cell*, *124*(4), pp.715-727.

Pizarro-Cerdá, J., Kühbacher, A. and Cossart, P., 2012. Entry of *Listeria monocytogenes* in mammalian epithelial cells: an updated view. *Cold Spring Harbor perspectives in medicine*, *2*(11), p.a010009.

Popowska, M., Krawczyk-Balska, A., Ostrowski, R. and Desvaux, M., 2017. InlL from *Listeria monocytogenes* is involved in biofilm formation and adhesion to mucin. *Frontiers in Microbiology*, *8*, p.660.

Portman, J.L., Huang, Q., Reniere, M.L., Iavarone, A.T. and Portnoy, D.A., 2017. Activity of the pore-forming virulence factor listeriolysin O is reversibly inhibited by naturally occurring S-glutathionylation. *Infection and Immunity*, *85*(4), pp.e00959-16.

Poyart, C., Abachin, E., Razafimanantsoa, I. and Berche, P., 1993. The zinc metalloprotease of *Listeria monocytogenes* is required for maturation of phosphatidylcholine phospholipase C: direct evidence obtained by gene complementation. *Infection and Immunity*, *61*(4), pp.1576-1580.

Quereda, J.J., Pizarro-Cerdá, J., Balestrino, D., Bobard, A., Danckaert, A., Aulner, N., Shorte, S., Enninga, J. and Cossart, P., 2016. A dual microscopy-based assay to assess *Listeria monocytogenes* cellular entry and vacuolar escape. *Applied and Environmental Microbiology*, *82*(1), pp.211-217.

Rabinovich, L., Sigal, N., Borovok, I., Nir-Paz, R. and Herskovits, A.A., 2012. Prophage excision activates *Listeria* competence genes that promote phagosomal escape and virulence. *Cell*, *150*(4), pp.792-802.

Radoshevich, L. and Cossart, P., 2018. *Listeria monocytogenes*: towards a complete picture of its physiology and pathogenesis. *Nature Reviews Microbiology*, *16*(1), pp.32-46.

Rafelski, S.M. and Theriot, J.A., 2005. Bacterial shape and ActA distribution affect initiation of *Listeria monocytogenes* actin-based motility. *Biophysical Journal*, *89*(3), pp.2146-2158.

Rafelski, S.M. and Theriot, J.A., 2006. Mechanism of polarization of *Listeria monocytogenes* surface protein ActA. *Molecular Microbiology*, *59*(4), pp.1262-1279.

Raven, J.A. and Beardall, J., 1981. The intrinsic permeability of biological membranes to H+: significance for the efficiency of low rates of energy transformation. *FEMS Microbiology Letters*, *10*(1), pp.1-5.

Raveneau, J., Geoffroy, C., Beretti, J.L., Gaillard, J.L., Alouf, J.E. and Berche, P., 1992. Reduced virulence of a *Listeria monocytogenes* phospholipase-deficient mutant obtained by transposon insertion into the zinc metalloprotease gene. *Infection and Immunity*, *60*(3), pp.916-921.

Reniere, M.L., Whiteley, A.T., Hamilton, K.L., John, S.M., Lauer, P., Brennan, R.G. and Portnoy, D.A., 2015. Glutathione activates virulence gene expression of an intracellular pathogen. *Nature*, *517*(7533), pp.170-173.

Reniere, M.L., Whiteley, A.T. and Portnoy, D.A., 2016. An *in vivo* selection identified *Listeria monocytogenes* genes required to sense the intracellular environment and activate virulence factor expression. PLoS Pathogens, *12(7), e1005741.*

Rinehart, E., Chapman, J. and Sun, Y., 2020. The Production of listeriolysin O and subsequent intracellular infections by *Listeria monocytogenes* are regulated by exogenous short chain fatty acid mixtures. *Toxins*, *12*(4), p.218.

Rinehart, E., Newton, E., Marasco, M.A., Beemiller, K., Zani, A., Muratore, M.K., Weis, J., Steinbicker, N., Wallace, N. and Sun, Y., 2018. *Listeria monocytogenes* response to propionate is differentially modulated by anaerobicity. *Pathogens*, *7*(3), p.60.

Rinehart, E.M., 2020. The Effects of Short Chain Fatty Acids and Oxygen Levels on *Listeria Monocytogenes Pathogenesis* (Doctoral dissertation, University of Dayton).

Ríos-Covián, D., Ruas-Madiedo, P., Margolles, A., Gueimonde, M., De Los Reyes-gavilán, C.G. and Salazar, N., 2016. Intestinal short chain fatty acids and their link with diet and human health. *Frontiers in Microbiology*, *7*, p.185.

Ripio, M.T., Brehm, K., Lara, M., Suarez, M. and Vazquez-Boland, J.A., 1997. Glucose-1-phosphate utilization by *Listeria monocytogenes* is PrfA dependent and coordinately expressed with virulence factors. *Journal of Bacteriology*, *179*(22), pp.7174-7180.

Roberts, B.N., Chakravarty, D., Gardner, J.C., Ricke, S.C. and Donaldson, J.R., 2020. *Listeria monocytogenes* Response to Anaerobic Environments. *Pathogens*, *9*(3), p.210.

Roe, A.J., O'Byrne, C., McLaggan, D. and Booth, I.R., 2002. Inhibition of *Escherichia coli* growth by acetic acid: a problem with methionine biosynthesis and homocysteine toxicity. *Microbiology*, *148*(7), pp.2215-2222.

Rolhion, N. and Cossart, P., 2017. How the study of *Listeria monocytogenes* has led to new concepts in biology. *Future Microbiology*, *12*(7), pp.621-638.

Ruan, Y., Rezelj, S., Bedina Zavec, A., Anderluh, G. and Scheuring, S., 2016. Listeriolysin O membrane damaging activity involves arc formation and lineaction--implication for *Listeria monocytogenes* escape from phagocytic vacuole. *PLoS Pathogens*, *12*(4), p.e1005597.

Russell, J.B., 1991. Intracellular pH of acid-tolerant ruminal bacteria. *Applied and Environmental Microbiology*, *57*(11), pp.3383-3384.

Ryan, S., Begley, M., Gahan, C.G. and Hill, C., 2009. Molecular characterization of the arginine deiminase system in *Listeria monocytogenes*: regulation and role in acid tolerance. *Environmental Microbiology*, *11*(2), pp.432-445.

Sabet, C., Lecuit, M., Cabanes, D., Cossart, P. and Bierne, H., 2005. LPXTG protein InlJ, a newly identified internalin involved in *Listeria monocytogenes* virulence. *Infection and Immunity*, *73*(10), pp.6912-6922.

Samarin, S., Romero, S., Kocks, C., Didry, D., Pantaloni, D. and Carlier, M.F., 2003. How VASP enhances actin-based motility. *The Journal of Cell Biology*, *163*(1), pp.131-142.

Samba-Louaka, A., Pereira, J.M., Nahori, M.A., Villiers, V., Deriano, L., Hamon, M.A. and Cossart, P., 2014. *Listeria monocytogenes* dampens the DNA damage response. *PLoS Pathogens*, *10*(10), p.e1004470.

Scaldaferri, F., Nardone, O., Lopetuso, L.R., Petito, V., Bibbò, S., Laterza, L., Gerardi, V., Bruno, G., Scoleri, I., Diroma, A. and Sgambato, A., 2013. Intestinal gas production and gastrointestinal symptoms: from pathogenesis to clinical implication. *European Review for Medical Pharmacological Scienice*, *17*(Suppl 2), pp.2-10.

Schuchat, A., Swaminathan, B. and Broome, C.V., 1991. Epidemiology of human listeriosis. *Clinical Microbiology Reviews*, *4*(2), pp.169-183

Schüller, S. and Phillips, A.D., 2010. Microaerobic conditions enhance type III secretion and adherence of enterohaemorrhagic Escherichia coli to polarized human intestinal epithelial cells. *Environmental Microbiology*, *12*(9), pp.2426-2435.

Schwerdtfeger, L.A., Nealon, N.J., Ryan, E.P. and Tobet, S.A., 2019. Human colon function ex vivo: Dependence on oxygen and sensitivity to antibiotic. *PloS One*, *14*(5), p.e0217170.

Scortti, M., Monzó, H.J., Lacharme-Lora, L., Lewis, D.A. and Vázquez-Boland, J.A., 2007. The PrfA virulence regulon. *Microbes and Infection*, *9*(10), pp.1196-1207.

Seifart Gomes, C., Izar, B., Pazan, F., Mohamed, W., Mraheil, M.A., Mukherjee, K., Billion, A., Aharonowitz, Y., Chakraborty, T. and Hain, T., 2011. Universal stress proteins are important for oxidative and acid stress resistance and growth of *Listeria monocytogenes* EGD-e in vitro and in vivo. *PLoS One*, *6*(9), p.e24965.

Shen, A., Higgins, D.E. and Panne, D., 2009. Recognition of AT-rich DNA binding sites by the MogR repressor. *Structure*, *17*(5), pp.769-777.

Shen, A., Kamp, H.D., Gründling, A. and Higgins, D.E., 2006. A bifunctional O-GlcNAc transferase governs flagellar motility through anti-repression. *Genes and Development*, *20*(23), pp.3283-3295.

Shetron-Rama, L.M., Marquis, H., Bouwer, H.A. and Freitag, N.E., 2002. Intracellular induction of *Listeria monocytogenes* actA expression. *Infection and Immunity*, *70*(3), pp.1087-1096.
Sibanda, T. and Buys, E.M., 2022. *Listeria monocytogenes* Pathogenesis: The Role of Stress Adaptation. *Microorganisms*, *10*(8), p.1522.

Singh, N., Thangaraju, M., Prasad, P.D., Martin, P.M., Lambert, N.A., Boettger, T., Offermanns, S. and Ganapathy, V., 2010. Blockade of dendritic cell development by bacterial fermentation products butyrate and propionate through a transporter (Slc5a8)-dependent inhibition of histone deacetylases. *Journal of Biological Chemistry*, *285*(36), pp.27601-27608.

Skogberg, K., Syrjänen, J., Jahkola, M., Renkonen, O.V., Paavonen, J., Ahonen, J., Kontiainen, S., Ruutu, P. and Valtonen, V., 1992. Clinical presentation and outcome of listeriosis in patients with and without immunosuppressive therapy. *Clinical Infectious Diseases*, *14*(4), pp.815-821.

Sleator, R.D., Wouters, J., Gahan, C.G., Abee, T. and Hill, C., 2001. Analysis of the role of OpuC, an osmolyte transport system, in salt tolerance and virulence potential of Listeria monocytogenes. *Applied and Environmental Microbiology*, *67*(6), pp.2692-2698.

Slonczewski, J.L., Fujisawa, M., Dopson, M. and Krulwich, T.A., 2009. Cytoplasmic pH measurement and homeostasis in bacteria and archaea. *Advances in Microbial Physiology*, *55*, pp.1-317.

Smith, G.A., Marquis, H., Jones, S., Johnston, N.C., Portnoy, D.A. and Goldfine, H., 1995. The two distinct phospholipases C of *Listeria monocytogenes* have overlapping roles in escape from a vacuole and cell-to-cell spread. *Infection and Immunity*, *63*(11), pp.4231-4237.

Spohn, S.N. and Mawe, G.M., 2017. Non-conventional features of peripheral serotonin signalling—the gut and beyond. *Nature Reviews Gastroenterology and Hepatology*, *14*(7), pp.412-420.

Spohn, S.N., Bianco, F., Scott, R.B., Keenan, C.M., Linton, A.A., O'Neill, C.H., Bonora, E., Dicay, M., Lavoie, B., Wilcox, R.L. and MacNaughton, W.K., 2016. Protective actions of epithelial 5-hydroxytryptamine 4 receptors in normal and inflamed colon. *Gastroenterology*, *151*(5), pp.933-9

Stavru, F., Palmer, A.E., Wang, C., Youle, R.J. and Cossart, P., 2013. Atypical mitochondrial fission upon bacterial infection. *Proceedings of the National Academy of Sciences*, *110*(40), pp.16003-16008.

Steckler, A.J., Cardenas-Alvarez, M.X., Ramsett, M.K.T., Dyer, N. and Bergholz, T.M., 2018. Genetic characterization of *Listeria monocytogenes* from ruminant listeriosis from different geographical regions in the US. *Veterinary Microbiology*, *215*, pp.93-97.

Suárez, M., González-Zorn, B., Vega, Y., Chico-Calero, I. and Vázquez-Boland, J.A., 2001. A role for ActA in epithelial cell invasion by *Listeria monocytogenes*. *Cellular Microbiology*, *3*(12), pp.853-864.

Sun, Y. and O'Riordan, M.X., 2013. Regulation of bacterial pathogenesis by intestinal short-chain fatty acids. In *Advances in applied microbiology* (Vol. 85, pp. 93-118). Academic Press.

Sun, Y., Wilkinson, B.J., Standiford, T.J., Akinbi, H.T. and O'Riordan, M.X., 2012. Fatty acids regulate stress resistance and virulence factor production for *Listeria monocytogenes*. *Journal of Bacteriology*, *194*(19), pp.5274-5284.

Sunkara, L.T., Achanta, M., Schreiber, N.B., Bommineni, Y.R., Dai, G., Jiang, W., Lamont, S., Lillehoj, H.S., Beker, A., Teeter, R.G. and Zhang, G., 2011. Butyrate enhances disease resistance of chickens by inducing antimicrobial host defense peptide gene expression. *PLoS One*, *6*(11), p.e27225.

Sunkara, L.T., Jiang, W. and Zhang, G., 2012. Modulation of antimicrobial host defense peptide gene expression by free fatty acids. *PloS One*, *7*(11), p.e49558.

Takaki, M., Misawa, H., Matsuyoshi, H., Kawahara, I., Goto, K., Zhang, G.X., Obata, K. and Kuniyasu, H., 2011. In vitro enhanced differentiation of neural networks in ES gut-like organ from mouse ES cells by a 5-HT4-receptor activation. *Biochemical and Biophysical Research Communications*, *406*(4), pp.529-533.

Tang, Y., Chen, Y., Jiang, H., Robbins, G.T. and Nie, D., 2011. G-protein-coupled receptor for short-chain fatty acids suppresses colon cancer. *International Journal of Cancer*, *128*(4), pp.847-856.

Tapia, N.C., Dorey, A.L., Gahan, C.G., den Besten, H.M., O'Byrne, C.P. and Abee, T., 2020. Different carbon sources result in differential activation of sigma B and stress resistance in *Listeria monocytogenes*. *International Journal of Food Microbiology*, *320*, p.108504.

Termén, S., Tollin, M., Rodriguez, E., Sveinsdóttir, S.H., Jóhannesson, B., Cederlund, A., Sjövall, J., Agerberth, B. and Gudmundsson, G.H., 2008. PU. 1 and bacterial metabolites regulate the human gene CAMP encoding antimicrobial peptide LL-37 in colon epithelial cells. *Molecular Immunology*, *45*(15), pp.3947-3955.

Tinevez, J.Y., Arena, E.T., Anderson, M., Nigro, G., Injarabian, L., André, A., Ferrari, M., Campbell-Valois, F.X., Devin, A., Shorte, S.L. and Sansonetti, P.J., 2019. Shigella-mediated oxygen depletion is essential for intestinal mucosa colonization. *Nature Microbiology*, *4*(11), pp.2001-2009

Travier, L. and Lecuit, M., 2014. *Listeria monocytogenes* ActA: a new function for a 'classic'virulence factor. *Current Opinion in Microbiology*, *17*, pp.53-60.

Trichet, L., Campàs, O., Sykes, C. and Plastino, J., 2007. VASP governs actin dynamics by modulating filament anchoring. *Biophysical Journal*, *92*(3), pp.1081-1089.

Tuchscherr, L., Bischoff, M., Lattar, S.M., Noto Llana, M., Pförtner, H., Niemann, S., Geraci, J., Van de Vyver, H., Fraunholz, M.J., Cheung, A.L. and Herrmann, M., 2015. Sigma factor

SigB is crucial to mediate *Staphylococcus aureus* adaptation during chronic infections. *PLoS Pathogens*, *11*(4), p.e1004870.

Turner, J.R., 2009. Intestinal mucosal barrier function in health and disease. *Nature Reviews Immunology*, *9*(11), pp.799-809.

Vadia, S., Arnett, E., Haghighat, A.C., Wilson-Kubalek, E.M., Tweten, R.K. and Seveau, S., 2011. The pore-forming toxin listeriolysin O mediates a novel entry pathway of *Listeria monocytogenes* into human hepatocytes. *PLoS Pathogens*, *7*(11), p.e1002356.

Vasanthakrishnan, R.B., de Las Heras, A., Scortti, M., Deshayes, C., Colegrave, N. and Vázquez-Boland, J.A., 2015. PrfA regulation offsets the cost of *Listeria* virulence outside the host. *Environmental Microbiology*, *17*(11), pp.4566-4579

Vazquez-Boland, J.A., Kocks, C., Dramsi, S., Ohayon, H., Geoffroy, C., Mengaud, J. and Cossart, P., 1992. Nucleotide sequence of the lecithinase operon of *Listeria monocytogenes* and possible role of lecithinase in cell-to-cell spread. *Infection and Immunity*, *60*(1), pp.219-230.

Vázquez-Boland, J.A., Kuhn, M., Berche, P., Chakraborty, T., Domínguez-Bernal, G., Goebel, W., González-Zorn, B., Wehland, J. and Kreft, J., 2001. *Listeria* pathogenesis and molecular virulence determinants. *Clinical Microbiology Reviews*, *14*(3), pp.584-640.

Vieira, E.L., Leonel, A.J., Sad, A.P., Beltrão, N.R., Costa, T.F., Ferreira, T.M., Gomes-Santos, A.C., Faria, A.M., Peluzio, M.C., Cara, D.C. and Alvarez-Leite, J.I., 2012. Oral administration of sodium butyrate attenuates inflammation and mucosal lesion in experimental acute ulcerative colitis. *The Journal of Nutritional Biochemistry*, *23*(5), pp.430-436.

Wallace, N., Zani, A., Abrams, E. and Sun, Y., 2016. The impact of oxygen on bacterial enteric pathogens. *In Advances in Applied Microbiology* (Vol. 95, pp. 179-204). Academic Press.

Wallace, N.C., 2018. Metabolic and Physiological Determinants in *Listeria monocytogenes* Anaerobic Virulence Regulation. University of Dayton.

Wang, J., 2012. *Modulation of Phosphoinositide Metabolism by Intracellular Pathogenic Bacteria Listeria monocytogenes*. The University of Manchester (United Kingdom).

Wang, S., Orsi, R.H., Tang, S., Zhang, W., Wiedmann, M. and Boor, K.J., 2014. Phosphotransferase system-dependent extracellular growth of *Listeria monocytogenes* is regulated by alternative sigma factors σL and σH. *Applied and Environmental Microbiology*, *80*(24), pp.7673-7682.

Ward, T.J., Gorski, L., Borucki, M.K., Mandrell, R.E., Hutchins, J. and Pupedis, K., 2004. Intraspecific phylogeny and lineage group identification based on the prfA virulence gene cluster of *Listeria monocytogenes*. *Journal of Bacteriology*, *186*(15), pp.4994-5002.

Weiglein, I., Goebel, W., Troppmair, J., Rapp, U.R., Demuth, A. and Kuhn, M., 1997. *Listeria monocytogenes* infection of HeLa cells results in listeriolysin O-mediated transient activation of the Raf-MEK-MAP kinase pathway. *FEMS Microbiology Letters*, *148*(2), pp.189-195.

Wemekamp-Kamphuis, H.H., Wouters, J.A., de Leeuw, P.P., Hain, T., Chakraborty, T. and Abee, T., 2004. Identification of sigma factor σB-controlled genes and their impact on acid

stress, high hydrostatic pressure, and freeze survival in *Listeria monocytogenes EGD-e*. *Applied and Environmental Microbiology*, *70*(6), pp.3457-3466.

Wesley, I.V., Borucki, M., Call, D.R., Larson, D. and Schroeder-Tucker, L., 2003. Detection and diagnosis of *Listeria* and listeriosis in animals. *Microbial Food Safety in Animal Agriculture: Current Topics*, pp.233-241.

Witte, C.E., Archer, K.A., Rae, C.S., Sauer, J.D., Woodward, J.J. and Portnoy, D.A., 2012. Innate immune pathways triggered by *Listeria monocytogenes* and their role in the induction of cell-mediated immunity. *Advances in Immunology*, *113*, pp.135-156.

Wollert, T., Pasche, B., Rochon, M., Deppenmeier, S., van den Heuvel, J., Gruber, A.D., Heinz, D.W., Lengeling, A. and Schubert, W.D., 2007. Extending the host range of *Listeria monocytogenes* by rational protein design. *Cell*, *129*(5), pp.891-902.

Xayarath, B. and Freitag, N.E., 2012. Optimizing the balance between host and environmental survival skills: lessons learned from *Listeria monocytogenes*. *Future Microbiology*, *7*(7), pp.839-852.

Yan, H., Neogi, S.B., Mo, Z., Guan, W., Shen, Z., Zhang, S., Li, L., Yamasaki, S., Shi, L. and Zhong, N., 2010. Prevalence and characterization of antimicrobial resistance of foodborne *Listeria monocytogenes* isolates in Hebei province of Northern China, 2005–2007. *International Journal of Food Microbiology*, *144*(2), pp.310-316.

Yildiz, O., Aygen, B., Esel, D., Kayabas, U., Alp, E., Sumerkan, B. and Doganay, M., 2007. Sepsis and meningitis due to *Listeria monocytogenes. Yonsei Medical Journal*, *48*(3), pp.433-439.

Yoshikawa, Y., Ogawa, M., Hain, T., Yoshida, M., Fukumatsu, M., Kim, M., Mimuro, H., Nakagawa, I., Yanagawa, T., Ishii, T. and Kakizuka, A., 2009. *Listeria monocytogenes* ActA-mediated escape from autophagic recognition. *Nature Cell Biology*, *11*(10), pp.1233-1240.

Yu, W.L., Dan, H. and Lin, M., 2007. Novel protein targets of the humoral immune response to *Listeria monocytogenes* infection in rabbits. *Journal of Medical Microbiology*, *56*(7), pp.888-895.

Zhang, Y., Yeh, E., Hall, G., Cripe, J., Bhagwat, A.A. and Meng, J., 2007. Characterization of *Listeria monocytogenes* isolated from retail foods. *International Journal of Food Microbiology*, *113*(1), pp.47-53

Zimmerman, M.A., Singh, N., Martin, P.M., Thangaraju, M., Ganapathy, V., Waller, J.L., Shi, H., Robertson, K.D., Munn, D.H. and Liu, K., 2012. Butyrate suppresses colonic inflammation through HDAC1-dependent Fas upregulation and Fas-mediated apoptosis of T cells. *American Journal of Physiology-Gastrointestinal and Liver Physiology*, *302*(12), pp.G1405-G1415.

Appendix

Appendix A The Western blot of PrfA, LLO, ActA and P60 proteins

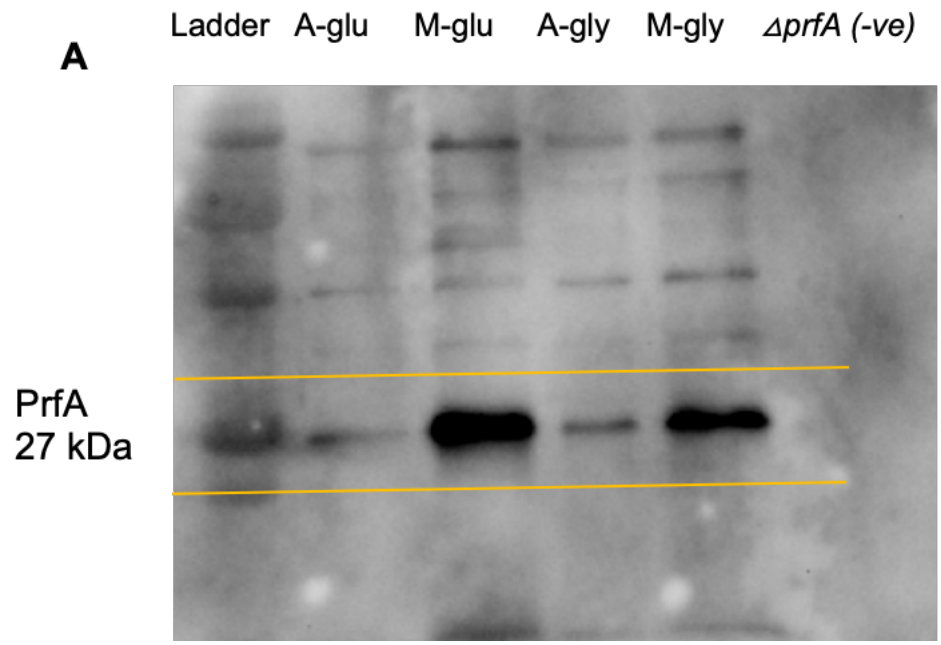

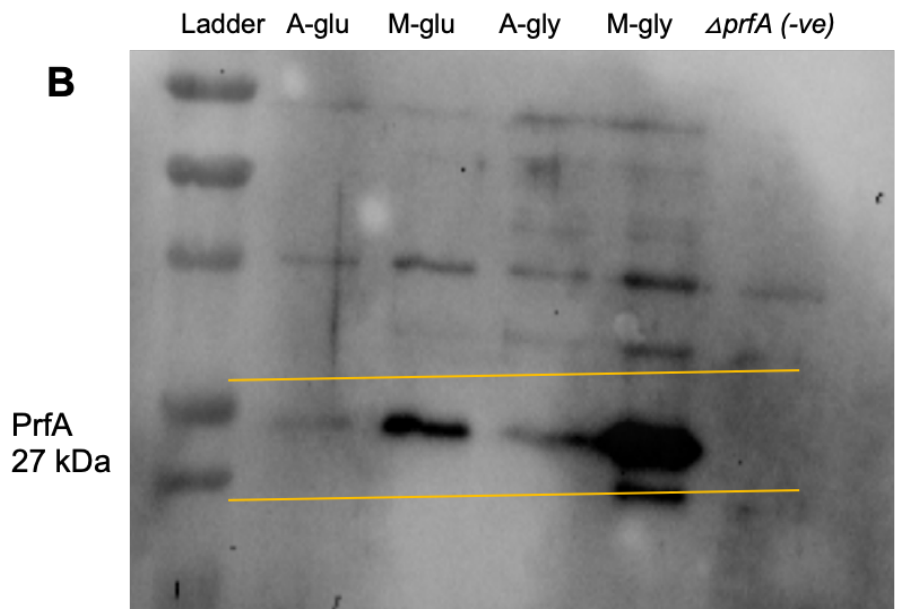

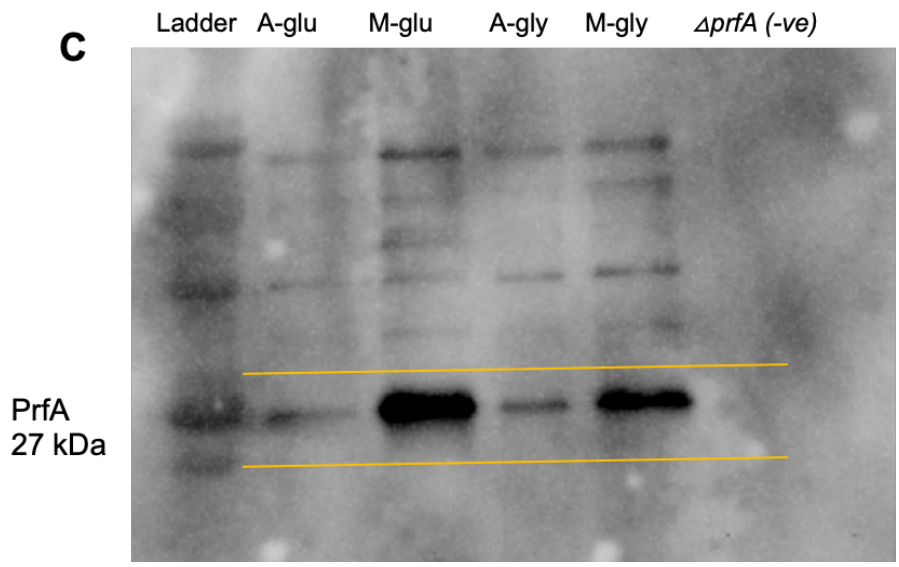
C
Ladder
A-glu
M-glu
A-gly
M-gly
ΔprfA (-ve)
PrfA
27 kDa

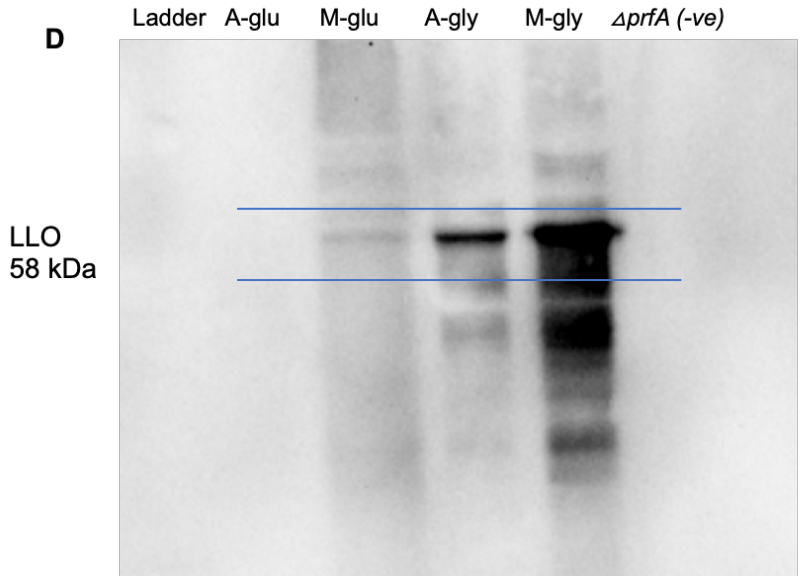
D
Ladder
A-glu
M-glu
A-gly
M-gly
ΔprfA (-ve)
LLO
58 kDa

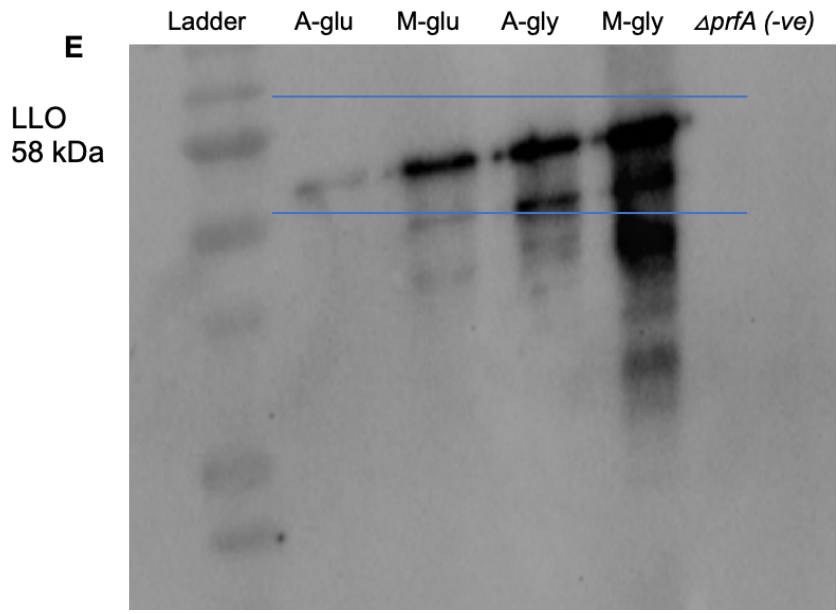
E
Ladder
A-glu
M-glu
A-gly
M-gly
ΔprfA (-ve)
LLO
58 kDa

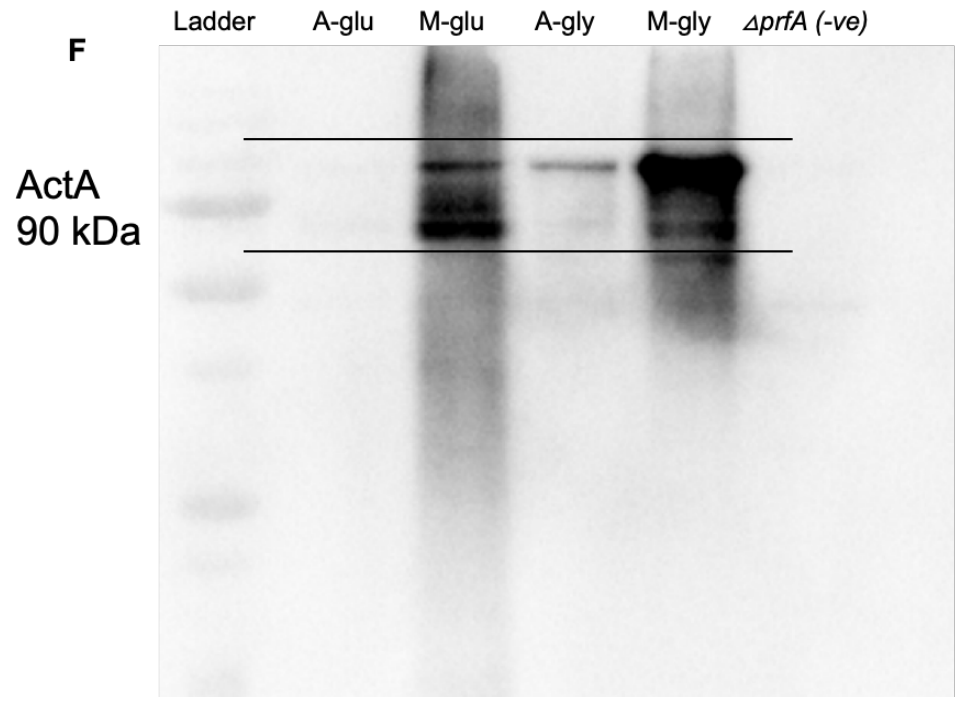
F
Ladder
A-glu
M-glu
A-gly
M-gly
ΔprfA (-ve)
ActA
90 kDa

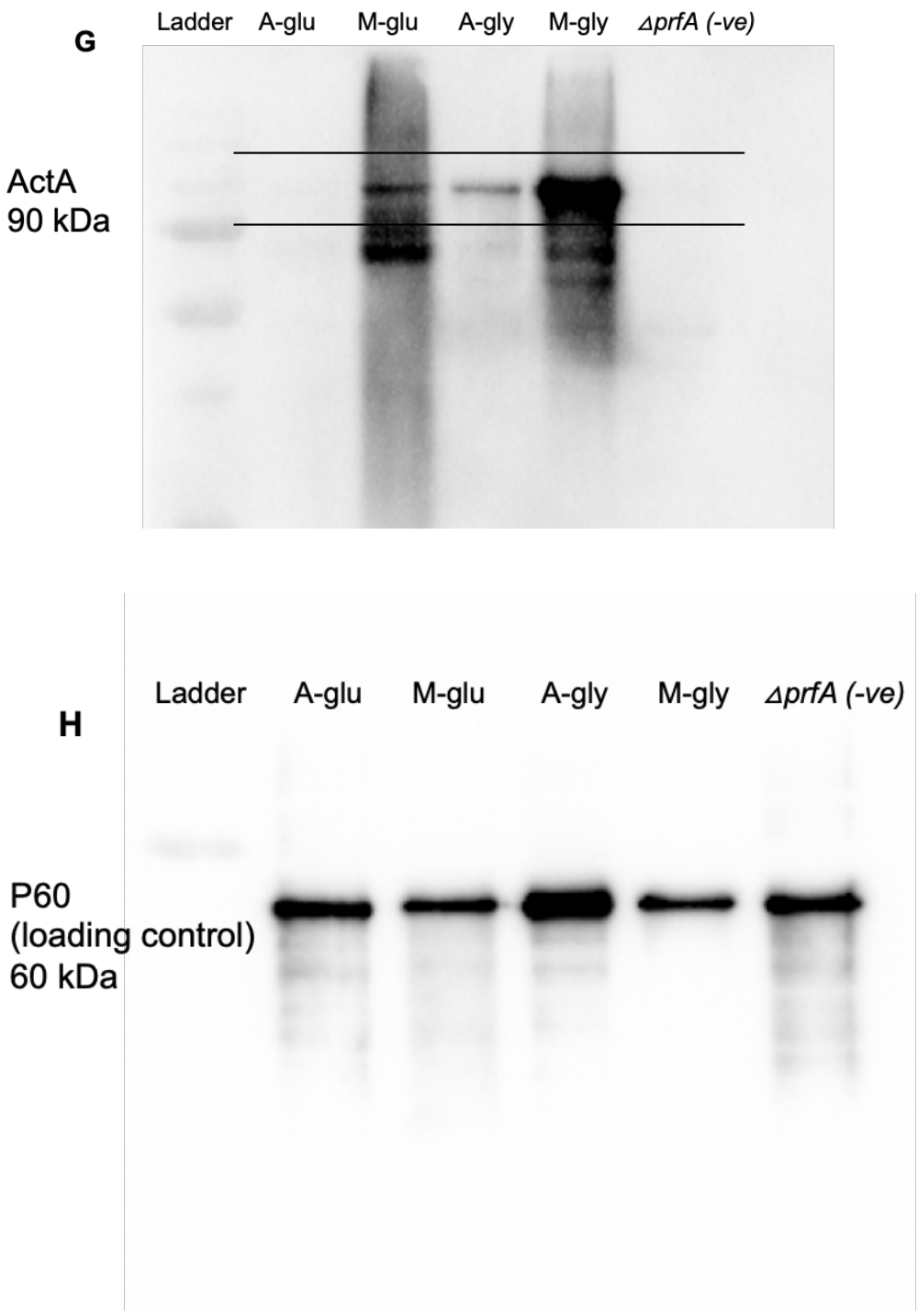

The protein was extracted from *L. monocytogenes InlA* wt grown in MD10 media to an OD_{600} of 1.1 and analysed by Western blotting with anti-PrfA, anti-LLO, anti-ActA and anti-P60 antibodies. A-glu and A-gly mean (under aerobic condition using glucose or glycerol as a carbon source respectively), M-glu and M-gly mean (under microaerobic condition using

glucose or glycerol as a carbon source respectively). Δ*prfA* was used as a negative control and P60 levels were used as a loading control.

Appendix B ArrayExpress submission id E-MTAB-12856 for RNA-seq data